UNIVERSIDADE FEDERAL DE SANTA MARIA
CENTRO DE CIÊNCIAS RURAIS
PROGRAMA DE PÓS-GRADUAÇÃO EM CIÊNCIA E TECNOLOGIA DOS ALIMENTOS

Mariana Manzoni Maroneze

DESENVOLVIMENTO DE EQUIPAMENTOS E PROCESSOS DE BASE MICROALGAL E CARACTERIZAÇÃO DE BIOPRODUTOS DE ORIGEM FOTOSSINTÉTICA

Santa Maria, RS
2019

Mariana Manzoni Maroneze

DESENVOLVIMENTO DE EQUIPAMENTOS E PROCESSOS DE BASE MICROALGAL E CARACTERIZAÇÃO DE BIOPRODUTOS DE ORIGEM FOTOSSINTÉTICA

Tese apresentada ao Curso de Doutorado do Programa de Pós-Graduação em Ciência e Tecnologia dos Alimentos, Área de Concentração em Qualidade de Alimentos, da Universidade Federal de Santa Maria (UFSM), como requisito parcial para obtenção do grau de **Doutora em Ciência e Tecnologia dos Alimentos**

Orientador: Prof. Dr. Eduardo Jacob-Lopes

Santa Maria, RS
2019

Maroneze, Mariana
DESENVOLVIMENTO DE EQUIPAMENTOS E PROCESSOS DE BASE MICROALGAL E CARACTERIZAÇÃO DE BIOPRODUTOS DE ORIGEM FOTOSSINTÉTICA / Mariana Maroneze.- 2019.
139 p.; 30 cm

Orientador: Eduardo Jacob Lopes
Tese (doutorado) - Universidade Federal de Santa Maria, Centro de Ciências Rurais, Programa de Pós Graduação em Ciência e Tecnologia dos Alimentos, RS, 2019

1. Microalgas 2. Fotobiorreator 3. Fotoperíodos 4. Biodiesel 5. Carotenoides I. Jacob Lopes, Eduardo II. Título.

Sistema de geração automática de ficha catalográfica da UFSM. Dados fornecidos pelo autor(a). Sob supervisão da Direção da Divisão de Processos Técnicos da Biblioteca Central. Bibliotecária responsável Paula Schoenfeldt Patta CRB 10/1728.

Mariana Manzoni Maroneze

DESENVOLVIMENTO DE EQUIPAMENTOS E PROCESSOS DE BASE MICROALGAL E CARACTERIZAÇÃO DE BIOPRODUTOS DE ORIGEM FOTOSSINTÉTICA

Tese apresentada ao Curso de Doutorado do Programa de Pós-Graduação em Ciência e Tecnologia dos Alimentos, Área de Concentração em Qualidade de Alimentos, da Universidade Federal de Santa Maria (UFSM), como requisito parcial para obtenção do grau de **Doutora em Ciência e Tecnologia dos Alimentos**

Aprovado em 8 de agosto de 2019:

Prof. Dr. Eduardo Jacob-Lopes (UFSM)
(Presidente/Orientador)

Prof. Drª. Leila Queiroz Zepka (UFSM)

Prof. Dr. Cristiano Ragagnim de Menezes (UFSM)

Prof. Drª. Maria Isabel Queiroz (FURG)

Prof. Dr. Valcenir Júnior Mendes Furlan (UNIPAMPA)

Santa Maria, RS
2019

AGRADECIMENTOS

A *Deus* pela força superior que guiou todos os meus passos para que chegasse até aqui, me permitindo errar, aprender e, principalmente crescer.

Ao meu orientador, Prof. Eduardo pelos quase oito anos de orientação, dedicação e amizade. Sou muito grata por poder carregar comigo os 70% de similaridade.

Aos meus pais, Gilberto e Cláudia, pela educação, por acreditarem e me apoiarem em todos os meus sonhos e por caminharem juntos comigo nessa jornada.

A Prof. Leila por toda ajuda e pelo pontapé inicial na realização do meu sonho de realizar o doutorado sanduíche.

A Prof. Maria Roca pela oportunidade de trabalhar em seu laboratório e por compartilhar um pouco do seu conhecimento comigo, que me possibilitou crescer tanto profissionalmente, quanto pessoalmente.

Aos pesquisadores e técnicos do Instituto de la Grasa pelos ensinamentos técnicos, trocas culturais, e pelos momentos compartilhados durante o período do intercâmbio.

As minhas colegas, que se tornaram grandes amigas e companheiras, Dani e Raquel, que dividiram tantos momentos, desde as aulas, a pesquisa, os perrengues e as conquistas.

Aos amigos da salinha de estudos, especialmente o Alisson, Alessandra, Mariane, Rafaela e Renata por todo apoio, amizade e companheirismo, com vocês tudo ficou mais leve e feliz.

Aos colegas do laboratório 111 pelos anos de convivência, parceria e trocas de experiência.

Aos amigos da vida, que mesmo sem entender bem o que eu falava, escutavam as histórias/dramas da pesquisa, apoiavam, torciam e vibravam a cada conquista.

A CAPES, que com o auxílio financeiro tanto no Brasil, quando na Espanha, tornou possível a realização desta tese.

Aos professores membros da banca, pela disponibilidade e por contribuírem para a qualidade desta tese.

A Universidade Federal de Santa Maria pela formação proporcionada.

“Se eu vi mais longe, foi por estar sobre ombros de gigantes.”

Isaac Newton

Depois de escalar uma grande montanha se descobre que existem muitas outras montanhas para escalar.

Nelson Mandela

RESUMO

DESENVOLVIMENTO DE EQUIPAMENTOS E PROCESSOS DE BASE MICROALGAL E CARACTERIZAÇÃO DE BIOPRODUTOS DE ORIGEM FOTOSSINTÉTICA

AUTORA: Mariana Manzoni Maroneze
ORIENTADOR: Eduardo Jacob Lopes

Processos e produtos baseados em microalgas são atualmente o foco de pesquisadores consideráveis, agências governamentais e empresas privadas em todo o mundo devido à sua ampla variedade de aplicações. Devido à alta produtividade e ao alto conteúdo lipídico, esses microrganismos aparecem como uma importante matéria-prima para a produção de biocombustíveis. Microalgas também são consideradas uma fonte potencial de compostos bioativos, especialmente pigmentos. No entanto, apesar das vantagens, os processos baseados em microalgas ainda apresentam vários desafios que precisam ser abordados, principalmente em termos de sistemas de cultivo. Em face disto, o trabalho teve por objetivos: (i) compreender os sistemas de cultivo de microalgas e suas implicações; (ii) desenvolver um fotobiorreator de bancada e câmara de fotoperíodo; (iii) obter o licenciamento de transferência de tecnologia do fotobiorreator e câmara de fotoperíodo de bancada; (iv) avaliar a influência de fotoperíodos em fotobiorreatores; (v) avaliar a influência de fotoperíodos na produção de biodiesel microalgal; (vi) determinar a presença de carotenoides esterificados em cianobactérias; (vii) determinar o perfil de carotenoides e clorofilas das microalgas *Chlorella vulgaris*, *Scenedesmus obliquus*, *Aphanothece microscopica* Nägeli e *Phormidium autumnale*, relacionando com o metabolismo desses microrganismos. O trabalho desenvolvido nessa tese de doutorado demonstrou que apesar de a área de desenvolvimento de sistemas de produção de microalgas ter evoluído muito nos últimos anos, até o momento, não há um sistema livre de limitações e, estas são intimamente relacionados ao aporte de energia luminosa às células. O biorreator e câmara de fotoperíodo de bancada desenvolvido depositado no INPI viabiliza estudos sobre estratégias de iluminação em cultivos microalgais a nível laboratorial nas mais diversas áreas do conhecimento. O uso de fotoperíodos demonstrou ser uma estratégia de iluminação artificial eficiente melhorar substancialmente o balanço de energia do processo de produção de biodiesel microalgal. Três carotenoides esterificados foram encontrados na caracterização do perfil de carotenoides em cianobactérias, miristoil-zeinoxantina e miristoil-β-criptoxantina em *Aphanothece microscopica* Nägeli e mixoxantofila em *Phormidum autumnale.* Vinte e nove pigmentos, entre carotenoides e clorofilas foram identificados em amostras de biomassa microalgal de *Chlorella vulgaris*, Scenedesmus *obliquus*, *Aphanothece microscopica* Nägeli e *Phormidum autumnale*, através da metodologia pepiline. Dois carotenoides ainda não encontrados em cianobactérias foram encontrados em *Aphanothece microscopica* Nägeli: 5,6-epoxy-β-criptoxantina, cis-5,8-furanoide-β-criptoxantina e 2'-dehidrodeoximixol. Um carotenoide nunca antes

identificado foi encontrado na biomassa de *Phormidum autumnale* (*Desertifilum*), a desertixantina.

Palavras chave: Microalgas, fotobiorreator, fotoperídos, biodiesel, carotenoides.

ABSTRACT

DEVELOPMENT OF MICROALGAL-BASED EQUIPMENT AND PROCESSES AND CHARACTERIZATION OF PHOTOSYNTHETIC ORIGIN BIOPRODUCTS

AUTHOR: Mariana Manzoni Maroneze
ADVISOR: Eduardo Jacob Lopes

Microalgae-based processes and products are currently the focus of considerable researchers, government agencies, and private companies around the world due to its wide variety of applications. Due to the high productivities and high lipid content, these microorganisms appear as an important raw material for biofuels production. Microalgae are also considered a potential source of bioactive compounds, especially pigments. However, despite the advantages, the processes based in microalgae still have several challenges that need to be addressed, mainly in terms of culture systems. In this sense, the aims of this work were: (i) understanding microalgae culture systems and their implications; (ii) developing a bench photobioreactor and photoperiod camera; (iii) obtain the technology transfer licensing of the photobioreactor and bench photoperiod camera; (iv) evaluate the influence of photoperiods on photobioreactors; (v) evaluate the influence of photoperiods on microalgal biodiesel production; (vi) determine the presence of esterified carotenoids in cyanobacteria; (vii) determine the carotenoid and chlorophyll profile of the microalgae *Chlorella vulgaris*, *Scenedesmus obliquus*, *Aphanothece microscopica* Nägeli and *Phormidium autumnale*, relating to the metabolism of these microorganisms. The work developed in this doctoral thesis has shown that although the area of development of microalgae production systems has evolved a lot in the last years, to date, there is no system free from limitations and these are closely related to the contribution of light energy the cells. The developed bioreactor and photoperiod camera deposited at INPI enables studies on lighting strategies in microalgal cultures at laboratory level in the most diverse areas of knowledge. The use of photoperiods has been shown to be an efficient artificial lighting strategy to improve the energy balance of the microalgal biodiesel production process. Three esterified carotenoids were found in the characterization of the carotenoid profile in cyanobacteria, myristoyl-zeinoxanthin and myristoyl-β-cryptoxanthin in *A. microscopica* Nägeli and mixoxantophyll in *P. autumnale*. Twenty-nine pigments between carotenoids and chlorophylls were identified in microalgal biomass samples of *C. vulgaris*, *Scenedesmus. obliquus*, *A. microscopica* Nägeli and *P.*

autumnale, using the pepiline methodology. Two carotenoids not yet found in cyanobacteria were found in A. microscopica Nägeli: 5,6-epoxy-β-cryptoxanthin, cis-5,8-furanoid-β-cryptoxanthin and 2'-dehydrodeoxymyxol. A previously unidentified carotenoid was found in the biomass of *P. autumnale* (*Desertifilum*), desertixanthin.

Keywords: Microalgae, photobioreactor, photoperiod, biodiesel, carotenoids.

SUMÁRIO

INTRODUÇÃO **11**
OBJETIVOS **13**
CAPÍTULO 1 ..... **14**
REVISÃO BIBLIOGRÁFICA 14
1.1 Microalgas 15
1.2 Metabolismo fotossintético 17
1.3 Sistemas de cultivo: biorreatores, operação e parâmetros de processo 18
1.4 Fotoperíodos 20
1.5 Metabolitos microalgais: lipídeos e pigmentos 22
CAPÍTULO 2 ..... **26**
Capítulo: Microalgal Production Systems with Highlights of Bioenergy Production 26
CAPÍTULO 3 ..... **57**
Patente: Câmara de Fotoperíodos e Biorreator de Bancada 57
CAPÍTULO 4 ..... **77**
Licenciamento de Tecnologia: Contrato de Licenciamento para Exploração do Pedido de Patente de Invenção Depositada junto ao INPI Intitulado "Câmara de Fotoperíodos e Biorreator de Bancada" 77
CAPÍTULO 5 ..... **79**
Manuscrito 1: Artificial lighting strategies in photobioreactors for bioenergy production by *Scenedesmus obliquus* CPCC05 79
CAPÍTULO 6 ..... **103**
Artigo 1: Esterified carotenoids as new food components in cyanobacteria 103
CAPÍTULO 7 ..... **112**
Manuscrito 2: Systematic high-through approach reveals new 2 carotenoid metabolism in cyanobacteria 112
CONCLUSÃO **131**
REFERÊNCIAS BIBLIOGRÁFICAS **133**

INTRODUÇÃO

As microalgas são um grupo diversificado de microrganismos fotossintéticos eucarióticos ou procarióticos, que podem crescer rapidamente e viver em condições adversas devido à sua estrutura robusta. Esses organismos são onipresentes e podem ser encontrados em uma variedade de ambientes aquáticos e terrestres. Eles desempenham um papel importante no ciclo global do carbono, usando a energia luminosa para produzir a matéria orgânica que suporta toda a vida na Terra. A fotossíntese microalgal é responsável pela assimilação de aproximadamente 50% do CO_2 do planeta, que é convertido em matéria orgânica (FALKOWSKI & RAVEN, 2007). Concomitante com a fixação de CO_2, eles também produzem O_2 e exibem um papel importante nos ciclos globais de nitrogênio, onde algumas espécies são capazes de fixar o N_2 em nitrogênio orgânico (BOROWITZKA, 2018).

Devido às mudanças climáticas e à crescente demanda por alimentos, rações, produtos químicos e energia, as microalgas da última década estão no foco de pesquisadores de todo o mundo (GIFUNI et al., 2019). A biomassa de microalgas surgiu como talvez a fonte mais promissora para a produção sustentável de biocombustíveis (biodiesel, biogás, bioetanol e biohidrogênio), produtos bioativos de alto valor (pigmentos, ácidos graxos, vitaminas, proteínas/enzimas e esteróis) para aplicação nutracêutica e farmacêutica, bem como suplementos alimentares humanos e animais (JACOB-LOPES et al., 2019; NWOBA et al., 2019). O número de potenciais bioprodutos isolados de microalgas atualmente é superior a 28.000, com centenas de novos compostos sendo descobertos a cada ano, devido ao avanço das técnicas analíticas, que permitem a detecção de metabólitos minoritários (LAURITANO et al., 2019).

Embora as microalgas apresentem várias vantagens (incluindo alta eficiência fotossintética, capacidade de sequestro de CO_2, capacidade de cultivo em terras agrícolas marginais e capacidade de reciclar nutrientes em águas residuárias e gases de combustão), a consolidação da produção industrial de biomassa ainda está em seus primeiros passos (PEREIRA et al., 2018). Atualmente, a barreira mais significativa e crítica para a expansão da comercialização da produção de outros produtos à base de microalgas continua sendo o alto custo de produção, principalmente em relação ao valor do cultivo e processamento a jusante (MARONEZE & QUEIROZ, 2018; HOLDMANN et al., 2019). Esse problema está diretamente relacionado com a necessidade do aporte de energia luminosa as células, uma vez que no ambiente natural, a intensidade luminosa e o regime de luz sofrem alterações contínuas, e a manutenção artificial de luz em períodos integrais de tempo pode

inviabilizar processo, sob o ponto de vista econômico (JACOB-LOPES et al., 2009; GROBBELAAR, 2009).

Pode-se dizer que a viabilidade de qualquer processo ou produto baseados em microalgas depende de dois fatores principais: alta produtividade e qualidade da biomassa com baixo custo de produção. Atualmente, mais de 90% da produção comercial global de biomassa de microalgas é conduzida em sistemas abertos tipo *raceway*, e em menor ocorrência em fotobiorreatores horizontais tubulares fechados ou biorreatores heterotróficos (BLANKEN et al., 2013; MAEDA et al. 2018, SCHADE & MEIER, 2019). Embora os sistemas abertos sejam econômicos em termos de construção, operação e manutenção, alguns problemas importantes incluem contaminação, evaporação, suscetibilidade a condições climáticas e elevada demanda por terra. Em contraste, os sistemas fechados podem eliminar problemas de contaminação e evaporação e alcançar concentrações mais altas de biomassa, mas com alto custo de capital, dificuldade de escalonamento. Devido ao alto controle operacional e a alta produtividade proporcionada pelos sistemas fechados, novos projetos de fotobiorreatores têm sido desenvolvidos por pesquisadores ao redor do mundo (CHANG et al. 2017).

Neste sentido, é necessário que os processos de produção de microalgas em termos de condições de cultivo e sistemas de cultivo sejam otimizados a fim de maximizar a viabilidade de produção e comercialização de produtos a base de microalgas. Além disso, é de extrema importância que todos os metabólitos sejam identificados para que cada vez mais produtos a base de microalgas possam ser comercializados e também para que possam contribuir para a consolidação das rotas metabólicas utilizadas por tais microrganismos. O presente trabalho é resultado de uma interação entre a Universidade Federal de Santa Maria e o Instituto de la Grasa (Sevilha-ES), viabilizado pelo Programa de Doutorado Sanduíche da Capes.

OBJETIVOS

Objetivo geral

Desenvolver equipamentos e processos de base microalgal e caracterizar bioprodutos de origem fotossintética.

Objetivos específicos

-Compreender os sistemas de cultivo de microalgas e suas implicações;

-Desenvolver um fotobiorreator de bancada e câmara de fotoperíodo;

-Obter o licenciamento de transferência de tecnologia do fotobiorreator e câmara de fotoperíodo de bancada;

-Avaliar a influência de fotoperíodos em fotobiorreatores;

- Avaliar a influência de fotoperíodos na produção de biodiesel microalgal;

- Determinar a presença de carotenoides esterificados em cianobactérias;

- Determinar o perfil de carotenoides e clorofilas das microalgas *Chlorella vulgaris, Scenedesmus obliquus*, *Aphanothece microscopica* Nägeli e *Phormidium autumnale,* relacionando com o metabolismo desses microrganismos.

CAPÍTULO 1

REVISÃO BIBLIOGRÁFICA

1. REVISÃO BIBLIOGRÁFICA

1.1 Microalgas

Microalgas é uma terminologia comercial sem valor taxonômico. Compreende um grupo diverso de microrganismos com cerca de 72.500 espécies catalogadas de forma consistente. Os principais critérios para classificar estes microrganismos são pigmentação, natureza química dos produtos de reserva e estrutura celular básica (JACOB-LOPES et al., 2019). Segundo Borowitzka (2018) sob a denominação de microalgas estão incluídos organismos com dois tipos de estrutura celular: estrutura procariótica, com representantes nos grupos *Cyanophyta* e *Prochlorophyta*; estrutura eucariótica, com representantes nos grupos *Glaucophyta, Rhodophyta, Ochrophyta, Haptophyta, Criptófitas, Dinophyta, Euglenophyta, Chlorarachniophyta* e *Chlorophyta*. No entanto, destacam-se sob o aspecto de exploração biotecnológica os grupos: cianobactérias (*Cyanophyta*), clorofíceas (*Chlorophyta*) e diatomáceas (*Ochrophyta*) (MATA et al., 2010).

As cianobactérias são classificadas no reino das eubactérias. Nunca apresentam flagelos e por terem sua organização celular do tipo procarionte, não possuem núcleo, nem organelas. Apresentam em sua estrutura a clorofila a e os fotossistemas I e II, ao contrário de outras bactérias fotossintetizantes, o que as permite realizar a fotossíntese na presença de oxigênio. Algumas espécies são estritamente fototróficas, enquanto outras atuam de modo facultativo, podendo crescer heterotroficamente (WIJFFELS et al., 2013). A composição pigmentar das cianobactérias é uma diferença notável de todos os demais grupos, podendo esses compostos serem usados como “impressões digitais” de determinadas espécies. Esses microrganismos são caracterizados por apresentar clorofila a e ficobiliproteinas (ficocianina, aloficocianina e ficoeritrina), o que lhe confere a cor verde-azul. Alguns gêneros podem conter ainda em sua composição outros tipos de clorofilas, em particular a clorofila d e f. Ainda com relação aos seus pigmentos, as cianobactérias têm sido detectadas como uma promissora fonte de carotenoides (RODRIGUES et al., 2014; PATIAS et al., 2017; BOROWITZKA, 2018).

Dentro do grupo das cianobactérias encontram-se os gêneros *Phormidium* e *Aphanothece*. *Phormidium* é um gênero de cianobactérias filamentosas, não ramificadas, com filamentos de cerca de 3-4 μm de diâmetro. Diversas espécies deste gênero são conhecidas por viverem em ambientes extremos, como fontes termais, solos desérticos e locais poluídos, e por isso possuem um amplo potencial para uso em bioprocessos, devido à sua robustez e exigências nutricionais simples (RODRIGUES et al., 2014; SHISHIDO

et al., 2019). As cianobactérias do gênero *Aphanothece* compreendem morfotipos unicelulares com células ovais ou cilíndricas dispostas irregularmente colônias mucilaginosas amorfas. *Aphanothece microscopica Nägeli* é uma cianobactéria de grande ocorrência no sul do Brasil, devido a sua robustez tem sido utilizada com sucesso tanto em cultivos heterotróficos quanto em fotossintéticos para produção de proteínas e óleos unicelulares (ZEPKA et al., 2007; JACOB-LOPES et al., 2008; QUEIROZ et al., 2013; QUEIROZ et al., 2018).

Por outro lado, as microalgas verdes ou clorofíceas, apresentam grande variedade nos níveis de organização, desde unicelulares, microalgas flageladas ou não, até talos morfologicamente complexos. Os organismos que compõem esse grupo são descritos como os mais abundantes e, assim como as cianobactérias, as clorofíceas podem ser encontradas em quase todos os ambientes, contudo, cerca de 90% do total de espécies (sobretudo as formas microscópicas) ocorrem em água doce (REVIERS, 2006). Apresentam clorofila a e b, e tem como reserva o amido. É o grupo mais promissor de microalgas para aplicações biotecnológicas. Além das clorofilas a e b como característica de toda microalga verde, estas contêm uma ampla gama de carotenoides, que podem ser acumulados e explorados comercialmente. Dentre todas as microalgas, o grupo das clorofíceas é um dos mais profundamente estudados. Um exemplo clássico é a *Chlorella*, que se se difundiu devido ao seu uso científico em estudos fundamentais sobre a fotossíntese e também por ser a primeira microalga a ser comercialmente explorada (SAFI et al., 2014).

Atualmente, 44 espécies de *Chlorella* são descritas, onde a *Chlorella vulgaris* é a espécie com maior produção ao redor do mundo, sendo reconhecida como importante fonte de proteína, ácidos graxos e pigmentos naturais. A *C. vulgaris* é uma célula microscópica esférica com diâmetro de 2-10 μm (SAFI et al., 2014). *Scenedesmus* é outro gênero pertencente à classe *Chlorophyta*, que tem ganhado destaque pelo seu potencial para produção de biodiesel devido a sua alta produtividade de biomassa com alto conteúdo lipídico e perfil de ácidos graxos desejado. Além disso, são microalgas bastante comuns em ambientes de água doce e, devido a sua robustez são relativamente fáceis de cultivar (ABOMOHRA et al., 2016; EL-SHEEKH et al., 2018).

Microalgas também podem ser classificadas quanto ao fornecimento de carbono. Algumas espécies utilizam carbono inorgânico, como o CO_2 e são consideradas autotróficas, pois realizam a fotossíntese para obtenção de energia. Alguns destes microrganismos possuem, no entanto, uma versatilidade no que se refere à manutenção de

suas estruturas, usufruindo de diferentes metabolismos energéticos, como a respiração e fixação de nitrogênio (RAZZAK et al., 2013; RASHID et al., 2014).

1.2 Metabolismo fotossintético

A reação global da fotossíntese é dividida em duas fases, que compreendem um conjunto de reações luminosas, que ocorrem apenas quando as células são iluminadas e reações de fixação de carbono, também chamadas de reações de escuro, que ocorrem tanto presença de luz quanto no escuro (JACOB-LOPES et al., 2009; WILLIANS & LAUREN, 2010).

As reações fotossintéticas ocorrem em organelas especiais, chamadas de cloroplastos. Onde, estes são envoltos por uma membrana, contendo um fluido aquoso chamado estroma, o qual contém o aparato bioquímico necessário para a fixação de CO_2, através das reações de carboxilação da fotossíntese, também conhecidas como ciclo de Calvin-Benson. O estroma contém pilhas de discos achatados delimitadas por uma membrana chamada tilacoide. Embebidos nas membranas tilacoides estão os pigmentos fotossintetizantes que promovem as reações luminosas e a síntese de ATP (FAY, 1983).

As reações luminosas são a etapa na qual ocorre a formação de compostos de alta energia, como ATP (adenosina trifosfato) e NADPH (nicotinamida adenina dinucleotídeo fosfato). Nesta etapa, a energia luminosa é absorvida pelas estruturas altamente organizadas dos pigmentos fotossintéticos e transportadores de elétrons, chamados fotossistemas. Os fotossistemas são constituídos pelo complexo do centro de reação e pelo complexo antena. Fazem parte do complexo antena os pigmentos acessórios: clorofilas b, c e d, carotenoides e ficobiliproteínas. Estes têm como função principal absorver os fótons e transferir a energia para o complexo do centro de reação. Onde, então as moléculas de clorofila a, que são excitadas e seus elétrons são transferidos para uma molécula aceptora de elétrons (ZHAO & SU, 2014).

Os elétrons então fluem através de uma série de transportadores ligados à membrana, incluindo citocromos, quinonas e proteínas ferro-enxofre. Simultaneamente, prótons são bombeados pela membrana tilacoide, a fim de gerar um potencial eletroquímico. Parte da energia liberada é incorporada durante este transporte de elétrons em ATP no processo de fosforilação. A última fonte de elétrons para a fotossíntese é a H_2O, o qual cede no processo de fotólise (reação de Hill), átomos de hidrogênio, elétrons e libera O_2, produto da fotossíntese das microalgas e das plantas verdes (FAY, 1983). A equação geral das reações dependentes de luz é (WILLIANS & LAUREN, 2010):

$$2H_2O+2NADP^{+}+3ADP+3P+Luz \rightarrow 2NADPH+2H^{+}+3ATP+ O_2$$

Na etapa independente de luz ou ciclo de Calvin, ocorre a síntese de açúcares monossacarídeos a partir da fixação de CO_2. O ciclo inicia-se com a reação da ribulose 1,5-bisfosfato (Ru5BP), que é catalisada pela enzima ribulose 1,5-difosfato carboxilase/oxigenase (rubisco), com o CO_2. O produto da reação é quebrado em duas moléculas de três carbonos, 3-fosfoglicerato (PGA). Na presença de ATP e NADPH, o PGA é reduzido em gliceraldeído 3-fosfato (G3P). A maior parte (5 de 6 moléculas) do G3P produzido é utilizado para regenerar Ru5BP, de modo que o ciclo possa ser fechado. Uma das seis moléculas de Ru5BP não é reciclada e, então se condensa para formar açúcares fosforados intermediários e, posteriormente glicose. A equação geral para as reações independentes de luz é (WILLIANS & LAUREN, 2010):

$$3CO_2 + 9ATP + 6NADPH + 6^{+}H \rightarrow C_3H_6O_3 - P + 9ADP + 8P + 6^{+}NADP + 3H_2O$$

1.3 Sistemas de cultivo: biorreatores, operação e parâmetros de processo

A escolha do fotobiorreator ideal é um fator crucial para o bom desempenho de qualquer sistema de cultura de microalgas, uma vez que este é uma função das condições ambientais e de cultivo. Sem levar em consideração qualquer aspecto econômico, fotobiorreatores devem apresentar alguns requisitos básicos de projeto: eficiente fornecimento de energia luminosa e CO_2, temperatura controlada, adequado sistema de mistura, disponibilidade de nutrientes, facilidade de controle das condições da reação e facilidade no aumento de escala (BOROWITZKA, 1999; MARONEZE & QUEIROZ, 2018).

O fornecimento de energia luminosa, devido ao seu caráter limitante no cultivo é o fator mais importante que regula a produtividade de culturas de microrganismos fotossintéticos (FERNÁNDES et al., 2013). Tanto a quantidade quanto a qualidade da fonte luminosa afetam a taxa de crescimento celular. Quando a intensidade da luz é baixa, a velocidade de crescimento é proporcional à intensidade luminosa. Porém, quando a intensidade luminosa é muito maior do que o valor da constante de saturação, ocorre a fotoinibição do crescimento, a qual, geralmente é causada pelo dano reversível ao aparato fotossintético. Iluminação natural ou artificial pode ser utilizada em função das características requeridas nos sistemas de cultivo (POSTEN et al., 2009).

No que se refere à nutrição, apesar das diferenças entre as espécies, para um crescimento ótimo o meio de cultura deve fornecer todos os macronutrientes e

micronutrientes demandados. No grupo dos macronutrientes, estão C, N, O, H e P, que são considerados como essenciais, e também Ca, Mg, S e K. No caso dos micronutrientes, tem-se Fe, Mn, Cu, Mo e Co, algumas espécies também necessitam de baixas concentrações de vitaminas (GEORGE et al., 2014).

A fonte de carbono mais utilizada em cultivos fotossintéticos é o dióxido de carbono, que pode estar em sua forma normal ou dissociada (HCO^{3-}) no meio de cultivo. A concentração ideal de CO_2 no meio ainda não está bem elucidada e varia de acordo com a espécie de microalga, porém, geralmente utiliza-se concentrações entre 2 e 15% (ZHAO & SU, 2014). Considerando a baixa solubilidade do CO_2 em líquidos, é necessário que haja uma eficiente transferência de CO_2 para o meio, de modo a elevar os coeficientes volumétricos de transferência de massa (KLa) para garantir um crescimento celular ótimo (FERNÁNDEZ et al., 2013).

O controle de temperatura também é imprescindível no sentido de garantir a estabilidade do cultivo. Em geral a ótima temperatura de cultivo ocorre na região mesófila (25-35ºC), embora algumas linhagens termófilas resistam a temperaturas na faixa dos 60ºC. A grande maioria dos sistemas de cultivo assume a variação da temperatura como um resultado da variação do ambiente, embora o uso de camisas de aquecimento, serpentinas e trocadores de calor externo possam ser instalados para o controle da temperatura de biorreatores microalgais (POSTEN et al., 2009, CHANG et al., 2017).

Finalmente, agitação é uma operação necessária no cultivo de microrganismos fotossintéticos, uma vez que assegura a uniformidade espacial dos vasos de reação, favorecendo a exposição das células a luz, a transferência de calor e estratificação térmica, além de melhorar a troca de gases. Uma mistura adequada minimiza ainda a formação de agregados celulares que aumentam a ineficiência global do biorreator. Embora fundamental para o adequado desenvolvimento do processo, a operação de mistura está relacionada a estresses hidrodinâmicos associados ao cisalhamento celular, que danifica e inibe o crescimento microalgal. Os biorreatores microalgais são normalmente equipados com sistemas de aeração pneumática e agitação mecânica, ou ainda uma combinação entre estes sistemas (BOROWITZKA, 1999).

Os cultivos de microalgas em larga escala, tiveram início antes da metade do século XX, desde então, uma ampla gama de sistemas de cultivo já foi relatado. A diferenciação destes sistemas de cultivo depende principalmente do custo, do tipo de produtos desejados, da fonte de nutrientes e da captura de CO_2. Os sistemas de cultura são geralmente

classificados de acordo com suas condições de projeto como sistemas abertos ou fechados (RAZZAK et al., 2013).

Tradicionalmente, os sistemas abertos têm sido amplamente utilizados para o cultivo em larga escala, devido à simplicidade e baixo custo. Estes sistemas de cultivo apresentam duas configurações principais: as lagoas circulares e os tanques raceway, que consistem em um tanque raso (20-30 cm de profundidade), de geometria circular ou oval, dotado de sistemas de agitação mecânica, que expõem o meio de cultura ao ar por turbilhonamento. Infelizmente, esses fotobiorreatores permitem apenas um controle limitado das condições de operação. Além disso, a produtividade é baixa devido à baixa absorção de luz no fundo do tanque e pela maior probabilidade de contaminação. Outras limitações desse tipo de cultivo incluem a grande necessidade de espaço de terra para o cultivo, perdas por evaporação, alta temperatura e, consequente baixa eficiência de transferência de massa (VASUMACHI et al., 2012).

Uma alternativa aos fotobiorreatores abertos são sistemas fechados, que possibilitam uma grande variedade de configurações e incrementam significantemente o desempenho dos cultivos. Três configurações principais dominam arranjos dos fotobiorreatores fechados, os sistemas tubulares, de placas planas e as colunas verticais. Estes sistemas são caracterizados por elevadas eficiências fotossintéticas associadas à maior precisão e controle das variáveis operacionais, menor risco de contaminação e minimização das perdas de água por evaporação (JACOB-LOPES et al., 2008; RAZZAK et al., 2013; MARONEZE & QUEIROZ, 2018).

1.4 Fotoperíodos

Para o desenvolvimento de um bioprocesso microalgal baseado em conceitos de tecnologia limpa, a fonte de energia ideal deve ser provida pela luz solar (ESSAM et al., 2007). A energia solar é um dos recursos naturais mais abundantes do planeta. Onde, a intensidade luminosa pode chegar a 1100 W m^{-2} durante o período do meio-dia, o que excede a intensidade necessária para a produção eficiente de microalgas. As vantagens desse tipo de abordagem são relacionadas principalmente ao fato de que a luz solar é livre, enquanto fontes de luz artificiais são onerosas (CHEN et al., 2013).

No entanto, as oscilações contínuas que a intensidade luminosa sofre ao longo do dia (fotoperíodo) são consideradas um fator limitante no uso da iluminação natural. O fotoperíodo é a quantidade de luz e escuro em um ciclo diário de 24 horas. No equador (latitude zero) o fotoperíodo é uma constante 12 horas de luz e 12 horas de escuro, mas,

sofre alterações em função da localização específica, condições meteorológicas, estação do ano e espectro solar (OGBONNA et al., 1999; JANSSEN et al., 2003).

A eficiência de sistemas de cultivo de microalgas pode ser mensurada através da produtividade ou da eficiência de conversão de energia luminosa em biomassa. Dentre os vários fatores que afetam a eficiência de fotobiorreatores, a energia luminosa é o substrato limitante do crescimento, uma vez que fornece toda a energia necessária para suportar seu metabolismo (HOLDMANN et al., 2019).

Por outro lado, as flutuações nos níveis de irradiação em sistemas de iluminação natural podem ser evitadas pela aplicação de iluminação artificial (KRZEMIŃSKA et al., 2014). O uso de iluminação contínua e controlada resulta em aumentos na produtividade do sistema. A exploração extensiva de luz artificial, no entanto, resulta em um aumento nos custos com eletricidade, aumentando consequentemente, os custos dos produtos finais (BLANKEN et al., 2013). Com o intuito de mitigar esse problema, diversas pesquisas têm sido desenvolvidas para utilizar ciclos de luz em cultivos microalgais. Além do apelo pela redução de custos com energia elétrica, a seleção de um fotoperíodo ideal pode melhorar significativamente o rendimento do processo e dos produtos nele gerado (ZHOU et al., 2015; XU et al., 2019). Tais fotoperíodos podem ser classificados em três principais grupos: os de longa duração, os de frequência e os de curta duração.

Os fotoperíodos de longa duração compreendem os períodos de luminosidade e escuro em uma proporção de horas. Os ciclos mais utilizados em cultivos microalgais são 24:0, 22:2, 16:8 e 12:12 (h:h), de claro:escuro. Nesta linha de trabalho, Jacob-Lopes et al. (2009) estudaram todos estes fotoperíodos no cultivo da cianobactéria *Aphanotece microscopia Nägelli* e verificaram que esta espécie conseguiu manter sua alta produtividade mesmo com fotoperíodo de 22:2 h de claro/escuro.

Já os fotoperíodos de frequência apresentam dois ou mais ciclos de claro/escuro por dia. Neste sentido Zhou et al. (2015) avaliaram cinco diferentes fotoperíodos de frequência: 2, 4, 8, 24 e 48 ciclos por dia. Estes autores verificaram que quanto maior o número de ciclos por dia, maior é a produtividade celular.

Por fim, os fotoperíodos de curta duração são assim denominados, pois abrangem os ciclos de claro/escuro em uma proporção de segundos ou milisegundos. Esse tipo de regime de luminosidade também é chamado de efeito flashing. Diversos estudos (JANSSEN et al., 1999; JANSSEN et al., 2001; JANSSEN et al., 2003) tem mostrado que esse tipo de iluminação favorece o crescimento de microalgas, podendo ter sua produtividade celular aumentada, quando comparada a sistemas com iluminação constante.

1.5 Metabolitos microalgais: lipídeos e pigmentos

As microalgas têm ganhado considerável atenção tanto de indústrias, quanto de pesquisadores em virtude de sua ampla variedade de aplicações. Através da fotossíntese, esses microrganismos têm a competência para usar água, energia luminosa e CO_2 para sintetizar a biomassa e metabólitos de interesse comercial, que podem ser usados como ingredientes alimentares, suplementos nutricionais, ração animal, combustíveis e outros produtos de valor agregado (RIZWAN et al., 2018; VENDRUSCOLO et al., 2019). Essas e outras aplicações são fundamentalmente suportadas pela composição química da biomassa microalgal (proteínas, lipídeos e pigmentos) além dos compostos extracelulares (carboidratos, lipídeos e compostos orgânicos voláteis) excretados pelas culturas (JACOB-LOPES et al., 2019). Sob o ponto de vista comercial, os metabólitos de maior interesse são os lipídeos e os pigmentos, principalmente em função do potencial para produção de bioenergia e da bioatividade dos ácidos graxos e dos carotenoides.

1.5.1 Lipídeos

Nas microalgas, os lipídeos desempenham papéis diferentes e podem ser classificados em lipídios de membrana (polares) e lipídeos de reserva (neutros e não polares). Lipídeos polares ou complexos incluem fosfolipídios e glicolipídios, os lipídios não-polares e neutros são aqueles que não contêm grupos carregados, o que inclui triacilgliceróis (TAGs), glicerídeos, esteróis e uma faixa limitada de hidrocarbonetos de alto peso molecular. Os triacilgliceróis são considerados produtos de armazenamento de energia, enquanto fosfolipídios e glicolipídios são estruturas lipídicas presentes na parede celular (MENEGAZZO & FONSECA, 2019). O teor lipídico em microalgas pode variar de 1 a 50 % do peso seco de sua biomassa, dependendo da espécie e condições de cultivo. Os lipídeos de origem microalgal, também conhecidos como óleos unicelulares podem ser usados como matéria-prima para biocombustíveis ou como ingrediente ou suplemento alimentar (SUN et al., 2019).

É consenso geral que limitar o consumo de combustíveis fósseis (carvão, gás natural e petróleo) tem sido uma exigência obrigatória do século XXI. Não apenas pelo esgotamento de suas fontes, mas também pelos impactos ambientais negativos por trás do uso massivo de tais combustíveis. Como resultado, foram desenvolvidas fontes alternativas sustentáveis e renováveis de energia, como os biocombustíveis da primeira, segunda, terceira e quarta geração. Ésteres metílicos de ácidos graxos, conhecidos como biodiesel,

são não-tóxicos, biodegradáveis e uma excelente alternativa ao diesel fóssil, uma vez que as propriedades de combustão desse biocombustível são semelhantes às do diesel à base de petróleo (SU et al., 2016). O óleo unicelular produzido por microalgas é considerado como uma das matérias-primas mais eficazes para a produção de biodiesel de terceira geração. As vantagens da produção de biodiesel a partir de microalgas incluem o rápido crescimento de culturas, alta produtividade de petróleo e baixa demanda de terras aráveis (DESHMUKH et al., 2019). Particularmente, espécies como *Chlorella* sp., *Nannochloropsis* sp. e *Scenedesmus* sp. são candidatos promissores para a produção do biocombustível devido as suas altas produtividades lipídicas e rápido crescimento (SUN et al., 2019).

Outros compostos produzidos por microalgas com grande potencial de exploração são os ácidos graxos ω-3 de cadeia longa, como linolênico, eicosapentaenoico (EPA) e docosaexaenoico (DHA) e ω-6, como linoleico, gama-linolênico (GLA) e araquidônico (ARA) (HU et al., 2019). A importância destes compostos baseia-se na incapacidade dos humanos para sintetizar alguns ácidos graxos, razão pela qual estes ácidos são chamados ácidos graxos essenciais. Estes compostos, especialmente ω-3 e ω-6 são determinantes para a integridade dos tecidos onde estão incorporados. O GLA encontra aplicações terapêuticas e na formulação de cosméticos, revitalizando a pele e, consequentemente, retardando o envelhecimento. Ácidos linoleico e linolênico são nutrientes essenciais para a síntese de prostaglandinas, o sistema imunológico e outros processos relacionados à regeneração tecidual. O ácido linoleico é também utilizado no tratamento de hiperplasias da pele em formulações tópicas. O DHA e o EPA estão associados à redução dos problemas associados a derrames cardiovasculares, artrite e hipertensão, e têm uma importante atividade hipolipidêmica, através da redução de triglicerídeos e aumento do colesterol da lipoproteína de alta densidade. Ácido DHA também atua no desenvolvimento e funcionamento do sistema nervoso. Os ácidos ARA e EPA apresentam ação agregadora e vasoconstritora de plaquetas e anti-agregantes e vasodilatadores no endotélio, além de ação quimiotática em neutrófilos (SAINI et al., 2018; JACOB-LOPES et al., 2019).

1.5.2 Pigmentos

Em termos de pigmentos, as microalgas podem sintetizar até três classes desses compostos (clorofilas, carotenoides e ficobiliproteínas). Os carotenoides são comuns em todos os gêneros de algas, enquanto que as ficobiliproteínas são encontradas apenas em cianobactérias. Quanto as clorofilas, já são reconhecidos cinco tipos: a, b, c (c_1, c_2), d e f,

sendo que a clorofila a é encontrada tanto em microalgas verdes quanto em cianobactérias, enquanto que a clorofila b não faz parte dos pigmentos das cianobactérias. Em 1996, pela primeira vez, a clorofila d foi identificada na cianobactéria *Acaryochloris marina* e, mais recentemente, em 2010, a clorofila f foi descoberta na cianobactéria *Halomicronema hongdchlores* (BOROWITZKA, 2018).

Entre os possíveis compostos que podem ser extraídos da biomassa de microalgas, os carotenoides e clorofilas são especialmente importantes devido à sua aplicação na saúde humana e como aditivo alimentar (GARCÍA-CAÑEDO, 2016). Além disso, esses pigmentos fotossintéticos são considerados excelentes biomarcadores quimiotaxonômicos para microalgas, devido à sua especificidade (PALIWAL et al., 2016).

Os carotenoides são pigmentos naturais lipofílicos amplamente distribuídos na natureza com uma estrutura de 40 átomos de carbono. A diversidade estrutural para os vários carotenoides é fornecida pela ciclização de uma ou ambas as extremidades, número e posição das duplas ligações conjugadas e oxigenação da cadeia principal (XAVIER & PÉREZ-GALVEZ, 2016). Até agora, cerca de 700 compostos já foram identificados e estão classificados em dois grandes grupos, baseados em seus grupos funcionais: xantofilas, contendo oxigênio como grupo funcional, os quais incluem luteína e zeaxantina; e carotenos, que são somente hidrocarbonetos, sem qualquer grupo funcional, β-caroteno e licopeno são exemplos de carotenos (HU et al., 2017). Nos organismos fotossintéticos, os carotenoides são pigmentos acessórios responsáveis pela captação de luz na fotossíntese e por proteger o aparelho fotossintético do excesso. Para os humanos, os carotenoides são essenciais como precursores da vitamina A. Além disso, os carotenoides têm um valor terapêutico importante, incluindo atividades anti-inflamatórias e anticancerígenas, que são amplamente atribuídas ao seu forte efeito antioxidante que é usado para proteger organismos contra o estresse oxidativo (SATHASIVAM et al., 2017).

Clorofilas são moléculas orgânicas complexas formadas por derivados da porfirina, uma estrutura macrocíclica, assimétrica, totalmente insaturada. Basicamente, estrutura está baseada num sistema tetrapirrólico, no qual os anéis de pirrol contendo quatro átomos de carbono (C) e um átomo de nitrogênio (N) formam um circuito conjugado fechado, coordenados com um átomo de magnésio (Mg) central. Esta estrutura também contém no C-17, uma cadeia de ácido propiônico esterificado com o fitol, um álcool diterpênico. Na fotossíntese, esses pigmentos são responsáveis pelas reações fotoquímicas e bioquímicas durante a absorção de luz. Os pigmentos de clorofila têm recebido atenção crescente devido aos seus potenciais benefícios para a saúde humana, que incluem atividade antineoplásica

(FERRUZI & BLAKESLEE, 2007; VESENICK et al., 2012), atividade antigenotóxica (NEGISHI et al., 1997), propriedades anti-inflamatórias (LARATO & PFAU, 1970; SUBRAMONIAM et al., 2012) e atividade antioxidante (FERNANDES et al., 2017). Além disso, a clorofila e seus derivados também tem sido proposta como corante natural em cosméticos, produtos farmacêuticos e embalagens de alimentos (FERREIRA & SANT'ANNA, 2017).

Embora os pigmentos fotossintéticos das microalgas tenham sido estudados, as informações detalhadas sobre o perfil desses pigmentos são limitadas a algumas espécies de microalgas.

CAPÍTULO 2

Capítulo: Microalgal Production Systems with Highlights of Bioenergy Production

Capítulo publicado no livro “Energy from Microalgae” (ISSN 1865-3529), publicado pela Springer Nature

Chapter 2
Microalgal Production Systems with Highlights of Bioenergy Production

Mariana Manzoni Maroneze and Maria Isabel Queiroz

Abstract The purpose of this chapter is to provide an overview of the main systems of microalgae production with highlights of biofuel production. The large-scale production systems (raceway ponds, horizontal tubular photobioreactors, and heterotrophic bioreactors) and small-scale photobioreactors (vertical and flat-plate photobioreactors) will be presented and discussed with a special emphasis on the main factors affecting its efficiency, biomass productivities reported in the literature, scaling-up, costs of construction and operation, and commercial applications. Besides this, the recent developments in microalgae cultivation systems will be reviewed in their main aspects. Finally, the criteria for selecting an appropriate bioreactor for microalgae cultivation will be presented, as well as the pros and cons of each system will be discussed in this chapter.

Keywords Photobioreactor · Heterotrophic bioreactor · Biomass Energy · Biofuel

1 Introduction

Historically microalgae have been of interest since 1942, when Harder and von Witsch (1942) suggested that microalgae could be viable sources of lipids to be used as food or to produce biofuels. Since then, an increasing amount of research involving microalgae and their bioproducts has been performed. Currently, these microorganisms are considered one of the most promising sources for bioenergy production (Chisti 2016; Chew et al. 2017; Raslavičius et al. 2018).

M. M. Maroneze
Department of Food Science and Technology, Federal University of Santa Maria (UFSM), Santa Maria, RS 97105-900, Brazil

M. I. Queiroz (✉)
School of Chemistry and Food, Federal University of Rio Grande (FURG), Rio Grande, RS 96201-900, Brazil
e-mail: queirozmariaisabel@gmail.com

E. Jacob-Lopes et al. (eds.), *Energy from Microalgae*, Green Energy and Technology, https://doi.org/10.1007/978-3-319-69093-3_2

Compared with conventional oil seeds, the biofuels produced from microalgae have several advantages that include the higher productivities, the ability to use nonarable land for microalgal cultivation and possibility to use wastewater and gas flue as source of nutrients and carbon to promote growth (Jacob-Lopes et al. 2014; Collotta et al. 2017). Microalgae also can produce different types of biofuels, such as biodiesel, bioethanol, biohydrogen, syngas, biobutanol, and bioelectricity (Chang et al. 2017; Su et al. 2017a, b). Unfortunately, until now, the majority of economic analyses conclude that microalgae biofuels cannot compete with conventional fuels (Lundquist et al. 2010; Sun et al. 2011). On the other hand, the concept of biorefinery can be explored with the aim to improve economic aspects. This is possible because of the wide variety of high-value compounds that microalgae can produce, such as carotenoids, proteins, long-chain polyunsaturated fatty acids, vitamins, and phycobilins (Chew et al. 2017).

Industrialization of microalgae products requires large-scale culture systems, which generally are raceway ponds, closed photobioreactors (PBRs), or heterotrophic bioreactors. Open systems are much cheaper and easier to operate than closed systems, however, have many operational problems, such as contamination, evaporation, susceptibility to weather conditions, and extensive land requirements. On the other hand, closed systems can eliminate these limitations, but with a high capital cost, difficulty in scaling-up, and high shear stress. However, due to the high operational control and the high productivity provided by the PBRs, researchers have been invested heavily in the development of new photobioreactors designs, in order to reduce these limitations, and thus make microalgae-based processes viable (Chang et al. 2017).

This chapter discusses the systems of microalgae production in large-scale (raceway ponds, horizontal tubular photobioreactors, and heterotrophic bioreactors) and small-scale (vertical tubular photobioreactors and flat-plate photobioreactors), with emphasis on major factors that influence their efficiency, biomass productivities, costs of biomass production, scaling-up, and commercial applications. Moreover, recent developments in microalgae cultivation systems are presented. Finally, the advantages and disadvantages of all microalgae production systems discussed are compared, and the criteria for selecting an appropriate PBR are presented.

2 Large-Scale Microalgae Biomass Production

2.1 Raceway Ponds

The raceway ponds were first developed in the 1950s for treating wastewater and, since the 1960s, outdoor open raceways have been used in commercial production of microalgae and cyanobacteria (Chisti 2016). Currently, it is the most utilized system for commercial microalgae production, accounting for more than 95% of

algae production worldwide, owing to their flexibility, low cost, and easy of scaling-up (Fernandez et al. 2013; Chang et al. 2017).

A raceway pond is a closed loop recirculation channel with a typical culture depth of about 0.25–0.30 m. The circulation mixes the nutrients, and cells are provided by the paddle wheels. The ponds are usually kept shallow because the algae need to be exposed to sunlight, and sunlight can only penetrate the pond water to a limited depth (Singh and Sharma 2012; Chang et al. 2017).

These ponds can be simply constructed in compacted soil with a 1- to 2-mm-thick plastic membrane. However, although it is cheaper, it is not commonly used for biomass production due to the high risk of contamination (Singh and Sharma 2012). To produce a biomass with high added value, the ponds are often made of concrete block walls and dividers lined with a plastic membrane to prevent seepage. Depending on the end use of the biomass, special care may be required to use liners that do not leach contaminating and inhibitory chemicals into the algal broth (Borowitzka 2005; Chisti 2016).

2.1.1 Major Factors Affecting the Raceway Pond Performance

Choice of Location

The choice of location of a raceway system has the greatest impact on biomass productivity. The factors to consider in the geographic location are average annual irradiance level, prevailing temperature, rainfall, land slope, potential nutrient sources, cost of the water, and land.

In terms of illumination, a minimum solar irradiation of 4.65 kWh/m^2/d is required to sustain high growth rates (Benemann et al. 1982). According to Chisti (2013), in an ideal condition, the temperature should be around 25 °C, with a minimum of diurnal and seasonal variations. A geographic location with rainfall not more than 1000 mm of rain per year facilitates the microalgae cultivation, since that can minimize the dilution of algae stock in the ponds (Bennett et al. 2014). In an ideal situation, the land slope should not be greater than 2% to avoid significant earthmoving costs during pond construction, but the US Department of Energy (DOE) cites a 5% maximum slope (DOE 2010; Bennett et al. 2014).

Other factor that depends on the local climate is the evaporation, which is influenced by the level of irradiance, the wind velocity, the air temperature, and the absolute humidity. An average freshwater evaporation rate of 10 L/m^2/d has been noted for some tropical regions. In this sense, freshwater needs to be added periodically to raceway to compensate the evaporation (Becker 1994; Chisti 2016).

Engineering Parameters

In raceways, the pond depth is one of the engineering parameters that has most influence on cultivation performance, because it is closely related to temperature

control, mixing, and light utilization efficiency. In general, the biomass productivity is higher in cultivations with lower depth raceways, but this also depends on the microalgae species used and the dimensions.

In raceway ponds, the mixing serves several purposes such as periodic exposure of cells to sunlight, keeping cells into suspension, availability of the nutrient to algal cells, and removal of photosynthetically generated oxygen. In this sense, an ideal mixing supply can increase productivity by nearly 10 times. Conventionally, the mixing is conventionally measured by the Reynolds number (Re), which in an ideal situation is about 257,000, considering a 1.5 m wide channel with a broth depth of 0.3 m and a culture velocity of 0.3 m/s (Chisti 2016).

Carbon Supply and pH

The carbon is the major constituent of microalgal cells, with approximately 50% of the cell mass. All carbon is photosynthetically assimilated from CO_2 and, this assimilation is closely related to the pH of the medium, since that, if CO_2 is consumed rapidly and not replenished, the pH becomes alkaline. In raceway ponds, generally, the pH is instable, because the CO_2 absorption from atmosphere through the surface of a raceway is insufficient to support the high photosynthesis rate for a good part of the day (Chisti 2013). An alkaline pH results in generation of toxic ammonia from dissolved ammonium salts, lowers the affinity of algae for CO_2, and increases the flexibility of mother cells, delaying completion of the cell cycle (Juneja et al. 2013). For this reason, to obtain better productivities in raceway, it is necessary to engineer a supply of CO_2.

Gas diffusers are used in raceways to inject CO_2 in the form of fine bubbles. According to Li et al. (2014), the CO_2 concentration greater than 73 μmol/L at a pH of 8.0 is optimal for the normal growth of microalgae. To produce high-value compounds, commercial pure carbon dioxide has been extensively used in microalgal cultures. However, this entails in additional economic costs and reduces the economic viability and sustainability of the process. It is estimated that the cost of the carbon source in microalgae production ranges from 8 to 27% of the daily production cost (Li et al. 2014). Furthermore, in this type of system, between 35 and 70% of the pure CO_2 injected into a pond is lost to the atmosphere. As an alternative, flue gas can be used, which also could contribute to the mitigation of environmental problems (de Godos et al. 2014).

Oxygen Accumulation

The photosynthesis reaction produces stoichiometrically 1.9 tons of oxygen to produce 1 ton of microalgal biomass. So, when there is intense microalgal growth, an excess of oxygen is generated. At high concentrations of O_2, the productivity of microalgae reduces considerably due to photorespiration and photoinhibition effects (Raso et al. 2012).

In raceway ponds, the only mechanism commonly used for removal of oxygen from the medium is the agitation by the paddle wheel and is not particularly effective. Even with high surface areas, the oxygen removal is insufficient during periods of maximum photosynthetic activity. At these photosynthesis peaks, the performance of the system can decrease up to 35% due to the excess dissolved oxygen in the medium, which can reach 300% of the air saturation value. Moreover, the biochemical composition of microalgae biomass can be influenced by the oxygen level in the pond (Richmond 1990; Chisti 2013).

Culture Contamination

As the raceway ponds are open to the environment, they are easily contaminated by bacteria, viruses, fungi, and other microalgae species and by predators. An alternative to control the contamination is to place the lakes inside greenhouses with controlled environmental conditions, but for the production of biofuels on a large scale, this is economically unfeasible.

However, it is known that not many contaminants can survive under extreme conditions. In this way, the contamination can be avoided by cultivating some highly resistant microalgal strains at high pH or high salinity. The species with the best performance in commercial cultivation in raceways includes *Chlorella* sp., *Spirulina* sp., and *Dunaliella* sp., which are cultivated under stringent conditions that inhibit the growth of other microorganisms or other species of microalgae (Chang et al. 2017).

2.1.2 Biomass Production in Raceway Ponds

Although biomass productivities of 0.40 g/L/d or higher have already been reported (Wen et al. 2016), values much lower than these are typically found, as shown in Table 1. The reported productivities are specific for the reactor designs, operating conditions, local weather conditions, and algae species. For this reason, the productivities obtained with a specific system cannot be simply extrapolated to other growth conditions. The biomass productivities in raceways are considered low, but generally are compensated by high product prices and low construction and operating costs.

2.1.3 Cost of Construction and Operation of Raceway Ponds

In terms of cost of construction, the plastic-lined earthen are the raceway ponds with the best cost-benefit, as unlined earth ponds are not generally considered satisfactory for producing algal biomass (Chisti 2013). According to Chisti (2016), the cost estimated to produce a 100-ha plastic-lined pond of compacted earth was about US$ 144,830 per ha in 2014. This cost data can be corrected for inflation and

Table 1 Biomass productivities of different open raceway ponds located in different countries

Microalgae	Location	Total volume (L)	Culture depth (cm)	Productivity (g/L/d)	References
Nannochloropsis salina	Arizona, USA	780	25.4	0.013	Crowe et al. (2012)
Spirulina (Arthrospira)	La Mancha, MX	2360–603	15–20	0.144–0.151	Olguín et al. (2003)
Scenedesmus rubescens	Florida, USA	900	20	0.020	Lin and Lin (2011)
Scenedesmus acutus	Arizona, USA	2300	7.5	0.066	Eustance et al. (2015)
Spirulina platensis	Málaga, ES	135,000	30	0.027	Jiménez et al. (2003)
Scenedesmus sp.	Almería, ES	20,000	20	0.170	de Godos et al. (2014)

thus provides a reasonable estimate of the current cost (Chisti 2013). In this way, the capital cost estimated for 2017 is of US$ 149,598 per ha. This estimate includes the earthworks, the plastic lining, the carbon dioxide supply tubing, inlets and outlets, the baffles, the paddle wheel, and motor.

To produce dry microalgae biomass in outdoor commercial raceway ponds, Nosker et al. (2011) and Chisti (2007) estimated a cost of € 4.95 and US$ 3.80 per kg of dry weight, respectively. According to Nosker et al. (2011), the factors which influence production costs are irradiation conditions, mixing, photosynthetic efficiency of systems, culture media, and carbon dioxide costs. Thus, by optimizing these factors, the production cost can reduce up to € 0.68 per kg.

2.1.4 Scaling-up in Raceway Ponds

The microalgae cultivation in open ponds is already a consolidated and widely practiced method for large-scale cultivation, since that are easily scaled up. There have been records of large-scale cultivation in raceways since 1987, where two 1000 m^2 raceway ponds were used as a test facility between 1987 and 1990 in New Mexico. These tests were conducted to verify the potential of microalgal biomass production for low-cost biodiesel production and were considered technically feasible (Rawat et al. 2013).

Although already a widely used technology, cultivations in raceway ponds still pose many challenges in terms of economic viability for large-scale biofuel production. This is mainly due to the low biomass productivity presented in these systems the need for extensive areas of land and substantial costs for harvesting (Scott et al. 2010).

2.1.5 Commercial Microalgae Cultivation in Raceway Ponds

The commercialization of biofuel from microalgae is still in its early gestation and has lot of challenges to achieve cost-competitive fuels. Currently, the industrial microalgae biomass production is restricted to high value.

Raceway ponds are under operation worldwide to produce a diverse range of products. For example, Cyanotech Corporation, in Hawaii, has cultivations in raceways of *Spirulina platensis* and *Haematococcus pluvialis*, to produce Spirulina Pacifica® and BioAstin® Natural Astaxanthin, respectively. Nikken Sohonsha Corporation (Japan) produces more than 40 different products (healthcare products, medical products, cosmetics, dietary supplements, fertilizers, and animal feeds) from microalgae as *Chlorella*, *Dunaliella*, *Monodus,* and *Isochlysis*. Tianjin Norland Biotech (China) cultivates *Spirulina*, *Chlorella,* and *H. pluvialis* to produce *Spirulina* tablets, *Chlorella* tablets, astaxanthin, astaxanthin oil, and phycocyanin.

However, it is important to point out that many companies are working with pilot plant tests for biofuels production. Examples of companies that are using open systems in their tests are the LiveFuels (USA), OriginOil Inc. (USA), PatroSun (USA), Neste Oil (FI), Ingrepo (NL), and Aquaflow Bionomics (NZ) (Su et al. 2017a, b).

2.2 Tubular Photobioreactor

Recently, closed PBRs, especially tubular photobioreactors have been successfully used for commercial microalgal biomass production. Unlike open raceways, tubular photobioreactors permit a good control of culture conditions and high solar radiation availability and, consequently, a high biomass productivity, which makes this type of system potential for biofuel production and compounds of high commercial value (Kunjapur and Eldridge 2010; Abomohra et al. 2016).

A tubular photobioreactor consists of an array of straight transparent tubes that are usually made of plastic or glass and have a diameter of 0.1 m or less. These transparent tubes can be arranged in different patterns (e.g., straight, bent, or spiral) and orientations (e.g., horizontal, inclined, vertical, or helical) in order to maximize the sunlight capture (Huang et al. 2017). However, to increase the scale, the tubes are usually arrayed in a horizontal fence-like, which improves the land utilization, and also have a better angle for incident light (Junying et al. 2013).

Besides the solar array for algae growth, a tubular photobioreactor is also composed of a harvesting unit to separate algae from the suspension, a degassing column for gas exchange and cooling (heating) and a circulation pump (Wang et al. 2012). The microalgal culture flows through solar collector tubing and is recirculated by maintaining highly turbulent flow, which is produced using either a mechanical pump or a gentler airlift pump (Abomohra et al. 2016; Chang et al. 2017).

This type of photobioreactor can be illuminated by artificial or natural light. The artificial illumination is technically possible, but expensive compared with outdoor cultivations, which is just viable for commercial production of high added value products.

2.2.1 Major Factors Affecting the Tubular Photobioreactor Performance

Light Supply

In autotrophic microalgae production, the light availability is the most important factor that influences the cell productivity and is one of the most difficult to control in outdoor cultures, due to the variation in solar radiation during the day and during the change of season (Fernandez et al. 1997).

In terms of design, the light capture is influenced by the transparency of the materials and the surface/volume ratio. The most common materials used for PBR construction are glass, plexiglass, polyvinyl chloride (PVC), acrylic-PVC, and polyethylene. All these materials have transparency suitable for the microalgae cultivations. However, they all have their pros and cons and need to be evaluated according to the type of process and desired product. Glass is strong and transparent and very good material for the construction of laboratory-*scale PBRs*. However, it requires many connection parts for the construction of large-scale PBRs, which could be costly. For this reason, the plastic type is most suitable for large-scale tubular photobioreactor, mainly of polyethylene (Wang et al. 2012).

Temperature

As already mentioned, the optimal temperature for microalgae cultures is generally around 25 °C, and most microalgae species can tolerate temperatures between 16 °C and 35 °C. In closed PBR, generally, the volume is small because a thin optical thick mixing ness is applied for the sake of light transfer. Therefore, variations in temperature during the day/night cycle and the seasons' changes have significant effects on microalgal cultivation. In this sense, it is necessary to set up a cost-effective cooling system (Huang et al. 2017).

Several methods have been tested to prevent overheating of the microalgae cultivation. Among them are as follows: (i) shading of the tubes with dark-colored sheets (Torzillo 1997), (ii) cooling of the culture by spraying water on the surface of the photobioreactor (Becker 1994), (iii) submerging part of the photobioreactor or the entire culture on a large body of water (Becker 1994), and (iv) installing a heat exchanger for the photobioreactor (Watanabe et al. 2011). However, shading the PBR is inefficient because it greatly reduces the illumination and consequently in the yield of biomass. Water spraying is efficient for cooling, but entails an increase in the cultivation costs. On the other hand, the method of submersion besides

efficient in the control of the temperature has been demonstrated to promote the average light intensity in the culture (Huang et al. 2017).

CO_2/O_2 Balance and Mixing

As explained in Sects. 2.1.1.3 and 2.1.1.4, the carbon dioxide and oxygen must be maintained in equilibrium and in moderate concentrations, since the excess of both causes damage to the cells. In this sense, the photobioreactor must contain a space for exhaust gases and an efficient mixing system, where promote turbulence and therefore mass transfer between the gas and liquid phases inside a photobioreactor (Wang et al. 2012).

In addition to its key role in the balance of gases and pH of the system, the mixing also is necessary to prevent sedimentation of algal cells, ensure that all cells of the population have uniform average exposure to light and nutrient and facilitate heat transfer and avoid thermal stratification. In tubular photobioreactor, the mixing is usually provided by aeration with CO_2-enriched gas bubbles or pumping, mechanical agitation, or a combination of these means. The choice depends on the scale of the system and the microalga species used, because some do not tolerate vigorous agitations (Suh and Lee 2003; Wang et al. 2012; Huang et al. 2017).

2.2.2 Biomass Productivity in Tubular Photobioreactor

The high biomass productivity is the greatest advantage of tubular photobioreactors, especially if compared to raceway ponds. Table 2 shows the biomass productivities in different tubular photobioreactors. The values range from 0.05 to 1.9 g/L/d. This variation is due to the type of geometric configuration used, microalgae species and operating and environmental conditions used in each study. If we compare these productivities values with those found in raceway ponds (Table 1), it is possible to see that except to the values found by Olaizola (2000), all the other productivities in tubular PRBs are greater than found in raceways.

2.2.3 Costs of Construction and Operation of Tubular Photobioreactors

The cost of PBRs has a major influence on production cost for large-scale biomass. The company AlgaeLink NV (Yerseke, The Netherlands) commercializes a horizontal serpentine PBR made of large-diameter transparent plastic tubes. For a system of 97 m^3, 1200 m^2 of occupied area, made of 2000 m long, 25 cm diameter PMMA tubes, according to Zitelli et al. (2013), the price was about € 194,000 in 2012. Through inflation calculation described in Chisti (2013), this price in 2017 is about € 202,798.

Table 2 Biomass productivities in tubular PBRs

Microalgae	Photobioreactor	Total volume (L)	Productivity (g/L/d)	References
Porphyridium cruentum	Airlift tubular	200	1.5	Camacho et al. (1999)
Phaeodactylon tricornutum	Airlift tubular	200	1.2	Fernández et al. (2001)
Phaeodactylon tricornutum	Airlift tubular	200	1.9	Grima et al. (2001)
Phaeodactylon tricornutum	Helical tubular	75	1.4	Ugwu et al. (2002)
Haematococcus pluvialis	Parallel tubular	25,000	0.05	Olaizola (2000)
Nannochloropsis gaditana	Fence-type tubular	340	0.59	San Pedro et al. (2014)

Norsker et al. (2011) calculated the cost for outdoor production of microalgae biomass in tubular photobioreactor and concluded that € 4.15 is the price for producing 1 kg of dry weight biomass, in a 100-ha plant. On the other hand, Grima (2009) found a cost of € 25 per kg of dry weight, in a horizontal tubular PBR of 4000 L. However, according to these authors, it is possible to reduce this cost up to € 0.5 per kg, through of process optimization.

2.2.4 Scaling-up

The scale-up of a tubular photobioreactor is not so simple in an open system, because it requires scaling-up of both the solar receiver and the airlift device. In principle, the volume of the solar receiver may be increased by increasing the diameter and the length of the tube. However, an increase in tube length can result in unacceptable concentrations of dissolved oxygen along the tubes. For this reason, in practice, only the tube diameter may be varied (Grima et al. 2001). Any change in tube diameter would imply a change in the light/dark cycle inside of photobioreactor. These cycles can improve the biomass productivity due to the ability of some species to store light energy to maintain their metabolism in the absence of light (Maroneze et al. 2016). Thus, the geometry of the PBR must be optimized according to the species used.

Grima et al. (2001) concluded that for *Phaeodactylum tricornutum,* the optimal photobioreactor (0.2 m^3) configuration and operations conditions were as follows: a solar receiver tube of 0.06 m diameter, 80 m long, connected to a 4 m tall airlift. Although not having a simple scaling-up, the tubular PBR is already quite widespread in large scale.

2.2.5 Commercial Applications of Horizontal Tubular PBRs

Currently, many biotech companies around the world are using tubular photobioreactors to produce microalgae biomass and several bioproducts. Among them are the Algaelink in the Netherlands that use horizontal and tubular photobioreactors for biomass and jet fuel production. The Heliae (USA) is using spiral tubular PBR to produce astaxanthin from *H. pluvialis.* In Cadiz, Spain, the Fitoplancton Marino SL uses a horizontal serpentine PBR cooled by immersion in a water pool to produce lyophilized microalgae biomass and slurries of several microalgae for aquaculture use (Torzillo et al. 2015; Chang et al. 2017).

2.3 Microalgal Heterotrophic Bioreactors

The heterotrophic bioreactors are a feasible alternative to overcome the light energy dependency that limits the scale-up and significantly complicates the design of photobioreactors (Vieira et al. 2012). Although restricted to a few microalgal species, the heterotrophic cultivation can be conducted in conventional reactor configurations such as stirred tank and bubble column reactors, which are relatively cheap, easily scalable, and generally present high kinetic performance (Queiroz et al. 2011; Perez-Garcia et al. 2011).

Moreover, to reduce the cost related to microalgae biofuel production, the organic carbon source and nutrients for the microalgae cultivation can be obtained from agro-industrial wastes (Queiroz et al. 2011; Francisco et al. 2015; Katiyar et al. 2017). In addition to meeting the demand for organic carbon, the use of wastewater in these cultivations also contributes to agro-industrial waste management (Maroneze et al. 2014).

On the other hand, the major limitations of these types of cultivation are the contamination and competition with other microorganisms that grow faster than the microalgae, inability to produce light-induced metabolites and inhibition of growth by excess organic substrate.

2.3.1 Major Factors Affecting Bioreactors in Heterotrophic Cultivations

Oxygen Supply

In aerobic bioprocesses, oxygen is a critical substrate for a cell metabolism that needs continuous supply, as it can easily become rate limiting due to its low solubility in water. According to Griffiths et al. (1960), independent of the organic substrate or the microalgae species, the biomass productivity is enhanced by higher levels of aeration.

In contrast, the aeration system energy requirement is a significant cost in bioreactors and also contributes to the carbon footprint of heterotrophic cultivations. So, for a viable biofuel production, a trade-off between the operating costs related to energy required for aeration and the productivity of the bioprocess (Santos et al. 2015). In this sense, Santos et al. (2015) concluded that for a heterotrophic bubble column bioreactor, the aeration of 0.5 VVM (volume of air per volume of medio per minute) is an equilibrium between kinetic performance and power requirements in bioreactor.

Mixing and Viscosity

Like in the cultivation systems already discussed, mixing is one of the most important operations in heterotrophic microalgal cultivation. This operation is necessary for uniformly distributing nutrients and for gas exchange. The adequate mixing can be provided by impellers and baffles or by aeration with airlift or bubble column systems (Perez-Garcia and Bashan 2015).

The viscosity of the medium is closely related to the mixing, where high viscosity in cultures requires higher impeller speed or airflow, which increases power consumption and operational costs. The viscosity comes mainly from the exogenous carbon source used, but is also increased with the high cell concentration and/or with the production of viscous cellular material.

2.3.2 Biomass Productivity in Heterotrophic Bioreactors

In terms of biomass production, the heterotrophic cultivations can present higher values of productivity, when compared to the other large-scale systems discussed in this chapter, as shown in Table 3, which summarizes the microalgal biomass productivities in heterotrophic cultivations with different carbon sources, bioreactors type, and microalgae species reported in the literature.

2.3.3 Costs in Heterotrophic Bioreactors

The production costs of the heterotrophic microalgae production depend on variables such as bioreactor, carbon source, microalgae strain, downstream processing operations, type and quality of the end product, among others. Tabernero et al. (2012) evaluated the production of microalgal biodiesel from *C. protothecoides* biomass grown heterotrophically. The cost estimated to produce one kilogram of biomass was US$ 1.29 per kg (corrected for 2017). This value was estimated for a biorefinery producing biomass in 465 continuously stirred bioreactors each of 150,000 L and producing 10 million/L/year of biodiesel.

A value below this (US$ 0.06/kg, corrected to 2017) was found by Roso et al. (2015) to produce *P. autumnale* biomass, in a techno-economic analysis of a

Table 3 Biomass microalgae productivity in heterotrophic cultivations

Microalgae	Bioreactor	Carbon source	Total volume (L)	Productivity (g/L/d)	References
Phormidium autumnale	Bubble column	Slaughterhouse wastewater	5	0.64	Roso et al. (2015)
Phormidium autumnale	Bubble column	Cassava starch	2	1.02	Francisco et al. (2014)
Phormidium autumnale	Bubble column	Cassava wastewater	2	6.68	Francisco et al. (2015)
Chlorella minutissima	Fermenter	Glycerol	7	0.44	Katiyar et al. (2017)
Chlorella protothecoides	Stirring tank	Glucose	5	7.40	Xiong et al. (2008)
Chlorella protothecoides	Fermenter	Cassava powder hydrolysate	5	7.66	Lu et al. (2010)
Chlorella pyrenoidosa	Stirred bioreactor	Food waste hydrolysate	2	3.45	Pleissner et al. (2013)
Aphanothece microscopica Nägeli	Bubble column	Fish processing wastewater	4.5	0.44	Queiroz et al. (2011)

simulated large-scale process to produce bulk oil and lipid-extracted algae in an agro-industrial biorefinery. These authors also found values of US$ 0.40/kg and US$ 0.07/kg (corrected to 2017) to produce bulk oil and lipid-extracted algae, respectively.

2.3.4 Scaling-up in Heterotrophic Bioreactors

Another differential of heterotrophic cultivation is the scaling-up relatively easy, and the bioreactors are available commercially for cultivation of several microorganisms with working volumes up to 100,000 L. Li et al. (2007) investigated the scale-up from 250 mL flasks to 11,000 L bioreactors of a heterotrophic cultivation with *C. protothecoides* to biodiesel production. The authors were successful in scaling-up and suggested that it is feasible to expand heterotrophic *Chlorella* cultivation for biodiesel production at the industry level.

According to Perez-Garcia and Bashan (2015), the practical aspects required for large-scale biofuel production from heterotrophic cultivation of microalgae are as follows: (i) the species must be robust and able to grow in the absence of light and under extreme conditions, such as high or low pH, high temperatures, or high salinity; (ii) the microalgae strain must also have a rapid growth to be able to compete with other heterotrophic microorganisms and thus avoid contamination; (iii) the exogenous carbon source must be inexpensive and easily found;

and (iv) the biofuel generated must present a quality standard required by the legislation and in quantity that makes the process economically viable.

2.3.5 Commercial Applications of Heterotrophic Bioreactors

The commercial production of microalgae via heterotrophic metabolism has been made by the Solazyme Inc., in Moema, São Paulo (Brazil). Solazyme's technology enables it to successfully convert a range of low-cost plant-based sugars into biofuels. The biofuels that this company has produced and tested are biodiesel (SoladieselBD®), renewable diesel (SoladieselRD®), aviation turbine fuel (Solajet™), and renewable jet fuel. Furthermore, Solazyme is producing renewable oils for the chemicals, nutrition and skin and personal care space utilizing today's existing industrial scale fermentation capacity.

3 Small-Scale Photobioreactors

3.1 Vertical Photobioreactors

Vertical reactors were among the first algal mass culture systems described in the literature (Cook 1950). These systems are compact, user-friendly bioreactors with a high ratio of surface area/volume, low contamination risk, and high biomass productivity. However, at present, these systems are not used as photobioreactors, except for investigational purposes, due to their difficult of scaling-up (Mirón et al. 1999).

Vertical photobioreactors consist of vertical tubes constructed with a transparent material (polyethylene or glass tubes) to allow the penetration of light. An air diffuser is located at the bottom of the reactor, where the sparged gas is converted into tiny bubbles. This sparging with gas mixture provides the constant agitation of the medium, mass transfer of CO_2 and also removes O_2 produced during photosynthesis. Based on their mode of liquid flow, vertical tubular photobioreactors can be divided into bubble column and airlift PBRs (Singh and Sharma 2012; Chang et al. 2017).

Bubble column photobioreactors are cylindrical vessel with height greater than twice the diameter, simply agitated by bubbling CO_2 and air from a sparger at the photobioreactor bottom without any special internal constructions and completely lack any moving parts (Singh and Sharma 2012; Koller 2015).

Airlift photobioreactors are cylindrical tubes with two interconnecting zones. One of the zones is called riser where gas mixture is sparged, whereas the other zone, the downcomer, does not receive the gas. The system can be with internal loop and external loop. In the first option, regions are separated either by a draft

tube or a split cylinder. On the other hand, in the external loop, riser and downcomer are separated physically by two different tubes.

3.1.1 Major Factors Affecting the Vertical PBRs Performance

Light Available

In vertical photobioreactors, the illumination is accomplished externally, which can be natural or artificial. The light available plays an essential role for the good performance of any photosynthetic culture. To obtain sufficient illumination, both the airlift and the bubble column photobioreactors cannot exceed about 0.2 m in diameter; otherwise, the light availability will be reduced severely, mainly in the center of cylinder. Additionally, it must also be considered that the height of the cylinder should not exceed 4 m due to structural reasons (Huang et al. 2017). Furthermore, in a vertical tubular photobioreactor, the light availability also is influenced by aeration rates, gas holdup, and superficial velocity (Mirón et al. 1999).

Aeration Rate, Gas Holdup, and Superficial Gas Velocity

As in horizontal photobioreactors, the agitation of the system gives only by pneumatic path, the aeration is responsible for culture mixing. In an ideal aeration rate, the microalgae are kept in suspension, the light/dark cycle is minimized, the CO_2 is diffused homogeneously, and its excess is removed, thus maintaining the pH stable and the produced oxygen is removed. In general, in airlift photobioreactors, the mixing is better than bubble column and thus can sustain better biomass production of different microalgae (Fernandes et al. 2014).

Gas holdup is one of the most important parameters characterizing airlift and tubular photobioreactors. It is necessary to the hydrodynamic design in different industrial processes because it governs gas phase residence time and gas–liquid mass transfer. The gas holdup is defined as the volume of the gas phase divided by the total volume. This parameter is influenced mainly by the superficial gas velocity and the type of gas diffuser (Mirón et al. 1999).

Superficial gas velocity is the ratio of the volumetric gas flow rate and cross-sectional area of the reactor. The photosynthetic efficiency of the culture is affected by the dark zone that may exist at the center of the photobioreactor. This dark zone is totally dependent on the gas superficial velocity, which is the ratio of the volumetric gas flow rate and cross-sectional area of the reactor. According to Janssen et al. (2003), high gas velocity (>0.05 m/s) is recommended for increasing the photosynthetic efficiency.

Table 4 Biomass productivity in vertical photobioreactors

Microalgae	Photobioreactor	Total volume (L)	Productivity (g/L/d)	References
Haematococcus pluvialis	Bubble column	55	0.06	López et al. (2006)
Chlorella ellipsoidea	Bubble column	6–200	0.03–0.04	Wang et al. (2014)
Anabaena sp.	Bubble column	9	0.31	López et al. (2009)
Aphanotece microscopica Nägueli	Bubble column	3	0.77	Jacob-Lopes et al. (2009)
Scenedesmus obliquus	Bubble column	2	0.21	Maroneze et al. (2016)
Chlorella sp.	Airlift	100	0.21	Xu et al. (2002)
Isochrysis galbana	Airlift	1	0.60	Hu and Richmond (1994)
Chlorella sp.	Airlift	4	0.37	Chiu et al. (2009)
Chlorella sp.	Airlift	1.6	0.25	Lal and Das (2016)

3.1.2 Biomass Productivity in Vertical PBR

Productivities of microalgal biomass in vertical photobioreactors vary with the type of mode of liquid flow, dimensions, microalgae species, and operating and environmental conditions implemented. The values of productivities in these systems of production reported in the literature vary between 0.031 and 0.77 g/L/d, as shown in Table 4.

3.1.3 Costs in Vertical Photobioreactors

According to Wang et al. (2014), for a 20 L indoor bubble column PBR, the cost of biomass production was about US$ 431.39 per kg. On the other hand, in a 200 L outdoor bubble column photobioreactor, the cost to produce 1 kg of dry weight biomass was US$ 58.69. The estimated cost by the methodology proposed by Chisti (2013) in 2017 for biomass production is of approximately US$ 445.58 and US$ 60.63 per kg of dry weight biomass in a 20 L indoor bubble column photobioreactor and a 200 L outdoor bubble column photobioreactor, respectively.

3.1.4 Scaling-up in Vertical Photobioreactors

The vertical tubular photobioreactors are limited to laboratory and pilot scales, which is attributed to fragility of the material, gas transfer at the top regions of the

system, temperature control, gas holdup, and a limited surface for illumination especially at up-scaled devices in case of algal species with high demands for illumination (Koller 2015). However, Mirón et al. (1999) affirm that such perceptions have never been substantiated and, according to their results, both bubble column and airlift photobioreactors are more suitable to scaling-up that horizontal PBRs.

A practical example of the difficulty of scale-up is the failure case of GreenFuel Technologies Corporation, at Arizona in 2007. Firstly, GreenFuel designs vertical inclined closed photobioreactors and installed pilot plant to recycle CO_2 emissions into microalgal biomass for biofuels production. With the success of the pilot plant, months later the company installed a photobioreactor at the same plant, but 100 times larger than its earlier test models. Due to incorrect scaling-up, the project of millions of dollars failed, its photobioreactors turned out to be twice as expensive as expected and the company had to fire nearly half its staff (Waltz 2009).

3.2 Flat-Plate Photobioreactors

Flat-plate photobioreactors have received much attention for microalgae biomass production due to their large illumination surface area (Ugwu et al. 2008). In this type of photobioreactor, a thin layer of culture is passed across a flat panel made of a transparent material, as glass, plexiglass, or polycarbonate (Faried et al. 2017). They can be oriented at different angles so as to modify the light intensity and use diffused and reflected light. Agitation can be provided either by bubbling air from its one side through perforated tube or by rotating it mechanically using a motor (Chang et al. 2017).

Flat-panel photobioreactors feature important advantages for biomass production of photoautotrophic microorganisms and may become a standard reactor type for the mass production of several algal species (Sierra et al. 2008). However, the capital and operational cost of such systems are still too high to produce microalgae biomass as feedstock for biofuels or other low-value products with currently available technologies (Li et al. 2014).

The construction of flat-plate reactors dates back to the early 1950s (Burlew 1953), since then, many different designs have been developed. Tredici and collaborators developed a rigid alveolar panel photobioreactor (Tredici et al. 1991; Tredici and Materassi 1992). Pulz and Scheibenbogen (1998) proposed a flat-plate PBR inner walls arranged to promote an ordered horizontal culture flow that was forced by a mechanical pump. Recently, Li et al. (2014) developed a flat-panel photobioreactor with internal bulk liquid flow and an external airlift with the purpose of developing a scalable industrial photobioreactor.

3.2.1 Major Factors Affecting the Flat-Plate Photobioreactor Performance

Light Supply

The flat-plate photobioreactors can be illuminated artificially or through sunlight. However, as the use of sunlight is much more economically feasible, and these systems have an excellent setting to capture sunlight, this is the most commonly used option.

The light absorption is totally dependent on the length of light path. In general, the biomass productivity is highest at the smallest light path and smallest at the longest light path PBR (Richmond and Cheng-Wu 2001). Other configuration that has an influence on light capture is the tilt angle of flat-plate photobioreactor. Throughout the year, the optimal tilt of the PBR that allows maximal incident light will change due to the position of the sun (Wang et al. 2012). Hu et al. (1998) described that as a general rule, the optimal angle for year-round biomass production is equal to the geographic latitude of the location.

Gas Balance and Mixing

A great advantage of flat-panel reactors is that they have a much shorter oxygen path than tubular reactors, so the accumulation of dissolved oxygen is low (Sierra et al. 2008; Chang et al. 2017). According to Sierra et al. (2008), in a flat-panel photobioreactor, an aeration of 0.25 VVM (volume of air per volume of liquid per minute) and a power supply of 53 W/m^3 are sufficient to maintain the balance of gases, mixing is ideally suited for most microalgal culture. Other authors reported even much higher aeration rates up to 2.0 VVM with positive effects (Alias et al. 2004; Wang et al. 2005).

Temperature

Microalgae cultivations in outdoor PBRs are exposed to seasonal and diurnal variation of temperature. These variations have a direct influence on the cellular growth and the chemical composition of the biomass, and therefore, for the development of an efficient and controlled process, the temperature must be maintained with the least possible variation.

Particularly, flat-plate photobioreactors are very susceptible to overheating due to its thin layer of cultivation and high light exposure. For this reason, the PBRs must have an efficient temperature control system. This control is usually done by water spraying (evaporative cooling) or alternatively, by using internal heat exchangers (Chang et al. 2017).

Table 5 Biomass productivities in flat-plate photobioreactor

Microalgae	Photobioreactor	Total volume (L)	Productivity (g/L/d)	References
Nannochloropsis sp.	Flat-plate	440	0.27	Cheng-Wu et al. (2001)
Spirulina platensis	Flat-plate inclined	6–50	0.3–4.3	Hu et al. (1996)
Chlorella vulgaris	Flat-plate airlift	30	0.16–0.95	Munkel et al. (2013)
Thermosynechococcus elongatus	Flat-plate airlift	10	2.9	Bergmann and Trösch (2016)
Nannochloropsis oculata	Short-light path flat-plate	–	12	Cuaresma et al. (2009)
Chlorella sorokiniana	Short-light path flat-plate	1	2.9–14.8	Tuantet et al. (2014)

3.2.2 Biomass Productivity in Flat-Plate Photobioreactor

Some values of biomass productivity reported in the literature are shown in Table 5, which range from 0.16–4.3 g/L/d. These values vary according to the species and parameters used for photobioreactor construction and cultivation. Due to the large light exposure surface area, high biomass productivity is found in these systems, however, are still limited to laboratory scale and pilot scale.

3.2.3 Costs in Flat-Plate PBRs

Tredici et al. (2016) evaluated the production cost of the microalga *Tetraselmis suecica* in a 1-ha plant made of "Green Wall Panel-II" (GWP®-II) photobioreactors located in Tuscany-Italy. The GWP® is flat disposable photobioreactor, designed and patented in 2004 and commercialized by Fotosintetica & Microbiologica S.r.l. Through a techno-economic analysis, they conclude that, for a 1-ha, the total capital investment is about € 1,661,777 and the total fixed capital per annum is of € 101,260. Also in this analysis, they found a cost of € 12.4 to produce 1 kg of biomass (dry weight). This cost can be reduced when the plant is installed in a region with more favorable climatic conditions. The authors related that in Tunisia, the cost of biomass production is of € 6.2 kg/in a 1-ha plant with the same PBR. Lower production costs (€ 5.96/kg) in a vertical flat-panel photobioreactor of commercial scale were found by Norsker et al. (2011), but if we update this value by calculating the inflation correction described in Chisti (2013), this value is of about € 6.36/kg.

3.2.4 Scaling-up in Flat-Plate Photobioreactors

The scale-up in flat-plate photobioreactors presents some challenges, which are usually caused by the large surface area of the photobioreactor. This type of design requires many modules and supports materials, shows difficulty in controlling culture temperature and is very susceptible to the fouling, which is the phenomena that occur when cells attach to the plastic walls, causing a reduction in light availability and an increased risk of contamination (Carvalho et al. 2014; Chang et al. 2017).

Despite the limitations, several commercial large-scale flat-plate photobioreactors have been developed. One example is the Green Wall Panel (GWP®) that has a concept of 'disposable panels' for large-scale applications. This system commercialized by Fotosintetica & Microbiologica S.r.l consists of vertical PBRs of 100-litre bags, made of a polyethylene foil enclosed in a rigid framework (Tredici et al. 2016). Other systems available commercially are the flat-plate airlift patented and produced by Subitec GmbH, in Germany. In this case, the photobioreactors are produced on scales varying from 6 to 180 L per unit.

4 Recent Developments in Microalgae Cultivation Systems

Recently, biofilm cultivation of microalgae emerged as a new biomass production strategy. These systems consist of a densely packed layer of microalgae that grow attached to a solid surface, which should be illuminated and should be frequently exposed to water containing nutrients. Among the advantages of the biofilm-based microalgae cultivation are the cost reduction related to microalgae harvesting, reduced light limitation, low footprint, low water consumption, and efficient CO_2 mass transfer. In contrast, the limitations of the system are the formation of gradients over the biofilm for pH, nutrients, and light (Gross et al. 2015; Hoh et al. 2015).

Another photobioreactor configuration that has attracted attention in recent years is the membrane photobioreactor, mainly for the cultivation of microalgae using wastewater. The membrane photobioreactor is a technology that integrates a conventional enclosed PBR with a submerged or side-stream membrane filtration process using microfiltration or ultrafiltration membranes for solid–liquid separation. These systems can operate in continuous mode, which increases the microalgal biomass production, they produce a high quality treated effluent with low levels of organic substances, pathogen, and suspended solids and are easy to operate and scale-up. However, only limited studies exist about these techniques and for a large-scale implementation, techno-economic analyses and environmental performance assessment are required to assess their viability (Billad et al. 2015; Luo et al. 2016).

Finally, hybrid photobioreactors have proved to be a promising technology for the mass production of microalgae compared with single PBRs. Hybrid photobioreactors are systems that combine different growth stages in two types of PBRs,

Table 6 Biomass productivities in emergent photobioreactors

Microalgae	Photobioreactor	Total volume (L)	Productivity (g/L/d)	References
Chlorella vulgaris	Biofilm photobioreactor	20.3	0.015	Tao et al. (2017)
Chlorella vulgaris	Biofilm photobioreactor	0.6–0.7	7.07	Pruvost et al. (2017)
Chlorella vulgaris	Membrane photobioreactor	25	0.06	Marbella et al. (2014)
Chlorella vulgaris	Membrane photobioreactor	10	0.04	Gao et al. (2014)
Chlorella vulgaris	Hybrid photobioreactor	1	0.05	Heidari et al. (2016)
Chlorella vulgaris	Hybrid photobioreactor	1.5	0.66	Jacob-Lopes et al. (2014)

closed and open, in which the disadvantage of one PBR is complemented by the other (Brennan and Owende 2010). These configurations aim to compensate the drawbacks caused by the limitation of surface/volume ratio and scale-up of open and closed conventional photobioreactors. These systems are based on a proper height/diameter ratio, generating configurations of reactors with heavy workloads in contrast to very long tubes or shallow ponds. The main advantages of these photobioreactors include low use of land area with high culture volume, low operating costs and are potential to scaling-up. On the other hand, this type of configuration is limited to the cultivation of microalgae species with the ability to store energy to sustain cell growth for periods in the dark, without affecting the rate of photosynthetic metabolism (Ramírez-Mérida et al. 2017).

The biomass productivities found in microalgae cultivation with these photobioreactors are shown in Table 6. All these systems are relatively new, and therefore, only a limited number of studies are found in the literature and are restricted to laboratory scale.

5 Criteria for the Selection of Microalgae Cultivation System

According to Chang et al. (2017), the main criteria to be considered in the choice of an ideal photobioreactor are as follows: (i) type and quality of the target product; (ii) tolerance of microalgal strains; and (iii) scale and performance versus cost.

The first criterion to be considered is the type and quality of the desired product. For the biofuel production, it is essential to produce a biomass rich in lipid or carbohydrate with a low cost to be competitive with conventional fossil fuels. In this case, a heterotrophic bioreactor integrated into a biorefinery system can be a good choice due to the high productivity, low cost, and low-land demand.

Additionally, these systems can operate in parallel in wastewater treatment, when they are used as a source of carbon and nutrients for algal growing. On the other hand, to produce light-induced metabolites and high-value products intended for human consumption, a closed PBR is more advisable (Li et al. 2014; Chang et al. 2017).

The characteristics of the microalgae strain that will be used must also be considered at the moment of the choice. Mainly in terms of adaptability and tolerance under outdoor conditions and shear forces and oxygen buildup generated by PBRs. In open ponds, strains must be able to compete with other microorganisms for nutrients and must have the ability to tolerate photoperiods and climate changes. In the case of closed photobioreactors, the strains must withstand strong shear forces generated by pumping or aeration and must be able to tolerate a possible excess of oxygen in the system (Brennan and Owende 2010; Chang et al. 2017).

When a biofuel is the target product, the most important issue is the cost of the biomass which will be processed to yield the fuel. For this, the systems must present a high kinetic performance at large-scale production. It is known that closed systems are significantly more efficient in biomass production compared with open systems. At the same time, most closed systems have a difficult and expensive scaling-up, and open systems can be scaled up easily and inexpensively to accommodate larger production rates. So, the choice of cultivation system must be based on the best trade-off between biomass productivity and production cost (Chang et al. 2017).

Table 7 Advantages and limitations of microalgae cultivation systems

Cultivation type	Cultivation system	Advantages	Limitations
Commercial			
	Raceway ponds	– Low investment – Low power consumption – Economical – Easy to clean – Easy maintenance	– Require large area of land – Cultures are easily contaminated – Low productivity – Limited to a few microalgal strains – Little control of culture conditions – Evaporation – Small illumination surface area
	Horizontal tubular photobioreactors	– High productivity – Large illumination surface area – Suitable for outdoor cultures – Relatively cheap	– Large land area demand – Poor mass transfer – Photoinhibition

(continued)

Table 7 (continued)

Cultivation type	Cultivation system	Advantages	Limitations
Lab-scale			
	Vertical photobioreactors	– High mass transfer – Good mixing – Potential for scalability – Easy to sterilize – Least land use – Reduced photoinhibition	– Small illumination area – Sophisticated construction materials – Support costs – Modest scalability
	Flat-plate photobioreactors	– High biomass productivity – Large illumination surface area – Suitable for outdoor cultures – Uniform distribution of light – Low power consumption	– Difficult to scale up – Difficult temperature control – Fouling – Photoinhibition – Shear damage from aeration
	Heterotrophic bioreactor	– High productivity	– Limited to a few microalgal strains
		– Low cost	– Susceptibility to contamination
		– Wastewater treatment	
		– Easy scaling-up	
Emergent			
	Biofilm photobioreactors	– Low cost of microalgae harvesting – Reduced light limitation – Low footprint – Low water consumption – Efficient CO_2 mass transfer	– Formation of gradients – Scaling-up
	Membrane photobioreactors	– High biomass productivity – High-quality treated effluent – Easy to operate	– Limited studies – Cost
	Hybrid photobioreactors	– Low use of land area – Low operating costs – High stability	– Limited to a few microalgal strains

In addition to considering all these factors, it is important to know all the advantages and limitations of each microalgae cultivation system. In this sense, Table 7 shows the pros and cons of all the systems presented in this chapter.

6 Final Considerations

The biofuels production from microalgae has been demonstrated to have broad potential of application, but these currently still remain at the exploratory stage. This chapter underlines several aspects involved in the microalgal production systems in order to help the development of biofuels from microalgae. Despite that a great deal of work has been done to develop systems for microalgae production, to date, there is no system without limitations. The main difficulties are related to the cost of construction and operation, scaling-up, contamination, and to a limited knowledge about the new cultivation systems. Therefore, to choose a system, trade-offs among productivity, costs, scaling-up, and value of final product should be carefully made.

References

Abomohra, A., Jin, W., Tu, R., Han, S., Eid, M., & Eladel, H. (2016). Microalgal biomass production as a sustainable feedstock for biodiesel: Current status and perspectives. *Renewable and Sustainable Energy Reviews, 64,* 596–606.

Alias, C. B., Lopez, M. C. G. M., Fernández, F. G. A., Sevilla, J. M. G., Sanchez, J. L. G., & Grima, E. M. (2004). Influence of power supply in the feasibility of *Phaeodactylum tricornutum* cultures. *Biotechnology and Bioengineering, 87,* 723–733.

Becker, E. W. (1994). *Microalgae-biotechnology and microbiology* (1st ed.). Cambridge: Cambridge University Press.

Benemann, J. R., Goebel, R. P., Augenstein, D. C., & Weissman, J. C. (1982). *Microalgae as a source of liquid fuels*. Final technical Report to U.S. DOE BER, viewed August 24, 2016, <https://www.osti.gov/scitech/biblio/6374113>.

Bennett, M. C., Turn, S. Q., & Chan, W. Y. (2014). A methodology to assess open pond, phototrophic, algae production potential: A Hawaii case study. *Biomass and Bioenergy, 66*, 168–75.

Bergmann, P., & Trösch, W. (2016). Repeated fed-batch cultivation of *Thermosynechococcus elongatus* BP-1 in flat-panel airlift photobioreactors with static mixers for improved light utilization: Influence of nitrate, carbon supply and photobioreactor design. *Algal Research, 17,* 79–86.

Billad, M. R., Arafat, H. A., & Vankelecom, I. F. J. (2015). Membrane technology in microalgae cultivation and harvesting: A review. *Biotechnology Advances, 32,* 1283–1300.

Borowitzka, M. A. (2005). Culturing microalgae in outdoor ponds. In R. A. Andersen (Ed.), *Algal culturing techniques* (pp. 205–218). Amsterdam: Elsevier Academic Press.

Brennan, L., & Owende, P. (2010). Biofuels from microalgae: A review of technologies for production, processing, and extractions of biofuels and co products. *Renewable and Sustainable Energy Reviews, 14,* 557–577.

Burlew, J. S. (1953). *Algal culture: From laboratory to pilot plant* (1st ed.). Washington: Carnegie Institution of Washington.

Camacho, R. F., Fernández, F. G. A., Pérez, J. A. S., Camacho, F. G., & Grima, E. M. (1999). Prediction of dissolved oxygen and carbon dioxide concentration profiles in tubular photobioreactors for microalgal culture. *Biotechnology and Bioengineering, 62,* 71–86.

Carvalho, J. C. M., Matsudo, M. C., Bezerra, R. P., Ferreira-Camargo, L. S., & Sato, S. (2014). Microalgae bioreactors. In R. Bajpai, A. Prokop, & M. Zappi (Eds.), *Algal biorefineries* (Vol. 1, pp. 83–126). Switzerland: Springer International Publishing.

Chang, J. S., Show, P. L., Ling, T. C., Chen, C. Y., Ho, S. H., Tan, C. H., et al. (2017). Photobioreactors. In C. Larroche, M. Sanroman, G. Du, & A. Pandey (Eds.), *Current developments in biotechnology and bioengineering: Bioprocesses, bioreactors and controls* (pp. 313–352). Atlanta: Elsevier.

Cheng-Wu, Z., Zmora, O., Kopel, R., & Richmond, A. (2001). An industrialsize flat glass reactor for mass production of *Nannochloropsis* sp. (*Eustigmatophyceae*). *Aquaculture, 195,* 35–49.

Chew, K. W., Yap, J. Y., Show, P. L., Suan, N. H., Juan, J. C., Ling, T. C., et al. (2017). Microalgae biorefinery: High value products perspectives. *Bioresource Technology, 229,* 53–62.

Chisti, Y. (2007). Biodiesel from microalgae. *Biotechnology Advances, 25,* 294–306.

Chisti, Y. (2013). Raceways-based production of algal crude oil In C. Posten & C. Walter (Eds.), *Microalgal biotechnology: Potential and production* (pp. 197–216). Berlin: de Gruyter.

Chisti, Y. (2016). Large-scale production of algal biomass: Raceway ponds. In F. Bux & Y. Chisti (Eds.), *Algae biotechnology: Products and processes* (pp. 21–40). New York: Springer.

Chiu, S. Y., Tsai, M. T., Kao, C. Y., Ong, S. C., & Lin, C. S. (2009). The air-lift photobioreactors with flow patterning for high-density cultures of microalgae and carbon dioxide removal. *Engineering in Life Sciences, 9,* 254–260.

Collotta, M., Champagne, P., Busi, L., & Alberti, M. (2017). Comparative LCA of flocculation for the harvesting of microalgae for biofuels production. *Procedia CIRP, 61,* 756760.

Cook, P. M. (1950). *Some problems in the large-scale culture of Chlorella* (pp. 53–75). Yellow Springs, OH: The Culture Foundation.

Crowe, B., Attalah, S., Agrawal, S., Waller, P., Ryan, R., Van Wagenen, J., et al. (2012). A comparison of *Nannochloropsis salina* growth performance in two outdoor pond designs: Conventional raceways versus the arid pond with superior temperature management. *International Journal of Chemical Engineering and Applications, 2012*, 9–21.

Cuaresma, M., Janssen, M., Vílchez, C., & Wijffels, R. H. (2009). Productivity of *Chlorella sorokiniana* in a short light-path (SLP) panel photobioreactor under high irradiance. *Biotechnology and Bioengineering, 104,* 352–359.

de Godos, I., Mendoza, J. L., Acién, F. G., Molina, E., Banks, C. J., Heaven, S., et al. (2014). Evaluation of carbon dioxide mass transfer in raceway reactors for microalgae culture using flue gases. *Bioresource Technology, 153,* 307–314.

Department of Energy (DOE). (2010). National algal biofuels technology roadmap, viewed August 24, 2016, <https://www1.eere.energy.gov/bioenergy/pdfs/algal_biofuels_roadmap.pdf>.

Eustance, E., Badvipour, S., Wray, J. T., & Sommerfeld, M. R. (2015). Biomass productivity of two Scenedesmus strains cultivated semi-continuously in outdoor raceway ponds and flat-panel photobioreactors. *Journal of Applied Phycology, 28,* 1471–1483.

Faried, M., Samer, M., Abdelsalam, E., Yousef, R. S., Attia, Y. A., & Ali, A. S. (2017). Biodiesel production from microalgae: Processes, technologies and recent advancements. *Renewable and Sustainable Energy Reviews, 79,* 893–913.

Fernandes, B. D., Mota, A., Ferreira, A., Dragone, D., Teixeira, J. A., & Vicente, A. A. (2014). Characterization of split cylinder airlift photobioreactors for efficient microalgae cultivation. *Chemical Engineering Science, 117,* 445–454.

Fernandez, F. G. A., Camacho, A. C., Pérez, J. A. S., Sevilla, J. M. F., & Grima, E. M. (1997). A model for light distribution and average solar irradiance inside outdoor tubular photobioreactors for the microalgal mass culture. *Biotechnology and Bioengineering, 55,* 701–714.

Fernandez, F. G. A., Sevilla, J. M. F., & Grima, E. M. (2013). Photobioreactors for the production of microalgae. *Reviews in Environmental Science and Bio/Technology, 12,* 131–151.

Fernández, F. G. A., Sevilla, J. M. F., Pérez, J. A. S., Grima, E. M., & Chisti, Y. (2001). Airlift-driven external-loop tubular photobioreactors for outdoor production of microalgae: Assessment of design and performance. *Chemical Engineering Science, 56,* 2721–2732.

Francisco, E. C., Franco, T. T., Wagner, R., & Jacob-Lopes, E. (2014). Assessment of different carbohydrates as exogenous carbon source in cultivation of cyanobacteria. *Bioprocess and Biosystems Engineering, 37*, 1497–505.

Francisco, E. C., Franco, T. T., Zepka, L. Q., & Jacob-Lopes, E. (2015). From waste-to-energy: The process integration and intensification for bulk oil and biodiesel production by microalgae. *Journal of Environmental Chemical Engineering, 3,* 482–487.

Gao, F., Yang, Z. H., Li, C., Wang, Y. J., Jin, W. H., & Deng, Y. B. (2014). Concentrated microalgae cultivation in treated sewage by membrane photobioreactor operated in batch flow mode. *Bioresource Technology, 167,* 441–446.

Griffiths, D. J., Thresher, C. L., & Street, H. E. (1960). The heterotrophic nutrition of *Chlorella vulgaris* (brannon no. 1 strain). *Annals of Botany, 24,* 1–11.

Grima, E. M. (2009). Algae biomass in Spain: A case study. In *First European Algae Biomass Association Conference & General Assembly*, Florence.

Grima, E. M., Fernández, J., Acién, F. G., & Chisti, Y. (2001). Tubular photobioreactor design for algal cultures. *Journal of Biotechnology, 92,* 113–131.

Gross, M., Jarboe, D., & Wen, Z. (2015). Biofilm-based algal cultivation systems. *Applied Microbiology and Biotechnology, 99,* 5781–5789.

Harder, R., & von Witsch, H. (1942). Ueber Massenkultur von Diatomeen. *Ber. Dtsch. Bot. Ges., 60,* 14–153.

Heidari, M., Kariminia, H. R., & Shayegan, J. (2016). Effect of culture age and initial inoculum size on lipid accumulation and productivity in a hybrid cultivation system of *Chlorella vulgaris*. *Process Safety and Environmental Protection, 104,* 111–122.

Hoh, D., Watson, S., & Kan, E. (2015). Algal biofilm reactors for integrated wastewater treatment and biofuel production: A review. *Chemical Engineering Journal, 287,* 466–473.

Hu, Q., Fairman, D., & Richmond, A. (1998). Optimal tilt angles of enclosed reactors for growing photoautotrophic microorganisms outdoors. *Journal of Fermentation and Bioengineering, 85,* 230–236.

Hu, Q., Guterman, H., & Richmond, A. (1996). A flat inclined modular photobioreactor for outdoor mass cultivation of photoautotrophs. *Biotechnology and Bioengineering, 51,* 51–60.

Hu, Q., & Richmond, A. (1994). Optimizing the population density in *Isochrysis galbana* grown outdoors in a glass column photobioreactor. *Journal of Applied Phycology, 6,* 391–396.

Huang, Q., Jiang, F., Wang, L., & Yang, C. (2017). Design of photobioreactors for mass cultivation of photosynthetic organisms. *Engineering, 3,* 318–329.

Jacob-Lopes, E., Scoparo, C. H. G., Lacerda, L. M. C. F., & Franco, T. T. (2009). Effect of light cycles (night/day) on CO_2 fixation and biomass production by microalgae in photobioreactors. *Chemical Engineering and Processing: Process Intensification, 48,* 306–310.

Jacob-Lopes, E., Zepka, L. Q., Merida, L. G. R., Maroneze, M. M., & Neves, C. (2014). Bioprocesso de conversão de dióxido de carbono de emissões industriais, bioprodutos, seus usos e fotobiorreator híbrido. BR n. PI2014000333.

Janssen, M., Tramper, J., Mur, L., & Wijffels, R. H. (2003). Enclosed outdoor photobioreactors: Light regime, photosynthetic efficiency, scale-up, and future prospects. *Biotechnology and Bioengineering, 81,* 193–210.

Jiménez, C., Cossío. B. R., & Niell, F. X. (2003). Relationship between physicochemical variables and productivity in open ponds for the production of *Spirulina*: A predictive model of algal yield. *Aquaculture, 221*, 331–45.

Juneja, A., Ceballos, R. M., & Murthy, G. S. (2013). Effects of environmental factors and nutrient availability on the biochemical composition of algae for biofuels production: A review. *Enegies, 6,* 4607–4638.

Junying, Z., Junfeng, R., & Baoning, Z. (2013). Factors in mass cultivation of microalgae for biodiesel. *Chinese Journal of Catalysis, 34,* 80–100.

Katiyar, R., Gurjar, B. R., Bharti, R. Q., Kumar, A., Biswas, S., & Pruthi, V. (2017). Heterotrophic cultivation of microalgae in photobioreactor using low cost crude glycerol for enhanced biodiesel production. *Renewable Energy, 113,* 1359–1365.

Koller, M. (2015). Design of closed photobioreactors for algal cultivation. In A. Prokop, R. K. Bajpai, & M. E. Zappi (Eds.), *Algal biorefineries volume 2: Products and refinery design* (pp. 139–186). Switzerland: Springer International Publishing.

Kunjapur, A. M., & Eldridge, R. B. (2010). Photobioreactor design for commercial biofuel production from microalgae. *Industrial and Engineering Chemistry Research, 49,* 3516–3526.

Lal, A., & Das, D. (2016). Biomass production and identification of suitable harvesting technique for *Chlorella* sp. MJ 11/11 and *Synechocystis* PCC 6803. *3 Biotech, 6,* 41–51.

Li, J., Stamato, M., Velliou, E., Jeffryes, C., & Agathos, S. N. (2014). Design and characterization of a scalable airlift flat panel photobioreactor for microalgae cultivation. *Journal of Applied Phycology, 27,* 75–86.

Li, X., Xu, H., & Wu, Q. (2007). Large-scale biodiesel production from microalga *Chlorella protothecoides* through heterotrophic cultivation in bioreactors. *Biotechnology and Bioengineering, 98,* 764–771.

Lin, Q., & Lin, J. (2011). Effects of nitrogen source and concentration on biomass and oil production of a *Scenedesmus rubescens* like microalga. *Bioresource Technology, 102,* 1615–1621.

Lopez, M. C. G., Del Rio Sanchez, E., Lopez, J. L. C., Fernandez, F. G. A., Sevilla, J. M. F., Rivas, J., et al. (2006). Comparative analysis of the outdoor culture of *Haematococcus pluvialis* in tubular and bubble column photobioreactors. *Journal of Biotechnology, 123*, 329–42.

López, C. V. G., Fernández, F. G. A., Sevilla, J. M. F., Fernández, J. F. S., García, M. C. F., & Grima, E. M. (2009). Utilization of the cyanobacteria *Anabaena* sp. ATCC 33047 in CO_2 removal processes. *Bioresource Technology, 100,* 5904–5910.

Lu, Y., Zhai, Y., Liu, M., & Wu, Q. (2010). Biodiesel production from algal oil using cassava (*Manihot esculenta* Crantz) as feedstock. *Journal of Applied Phycology, 22,* 573–578.

Lundquist, T. J., Woertz, I. C., Quinn, N. W. T., & Benemann, A. (2010). *Realistic technology and engineering assessment of algae biofuel production*. Berkeley: Energy Biosciences Institute, University of California.

Luo, Y., Le-Clech, P., & Henderson, R. K. (2016). Simultaneous microalgae cultivation and wastewater treatment in submerged membrane photobioreactors: A review. *Algal Research, 24,* 425–437.

Marbella, L., Bilad, M. R., Passaris, I., Discart, V., Bañadme, D., Beuckels, A., et al. (2014). Membrane photobioreactors for integrated microalgae cultivation and nutrient remediation of membrane bioreactors effluent. *Bioresource Technology, 163,* 228–235.

Maroneze, M. M., Barin, J. S., Menezes, C. R., Queiroz, M. I., Zepka, L. Q., & Jacob-Lopes, E. (2014). Treatment of cattle-slaughterhouse wastewater and the reuse of sludge for biodiesel production by microalgal heterotrophic bioreactors. *Scientia Agricola, 71,* 521–524.

Maroneze, M. M., Siqueira, S. F., Vendruscolo, R. G., Wagner, R., Menezes, C. R., Zepka, L. Q., et al. (2016). The role of photoperiods on photobioreactors—a potential strategy to reduce costs. *Bioresource Technology, 219,* 493–499.

Mirón, A. S., Gómez, A. C., Camacho, F. G., Grima, E. M., & Chisti, Y. (1999). Comparative evaluation of compact photobioreactors for large-scale monoculture of microalgae. *Journal of Biotechnology, 70,* 249–270.

Münkel, R., Schmid-Staiger, U., Werner, A., & Hirth, T. (2013). Optimization of outdoor cultivation in flat panel airlift reactors for lipid production by *Chlorella vulgaris*. *Biotechnology and Bioengineering, 110,* 2882–2893.

Norsker, N. H., Barbosa, M. J., Vermuë, M. H., & Wijffels, R. H. (2011). Microalgal production-a close look at the economics. *Biotechnology Advances, 29,* 24–27.

Olaizola, M. (2000). Commercial production of astaxanthin from *Haematococcus pluvialis* using 25,000-liter outdoor photobioreactors. *Journal of Applied Phycology, 12,* 499–506.

Olguín, E., Galicia, S., Mercado, G., & Pérez, T. (2003). Annual productivity of *Spirulina* (*Arthrospira*) and nutrient removal in a pig wastewater recycling process under tropical conditions. *Journal of Applied Phycology, 15,* 249–257.

Perez-Garcia, O., & Bashan, Y. (2015). Microalgal heterotrophic and mixotrophic culturing for bio-refining: From metabolic routes to techno-economics. In A. Prokop, R. K. Bajpai, & M. E. Zappi (Eds.), *Algal biorefineries volume 2: Products and refinery design* (pp. 61–132). Switzerland: Springer International Publishing.

Perez-Garcia, O., Escalante, F. M. E., de-Bashan, L. E., & Bashan, Y. (2011). Heterotrophic cultures of microalgae: Metabolism and potential products. *Water Research, 45,* 11–36.

Pleissner, D., Lam, W. C., Sun, Z., & Lin, C. S. K. (2013). Food waste as nutrient source in heterotrophic microalgae cultivation. *Bioresource Technology, 137,* 139–146.

Pruvost, J., Le Borgne, F., Artu, A., & Legrand, J. (2017). Development of a thin-film solar photobioreactor with high biomass volumetric productivity (AlgoFilm©) based on process intensification principles. *Algal Research, 21,* 120–137.

Pulz, O., & Scheibenbogen, K. (1998). Photobioreactors: Design and performance with respect to light energy input. *Advances in Biochemical Engineering/Biotechnology, 59,* 123–152.

Queiroz, M. I., Hornes, M. O., Silva-Manetti, A. G., & Jacob-Lopes, E. (2011). Single-cell oil production by cyanobacterium *Aphanothece microscopica Nägeli* cultivated heterotrophically in fish processing wastewater. *Applied Energy, 88,* 3438–3443.

Ramírez-Mérida, L. G. R., Zepka, L. Q., & Jacob-Lopes, E. (2017). Current production of microalgae at industrial scale. In J. C. M. Pires (Ed.), *Recent advances in renewable energy* (pp. 242–260). Sharjah: Bentham Science Publishers.

Raslavičius, L., Striūgas, N., & Felneris, M. (2018). New insights into algae factories of the future. *Renewable and Sustainable Energy Reviews, 81,* 643–654.

Raso, S., van Genugten, B., Vermuë, M., & Wijffels, R. H. (2012). Effect of oxygen concentration on the growth of *Nannochloropsis* sp. at low light intensity. *Journal of Applied Phycology, 24,* 863–871.

Rawat, I., Kumar, R. R., Mutanda, T., & Bux, F. (2013). Biodiesel from microalgae: A critical evaluation from laboratory to large scale production. *Applied Energy, 103,* 444–467.

Richmond, A. (1990). Large scale microalgal culture and applications. In F. E. Round & D. J. Chapman (Eds.), *Progress in phycological research* (pp. 269–330). Britol: Biopress Ltd.

Richmond, A., & Cheng-Wu, Z. (2001). Optimization of a flat plate glass reactor for mass production of *Nannochloropsis* sp. outdoors. *Journal of Biotechnology, 85,* 259–269.

Roso, G. R., Santos, A. M., Zepka, L. Q., & Jacob-Lopes, E. (2015). The econometrics of production of bulk oil and lipid extracted algae in an agroindustrial biorefinery. *Current Biotechnology, 4,* 547–553.

San Pedro, A., González-López, C. V., Acién, F. G., & Grima, E. M. (2014). Outdoor pilot-scale production of *Nannochloropsis gaditana*: Influence of culture parameters and lipid production rates in tubular photobioreactors. *Bioresource Technology, 169,* 667–676.

Santos, A. M., Deprá, M. C., Santos, A. M., Zepka, L. Q., & Jacob-Lopes, E. (2015). Aeration energy requirements in microalgal heterotrophic bioreactors applied to agroindustrial wastewater treatment. *Current Biotechnology, 4,* 249–254.

Scott, S. A., Davey, M. P., Dennis, J. S., Horst, O., Howe, C. J., Lea-Smith, D. J., et al. (2010). Biodiesel from algae: Challenges and prospects. *Current Opinion in Biotechnology, 21,* 277–286.

Sierra, E., Acién, F. G., Fernández, J. M., García, J. L., González, C., & Molina, E. (2008). Characterization of a flat plate photobioreactor for the production of microalgae. *Chemical Engineering Journal, 138,* 136–147.

Singh, R. N., & Sharma, S. (2012). Development of suitable photobioreactor for algae production —a review. *Renewable and Sustainable Energy Reviews, 16,* 2347–2353.

Su, H., Zhou, X., Xia, X., Sun, Z., & Zhang. Y. (2017a). Progress of microalgae biofuel's commercialization. *Renewable and Sustainable Energy Reviews, 74*, 402–411.

Su, Y., Song, K., Zhang, P., Su, Y., Cheng, J., & Chen, X. (2017b). Progress of microalgae biofuel's commercialization. *Renewable and Sustainable Energy Reviews, 74*, 402–411.

Suh, I. S., & Lee, C. G. (2003). Photobioreactor engineering: Design and performance. *Biotechnology and Bioprocess Engineering, 8,* 313–321.

Sun, A., Davis, R., Starbuck, M., Ben-Amotz, A., Pate, R., & Piencos, P. T. (2011). Comparative cost analysis of algal oil production for biofuels. *Energy, 36,* 5169–5179.

Tabernero, A., Martín del Valle, E. M., & Galán, M. A. (2012). Evaluating the industrial potential of biodiesel from a microalgae heterotrophic culture: Scale-up and economics. *Biochemical Engineering Journal, 63,* 104–115.

Tao, Q., Gao, F., Qian, C. Y., Guo, X. Z., Zheng, Z., & Yang, Z. H. (2017). Enhanced biomass/biofuel production and nutrient removal in an algal biofilm airlift photobioreactor. *Algal Research, 21,* 9–15.

Torzillo, G. (1997). Tubular bioreactors. In A. Vonshak (Ed.), *Spirulina platensis (Arthrospira): Phisiology, cell-biology and biotechnology* (1st ed., pp. 101–115). London: Taylor and Francis.

Torzillo, G., Zittelli, G. C., & Chini Zittelli, G. (2015). Tubular photobioreactors. In A. Prokop, R. K. Bajpai, & M. E. Zappi (Eds.), *Algal biorefineries volume 2: Products and refinery design* (pp. 187–212). Switzerland: Springer International Publishing.

Tredici, M. R., Carlozzi, P., Zittelli, G. C., & Materassi, R. (1991). A vertical alveolar panel (VAP) for outdoor mass cultivation of microalgae and cyanobacteria. *Bioresource Technology, 38,* 153–159.

Tredici, M. R., & Materassi, R. (1992). From open ponds to vertical alveolar panels: The Italian experience in the development of reactors for the mass cultivation of photoautotrophic microorganisms. *Journal of Applied Phycology, 4,* 221–231.

Tredici, M. R., Rodolfi, L., Biondi, N., Bassi, N., & Sampietro, G. (2016). Techno-economic analysis of microalgal biomass production in a 1-há Green Wall Panel (GWP®) plant. *Algal Research, 19,* 253–263.

Tuantet, K., Temmink, H., Zeeman, G., Janssen, M., Wijffels, R. H., & Buisman, C. J. N. (2014). Nutrient removal and microalgal biomass production on urine in a short light-path photobioreactor. *Water Research, 55,* 162–174.

Ugwu, C. U., Aoyagi, H., & Uchiyama, H. (2008). Photobioreactors for mass cultivation of algae. *Bioresource Technology, 99,* 4021–4028.

Ugwu, C. U., Ogbonna, J. C., & Tanaka, H. (2002). Improvement of mass transfer characteristics and productivities of inclined tubular photobioreactors by installation of internal static mixers. *Applied Microbiology and Biotechnology, 58,* 600–607.

Vieira, J. G., Manetti, A. G. S., Jacob-Lopes, E., & Queiroz, M. I. (2012). Uptake of phosphorus from dairy wastewater by heterotrophic cultures of cyanobacteria. *Desalination and Water Treatment, 40,* 224–230.

Waltz, E. (2009). Biotech's green gold? *Nature Biotechnology, 27,* 15–18.

Wang, B., Lan, C. Q., & Horsman, M. (2012). Closed photobioreactors for production of microalgal biomasses. *Biotechnology Advances, 30,* 904–912.

Wang, S. K., Hu, Y. R., Wang, F., Stiles, M. R., & Liu, C. Z. (2014). Scale-up cultivation of *Chlorella ellipsoidea* from indoor to outdoor in bubble column bioreactors. *Bioresource Technology, 156,* 117–122.

Wang, C. H., Sun, Y. Y., Xing, R. L., & Sun, L. Q. (2005). Effect of liquid circulation velocity and cell density on the growth of *Parietochloris incisa* in flat plate photobioreactors. *Biotechnology and Bioprocess Engineering, 10,* 103–108.

Watanabe, Y., de la Noue, J., & Hall, D. O. (2011). Photosynthetic performance of a helical tubular photobioreactor incorporating the cyanobacterium *Spirulina platensis*. *Biotechnology and Bioengineering, 47,* 261–269.

Wen, X., Du, K., Wang, Z., Peng, X., Luo, L., Tao, H., et al. (2016). Effective cultivation of microalgae for biofuel production: A pilot-scale evaluation of a novel oleaginous microalga *Graesiella* sp. WBG-1. *Biotechnology for Biofuels, 9,* 123–135.

Xiong, W., Li, X., Xiang, J., & Wu, Q. (2008). High-density fermentation of microalga *Chlorella protothecoides* in bioreactor for microbial-diesel production. *Applied Microbiology and Biotechnology, 78,* 29–36.

Xu, Z., Baicheng, Z., Yiping, Z., Zhaoling, C., Wei, C., & Fan, O. (2002). A simple and low-cost airlift photobioreactor for microalgal mass culture. *Biotechnology Letters, 24,* 1767–1771.

Zitelli, G. C., Rodolfi, L., Bassi, N., Biondi, N., & Tredici, M. R. (2013). Photobioreactors for biofuel production. In M. A. Borowitzka & N. R. Moheimani (Eds.), *Algae for biofuels and energy* (pp. 115–131). Dordrecht: Springer.

CAPÍTULO 3

Patente: Câmara de Fotoperíodos e Biorreator de Bancada

Depositada no Instituto Nacional da Propriedade Industrial (INPI)

Processo BR 10 2016 030619 1

INSTITUTO NACIONAL DA PROPRIEDADE INDUSTRIAL

27/12/2016 870160079272 09:56

00.000.2.2.16.0859138.1

Pedido nacional de Invenção, Modelo de Utilidade, Certificado de Adição de Invenção e entrada na fase nacional do PCT

Número do Processo: BR 10 2016 030619 1

Dados do Depositante (71)

Depositante 1 de 2

Nome ou Razão Social: UNIVERSIDADE FEDERAL DE SANTA MARIA

Tipo de Pessoa: Pessoa Jurídica

CPF/CNPJ: 95591764000105

Nacionalidade: Brasileira

Qualificação Jurídica: Instituição de Ensino e Pesquisa

Endereço: Avenida Roraima, nº 1000, Cidade Universitária - Bairro Camobi

Cidade: Santa Maria

Estado: RS

CEP: 97105-900

País: Brasil

Telefone: (55) 3220-8887

Fax:

Email: agittec.pi@ufsm.br

Depositante 2 de 2

Nome ou Razão Social:	TECNAL INDÚSTRIA, COMÉRCIO, IMPORTAÇÃO E EXPORTAÇÃO DE EQUIPAMENTOS PARA LABORATÓRIO LTDA
Tipo de Pessoa:	Pessoa Jurídica
CPF/CNPJ:	47010566000168
Nacionalidade:	Brasileira
Qualificação Jurídica:	Pessoa Jurídica
Endereço:	Rua João Leonardo Fustaino, 325.
Cidade:	Piracicaba
Estado:	SP
CEP:	13413-102
País:	BRASIL
Telefone:	(19) 210 56161
Fax:	
Email:	fernando@tecnallab.com.br

Dados do Pedido

Natureza Patente:	10 - Patente de Invenção (PI)
Título da Invenção ou Modelo de Utilidade (54):	CÂMARA DE FOTOPERÍODOS E BIORREATOR DE BANCADA
Resumo:	A presente invenção descreve uma câmara de fotoperíodo e um biorreator capazes de expor um material a ciclos de iluminação e intensidade luminosa variáveis, o sistema também é capaz de realizar a análise dos fluidos de saída do biorreator. Especificamente, a presente invenção compreende uma câmara de fotoperíodo dotada de LEDs e um controlador comandado por um software que é capaz de variar os ciclos de iluminação e a intensidade luminosa, o biorreator é dotado de um vaso de reação de borosilicato e ao menos um sistema de agitação. A presente invenção se situa nos campos da engenharia mecânica e química.
Figura a publicar:	1

Dados do Inventor (72)

Inventor 1 de 5

Nome: EDUARDO JACOB LOPES

CPF: 98623273087

Nacionalidade: Brasileira

Qualificação Física: Professor do ensino superior

Endereço: Rua João Atílio Zampieri, 62/603.

Cidade: Santa Maria

Estado: RS

CEP: 97105-450

País: BRASIL

Telefone: (55) 322 08822

Fax:

Email: jacoblopes@pq.cnpq.br

Inventor 2 de 5

Nome: MARIANA MANZONI MARONEZE

CPF: 03101901006

Nacionalidade: Brasileira

Qualificação Física: Estudante de Pós Graduação

Endereço: Rua Floriano Peixoto, 1321/402.

Cidade: Santa Maria

Estado: RS

CEP: 97015-373

País: BRASIL

Telefone: (55) 996 635110

Fax:

Email: mariana_maroneze@hotmail.com

Inventor 3 de 5

Nome: LEILA QUEIROZ ZEPKA

CPF: 96427655000

Nacionalidade: Brasileira

Qualificação Física: Professor do ensino superior

Endereço: Rua João Atílio Zampieri, 62/603.

Cidade: Santa Maria

Estado: RS

CEP: 97105-450

País: BRASIL

Telefone: (55) 331 71410

Fax:

Email: zepkaleila@yahoo.com.br

Inventor 4 de 5

Nome: STEFANIA FORTES SIQUEIRA

CPF: 02410998038

Nacionalidade: Brasileira

Qualificação Física: Estudante de Pós Graduação

Endereço: Rua Nove. Parque Alto da Colina, 130.

Cidade: Santa Maria

Estado: RS

CEP: 97110-795

País: BRASIL

Telefone: (55) 330 70062

Fax:

Email:

Inventor 5 de 5

Nome: MARIANY COSTA DEPRÁ

CPF: 03412411051

Nacionalidade: Brasileira

Qualificação Física: Estudante de Pós Graduação

Endereço: Rua General Neto, 277/202.

Cidade: Santa Maria

Estado: RS

CEP: 97050-241

País: BRASIL

Telefone: (55) 302 73201

Fax:

Email: marianydepra@gmail.com

Documentos anexados

Tipo Anexo	Nome
Comprovante de pagamento de GRU 200	Comprovante de pagamento - processo 377.pdf
Declarações de inventor	Declarações de inventores.pdf
Relatório Descritivo	UFSM - Processo 00377-PI2016 - Relatório Descritivo - 13Dez2016.pdf
Reivindicação	UFSM - Processo 00377-PI2016 - Reivindicações - 13Dez2016.pdf
Desenho	UFSM - Processo 00377-PI2016 - Figuras - 13Dez2016.pdf
Resumo	UFSM - Processo 00377-PI2016 - Resumo - 13Dez2016.pdf

Acesso ao Patrimônio Genético

☑ Declaração Negativa de Acesso - Declaro que o objeto do presente pedido de patente de invenção não foi obtido em decorrência de acesso à amostra de componente do Patrimônio Genético Brasileiro, o acesso foi realizado antes de 30 de junho de 2000, ou não se aplica.

Declaração de veracidade

☑ Declaro, sob as penas da lei, que todas as informações acima prestadas são completas e verdadeiras.

Relatório Descritivo de Patente de Invenção

CÂMARA DE FOTOPERÍODOS E BIORREATOR DE BANCADA

Campo da Invenção

[0001] A presente invenção descreve uma câmara de fotoperíodo e um biorreator capazes de expor um material a ciclos de iluminação e intensidade luminosa variáveis, o sistema também é capaz de realizar a análise dos fluidos de saída do biorreator. A presente invenção se situa nos campos da engenharia mecânica e química.

Antecedentes da Invenção

[0002] Biorreatores são amplamente utilizados em diversos processos químicos para a obtenção de diversos produtos a partir de inúmeras reações. Uma entre sua vasta aplicação envolve reações fotossintéticas, que necessitam de luz para que possam ocorrer.

[0003] Deste modo, para que estas reações possam ocorre em ambientes laboratoriais e não necessite ficar exposto a ambientes externos para absorção de luz solar, cria-se a necessidade de um equipamento que gere luz que seja aproveitada pelo sistema.

[0004] Alguns equipamentos foram criados com tal propósito, porém os mesmos não são capazes de executar diferentes ciclos de fotoperíodo e intensidade luminosa.

[0005] Os biorreatores atuais realizam a análises dos gases do interior do mesmo através da retirada de uma amostragem, que deve ser executada toda vez que se deseja realizar a análise.

[0006] Na busca pelo estado da técnica em literaturas científica e patentária, foram encontrados os seguintes documentos que tratam sobre o tema:

[0007] O produto Biorreator para algas e cianobactérias, comercializado pela empresa Tecnal, desenvolvedora de equipamentos científicos, é dotado

de um biorreator do tipo air-lift dotado de uma câmara de fotoperíodos. A câmara de fotoperíodos do produto possui de 6 painéis LED que podem atingir intensidade luminosa máxima de 1.500 µmol-photon.m^{-2}.s^{-1}/painel, porém a intensidade incidida sobre diferentes pontos da parede do biorreator não é uniforme, apresentando variações de até 90%, fator que prejudica a eficiência do processo fotossintético, sendo que tal variabilidade espacial tem como um de seus agravantes a presença de espelhos na face interna da câmara de fotoperíodos. Ademais, a câmara de fotoperíodos apresenta apenas a possibilidade de período de longa duração ou frequência.

[0008] O documento PI0701608-5 revela um sistema reacional pneumático, o qual inclui três modelos: coluna de bolhas ou torre, air-lift de cilindros concêntricos e air-lift tipo “split”. O sistema proposto não apresenta sistema de fotoperíodo e não apresenta capacidade de análise dos gases de saída. Ademais somente metade do cilindro reacional é construída em vidro borossilicato, sendo a outra metade encamisada em aço inoxidável fator que reduz a luz absorvida.

[0009] O documento CN201801523 revela O sistema consiste em um fotobiorreator laminado, um dispositivo de iluminação e um disco. O fotobiorreator é utilizado para o cultivo de microalgas ou outros microrganismos fotossintéticos, o dispositivo de iluminação fornece a energia luminosa para as células e controla o liga/desliga da fonte de luz através de um relé eletromagnético, o que permite a realização dos ciclos de luz de longa duração. O disco é induzido a rodar por motor ligado a ele, de modo a transmitir e irradiar a luz fornecida pela fonte de luz para a superfície do reator em ciclos de luz de curta duração. A geometria do dispositivo gera uma incidência luminosa não uniforme sobre a superfície do reator, reduzindo a eficiência das reações.

[0010] Assim, do que se depreende da literatura pesquisada, não foram encontrados documentos antecipando ou sugerindo os ensinamentos da presente invenção, de forma que a solução aqui proposta possui novidade e atividade inventiva frente ao estado da técnica.

[0011] Deste modo a eficiência das reações provenientes do biorreator é minimizada, pois não há dispositivo capaz de variar os ciclos e a intensidade luminosa fornecida ao biorreator para que a reação pretendida seja ampliada.

Sumário da Invenção

[0012] Dessa forma, a presente invenção tem por objetivo resolver os problemas constantes no estado da técnica a partir de uma câmara fotossintética e um biorreator que são capazes de criar diferentes ciclos de iluminação e intensidade luminosa e realizar a análise constante dos gases de saída.

[0013] Em um primeiro objeto, a presente invenção apresenta uma câmara de fotoperíodo apresentando geometria capaz de envolver um biorreator e compreendendo painéis de LED posicionados na face interna da câmara, distados uniformemente entre si, e ao menos um controlador capaz de programar ciclos de iluminação e intensidade luminosa, em que o controlador é adaptado para configurar:

a. ciclos de longa duração;
b. ciclos de média duração;
c. ciclos de curta duração;
d. frequência; e
e. rampas de luminosidade.

[0014] Em um segundo objeto, a presente invenção apresenta um biorreator de bancada que compreende uma câmara de fotoperíodo capaz de simular diferentes ciclos de iluminação e intensidade luminosa, em que a dita câmara de fotoperíodo é conforme definido anteriormente.

[0015] Ainda, o conceito inventivo comum a todos os contextos de proteção reivindicados fazem referência a uma câmara de fotoperíodo e um biorreator que são capazes de realizar cultivo de materiais fotossintéticos com alta eficiência, pois apresentam a capacidade de expor tal material a variados

ciclos e intensidades de iluminação, regulados a partir de uma análise dos gases de saída do biorreator.

[0016] Estes e outros objetos da invenção serão imediatamente valorizados pelos versados na arte e pelas empresas com interesses no segmento, e serão descritos em detalhes suficientes para sua reprodução na descrição a seguir.

Breve Descrição das Figuras

[0017] São apresentadas as seguintes figuras:

[0018] A figura 1 mostra uma concretização de uma câmara de fotoperíodo envolvendo um biorreator.

[0019] A figura 2 mostra uma concretização da tampa do biorreator.

[0020] A figura 3 mostra o sistema de agitação do biorreator por injeção de gases.

[0021] A figura 4 mostra um detalhamento da câmara de fotoperíodo aberta, independentemente de associação ao biorreator, exemplificando pontos de medição utilizados nos testes de averiguação de intensidade luminosa.

Descrição Detalhada da Invenção

[0022] As descrições que seguem são apresentadas a título de exemplo e não limitativas ao escopo da invenção e farão compreender de forma mais clara o objeto do presente pedido de patente.

[0023] Em um primeiro objeto, a presente invenção apresenta uma câmara de fotoperíodo apresentando geometria capaz de envolver um biorreator e compreendendo painéis de LED posicionados na face interna da câmara, distados uniformemente entre si, e ao menos um controlador capaz de programar ciclos de iluminação e intensidade luminosa.

[0024] Em uma concretização, a câmara de fotoperíodo foi confeccionada com capacidade de acomodação para 12 painéis LED, que podem ser ligados individualmente. Cada painel é composto por um canal de

LED, o qual pode ser substituído manualmente pelo usuário. A configuração com 12 painéis LED faz com que a incidência luminosa na parede do biorreator seja uniforme.

[0025] Foram realizados testes no antecedente dotado de seis painéis LED para medição da intensidade luminosa incidida sobre as paredes do biorreator. Com a utilização de um sensor quântico para a medição da intensidade luminosa, foram determinados pontos de medição, os pontos escolhidos são distribuídos pelo biorreator de forma a verificar as variações de intensidade luminosa, dessa forma foram escolhidos três pontos sobre um painel LED (A, B e C) e três pontos em uma superfície sem painel (D, E e F), sendo os três pontos que cada local divididos entre a parte inferior, a central e a superior. Os valores de intensidade luminosa na parede do biorreator entre os pontos escolhidos mostraram que com a disposição de seis painéis a incidência luminosa na parede do biorreator varia em até 90%, esta variação reduz a eficiência do processo fotossintético e ocasiona um consumo energético desnecessário. Desta forma, surgiu a necessidade de determinar uma geometria capaz de manter a uniformidade da intensidade luminosa, em novos testes com outras geometrias foi obtido melhor resultado de uniformidade na incidência luminosa na parede do biorreator em uma concretização onde a câmara de fotoperíodos é dotada de 12 painéis LED.

[0026] Em uma concretização, foram instalados canais com capacidade de atingir intensidade de 750 µmol-photon.m^{-2}.s^{-1}/painel, os canais de LED podem ser nas cores/comprimento de onda de azul royal (450nm), verde (525nm), vermelho (630nm), vermelho (660nm), branco-frio, branco-neutro ou branco-quente.

[0027] A câmara de fotoperíodo é dotada de um controlador de fotoperíodos, tal controlador é capaz de programar a quantidade de painéis ligados e a intensidade luminosa de cada painel.

[0028] Em uma concretização, o controlador é dotado de 5 ajustes programados: longa duração, média duração (pulsado lento), curta duração

(pulsado), frequência e rampas de luminosidade. Os fotoperíodos de longa duração compreendem os períodos de luminosidade e escuro em uma proporção de horas. Os fotoperíodos de curta duração, também de chamados de pulsados são assim denominados, pois abrangem os ciclos de claro/escuro em uma proporção de segundos ou milissegundos. Os fotoperíodos de frequência apresentam dois ou mais ciclos de claro/escuro por dia. Já as rampas de luminosidade permitem escolher a intensidade luminosa máxima, o tempo que o sistema permanece nessa intensidade máxima, o tempo que permanece no escuro e o tempo que a luminosidade leva para atingir a luminosidade máxima, e então um software projeta uma curva da intensidade luminosa pelo tempo determinando qual deve ser a variação de aumento da luminosidade e da mesma forma irá reduzir até a intensidade zero, esse tipo de fotoperíodo permite simular condições naturais de iluminação. Independente do regime de luminosidade, o software permite selecionar a quantia de canais a serem ligados, assim como sua intensidade, que pode variar de 0 a 100%.

[0029] A literatura reporta que para se obter um cultivo fotossintético microalgal com eficiências fotossintéticas elevadas deve-se utilizar iluminação contínua (100%) nos fotobiorreatores. No entanto, foram realizados diversos testes expondo um cultivo a diferentes ciclos de iluminação e foi comprovado, através dos resultados mostrados na Tabela 1 a seguir, que é possível aumentar a eficiência do processo fotossintético.

Ciclos		Eficiência
Iluminação Contínua	24h	100%
Longa duração	22:02h	98,10%
	22:04h	81,88%
	18:06h	67,53%
	12:12h	15,07%
Frequência	2 c/d	93,47%
	4 c/d	99,56%

	8 c/d	106,60%
	12 c/d	124,78%
	24 c/d	132,60%
	48 c/d	132,75%
Curta duração	0,91:0,09s	138,80%
	0,83:0,17s	105,20%
	0,75:,025s	102,60%
	0,50:0,50s	73,76%

Tabela 1

[0030] Os resultados obtidos evidenciam a necessidade da câmara de fotoperíodos possuir diferentes ciclos de iluminação.

[0031] Em uma concretização, a câmara de fotoperíodo foi confeccionada em formato cilíndrico, em aço inox 304 polido, para ser utilizado juntamente a um biorreator de bancada, com escalas de bancada de 2L, 5L ou 10L.

[0032] Em uma concretização, a câmara de fotoperíodo é dotada de uma interface homem máquina por ondo pode ser realizado a programação do mesmo e armazenamento de dados.

[0033] Em um segundo objeto, a presente invenção apresenta um biorreator de bancada que compreende uma câmara de fotoperíodo capaz de simular diferentes ciclos de iluminação e intensidade luminosa.

[0034] Em uma concretização, o vaso de reação é construído em vidro borosilicato (1), geometria cilíndrica, relação altura/diâmetro de 4,45.

[0035] Em uma concretização, a tampa do vaso de reação é dotada de aberturas para sensores de temperatura (6), pH (7), O_2 (8), Saída para analisador de gases (CO_2 e O_2)(9), quatro entradas simples para adição de ácido (10), base (11), anti-espumante (12) e nutrientes (13), sensor de nível de espuma (14), septo (16), entrada (17) para o condensador de refluxo e saída

para amostragem líquida (15) sendo que a amostragem é realizada por meio de um sistema baseado em seringa com um reservatório autoclavável.

[0036] Em uma concretização, a tampa (2) foi confeccionada em aço inoxidável 316L e é dotada de manípulos para fechamento em aço inoxidável 304. Para vedação da tampa foi utilizado anéis de vedação.

[0037] O vaso de reação é sustentado por uma base horizontal (4), com saídas para o sistema de arrefecimento e entrada de gases para o aspersor. O fluxo ascendente de gases provenientes do aspersor é responsável pela agitação odo sistema.

[0038] Em uma concretização, a entrada de gases para agitação do sistema é realizada pelo método coluna de bolhas, por onde o ar ou mistura gasosa é introduzido na base do sistema através de um duto (18) e é aspergido via um aspersor em cruzeta (19).

[0039] Em uma concretização a entrada de gases para agitação do sistema é realizada pelo método air-lift, nesta concretização é inserido no interior do vaso reacional um cilindro interno (20), o ar ou mistura de gases é introduzido no sistema através do duto (18) e é aspergido via aspersor (19).

[0040] O biorreator possui a capacidade de adição de equipamentos auxiliares, entre eles:

a. Misturador automático de gases com controlador mássico de vazão;
b. - Misturador manual de gases com bloco de rotâmetros;
c. - Eletrodo de pH digital e autoclavável;
d. - Sensor de oxigênio dissolvido digital e autoclavável;
e. - Sensor de dióxido de carbono dissolvido digital e autoclavável;
f. - Sensor de gases CO_2 e O_2;
g. - Sensor de turbidez autoclavável;
h. - Sensor de radiação PAR;
i. - Bombas peristálticas para dosagem de líquidos (ácido, base, anti-espumante e nutrientes);

j. - Banho termostatizado com circulação externa com controle de temperatura de -10ºC a 100ºC.

Exemplo 1. Realização Preferencial

[0041] Os exemplos aqui mostrados têm o intuito somente de exemplificar uma das inúmeras maneiras de se realizar a invenção, contudo sem limitar, o escopo da mesma.

[0042] Em uma concretização preferencial, a câmara de fotoperíodos é dotada de 12 painéis LED, sendo que a seção da sua parte interna é um dodecágono onde é instalado um painel em cada face, de forma que a superfície interna seja formada apenas pelos painéis LED.

[0043] Os versados na arte valorizarão os conhecimentos aqui apresentados e poderão reproduzir a invenção nas modalidades apresentadas e em outras variantes, abrangidas no escopo das reivindicações anexas.

Reivindicações

1. Câmara de fotoperíodos **caracterizada** por apresentar geometria capaz de envolver um biorreator e por compreender painéis de LED posicionados na face interna da câmara, distados uniformemente entre si, e ao menos um controlador capaz de programar ciclos de iluminação e intensidade luminosa, em que o controlador é adaptado para configurar:
    a. ciclos de longa duração;
    b. ciclos de média duração;
    c. ciclos de curta duração;
    d. frequência; e
    e. rampas de luminosidade.
2. Câmara de fotoperíodos, de acordo com a reivindicação 1, **caracterizada** por compreender 12 painéis LED dispostos na face interna da câmara de fotoperíodos.
3. Câmara de fotoperíodos, de acordo com qualquer uma das reivindicações 1 a 2, **caracterizada** pelo ciclo de iluminação compreender duração na faixa de 0,88 a 0,94 segundos de iluminação e 0,06 a 0,12 segundo de escuro.
4. Câmara de fotoperíodos, de acordo com qualquer uma das reivindicações 1 a 3, **caracterizada** pelo fato dos LEDs atingirem uma intensidade luminosa de 750 µmol-photon.m^{-2}.s^{-1}/painel.
5. Câmara de fotoperíodos, de acordo com qualquer uma das reivindicações 1 a4,**caracterizada**por ser utilizada em biorreatores entre 1L e 15L.
6. Câmara de fotoperíodos, de acordo com qualquer uma das reivindicações 1 a 5, **caracterizada** por ser dotada de ao menos uma interface homem máquina.
7. Biorreator de bancada **caracterizado** por compreender uma câmara de fotoperíodo capaz de simular diferentes ciclos de iluminação e intensidade luminosa, em que a referida câmara de fotoperíodo é conforme descrito nas reivindicações 1 a 6.

8. Biorreator de bancada, de acordo com a reivindicação 7,**caracterizado** por compreender um vaso de reação inteiramente em vidro borosilicato, ao menos uma entrada, ao menos um sistema de agitação e ao menos uma câmara de fotoperíodo, dotada de ao menos um conjunto de LEDs, em que a referida câmara de fotoperíodo envolve o biorreator.
9. Biorreator de bancada, de acordo com qualquer uma das reivindicações 7 e 8, **caracterizado** por compreender um detector de fluidos na saída de fluidos realizando análise contínua dos fluidos de saída.
10. Biorreator de bancada, de acordo com a reivindicação 9, **caracterizado** por utilizar os resultados da análise constante dos gases para ajustar o ciclo de iluminação e a intensidade luminosa da câmara de fotoperíodo.

FIGURAS

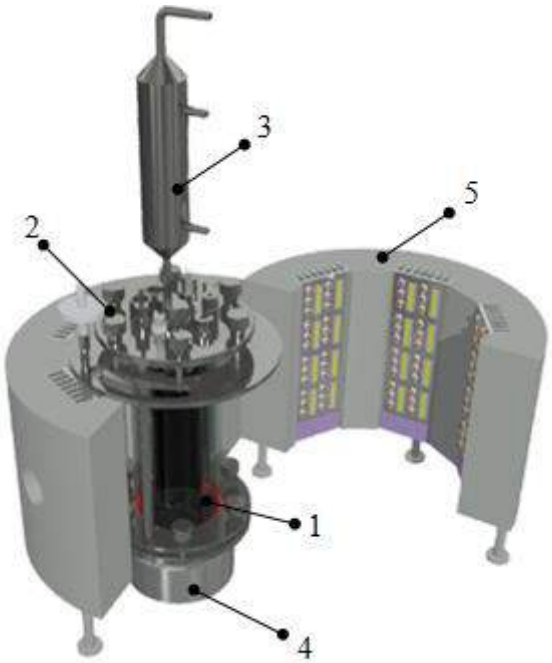

Figura 1

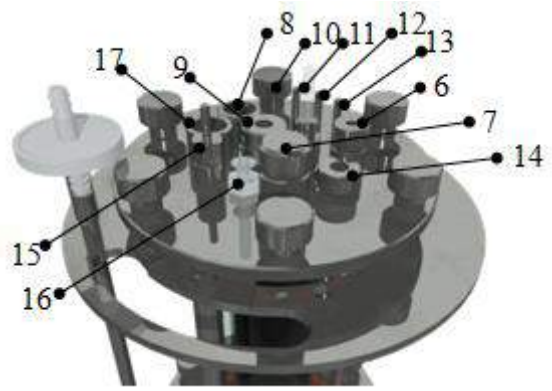

Figura 2

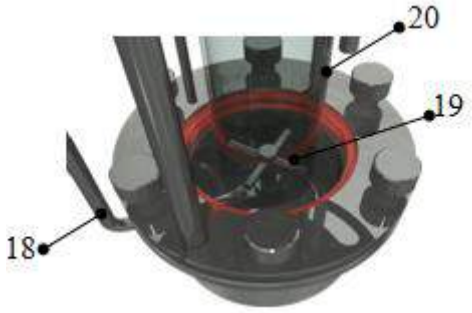

Figura 3

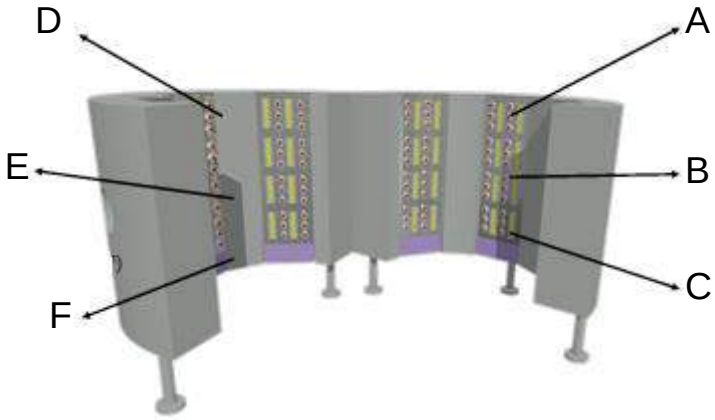

Figura 4

Resumo

CÂMARA DE FOTOPERÍODOS E BIORREATOR DE BANCADA

A presente invenção descreve uma câmara de fotoperíodo e um biorreator capazes de expor um material a ciclos de iluminação e intensidade luminosa variáveis, o sistema também é capaz de realizar a análise dos fluidos de saída do biorreator. Especificamente, a presente invenção compreende uma câmara de fotoperíodo dotada de LEDs e um controlador comandado por um software que é capaz de variar os ciclos de iluminação e a intensidade luminosa, o biorreator é dotado de um vaso de reação de borosilicato e ao menos um sistema de agitação. A presente invenção se situa nos campos da engenharia mecânica e química.

CAPÍTULO 4

Licenciamento de Tecnologia: Contrato de Licenciamento para Exploração do Pedido de Patente de Invenção Depositada junto ao INPI Intitulado “Câmara de Fotoperíodos e Biorreator de Bancada”

MINISTÉRIO DA EDUCAÇÃO
UNIVERSIDADE FEDERAL DE SANTA MARIA

PORTARIA N. 87.343, DE 02 DE JANEIRO DE 2018.

O REITOR DA UNIVERSIDADE FEDERAL DE SANTA MARIA, no uso de suas atribuições legais e estatutárias, e em atendimento o art. 67 da Lei n. 8.666/93, e tendo em vista o que consta do Memorando n. 199/2017-DIMECI, resolve:

DESIGNAR o servidor **EDUARDO JACOB LOPES**, SIAPE 1655518, como Gestor do Contrato nº 001/2018, cujo objeto: **CONTRATO DE LICENCIAMENTO PARA EXPLORAÇÃO DO PEDIDO DE PATENTE DE INVENÇÃO DEPOSITADA JUNTO AO INPI INTITULADO "CÂMARA DE FOTOPERÍODOS E BIORREATOR DE BANCADA**,e firmado com a empresa **TECNAL INDÚSTRIA, COMÉRCIO, IMPORTAÇÃO E EXPORTAÇÃO DE EQUIPAMENTOS PARA LABORATÓRIOS LTDA,** conforme art. 67 §§ 1º e 2º da Lei 8.666/93:

> ***Art. 67. A execução do contrato deverá ser acompanhada e fiscalizada por um representante da Administração especialmente designado, permitida a contratação de terceiros para assisti-lo e subsidiá-lo de informações pertinentes a essa atribuição.***
> ***§ 1º O representante da Administração anotará em registro próprio todas as ocorrências relacionadas com a execução do contrato, determinando o que for necessário à regularização das faltas ou defeitos observados.***
> ***§ 2º As decisões e providências que ultrapassarem a competência do representante deverão ser solicitadas a seus superiores em tempo hábil para a adoção das medidas convenientes.***

O Gestor do contrato terá as seguintes atribuições e responsabilidades:
- Acompanhar rotineiramente a execução contratual de forma a manter a sua qualidade, atuando tempestivamente na solução de eventuais problemas;
- Solicitar garantia contratual à empresa contratada;
- Zelar pela fiel execução do contrato, de acordo com as cláusulas acordadas e as normas da Lei 8.666/93;
- Solicitar com as devidas justificativas, caso haja necessidade, acréscimos ou supressões e outros ajustes do objeto contratado;
- Sanar qualquer dúvida com as demais áreas responsáveis da Administração, objetivando o fiel cumprimento do contrato;
- Anotar em registros próprios todas as ocorrências relacionadas com a execução do contrato, com a finalidade de regularizar as faltas e defeitos observados;
- Atestar as respectivas notas fiscais, após a certificação de que os serviços foram efetivamente realizados, conforme as cláusulas contratuais;
- Encaminhar ao DEMAPA, devidamente documentado, os eventuais problemas na execução contratual;
- Encaminhar no prazo mínimo de 90 dias, antes do término da vigência do contrato, a solicitação de renovação contratual, caso o contrato permita prorrogações e haja interesse da contratante e contratada,
- Solicitar a abertura de processo licitatório para a nova contratação, no prazo mínimo de 90 dias antes do término da vigência do contrato.

PAULO AFONSO BURMANN.

CAPÍTULO 5

Manuscrito 1: Artificial lighting strategies in photobioreactors for bioenergy production by *Scenedesmus obliquus* CPCC05

Em processo de revisão no periódico SN Applied Sciences

Artificial lighting strategies in photobioreactors for bioenergy production by *Scenedesmus obliquus* CPCC05

Mariana Manzoni Maroneze, Mariany Costa Deprá, Leila Queiroz Zepka, Eduardo Jacob-Lopes*

Department of Food Science and Technology, Federal University of Santa Maria (UFSM), 97105-900, Santa Maria, RS, Brazil

Email: ejacoblopes@gmail.com

Abstract

The aim of this work was to evaluate the artificial lighting strategies to produce microalgal biodiesel. Different long-term, frequency, and short photoperiods were examined. Were measured the productivities of the process, chemical composition of the biomass, biodiesel quality, and energy balance. The results showed that *Scenedesmus obliquus* CPCC05 can store sufficient energy to sustain cell growth for continuous periods of up to 2 h in the dark, without affecting the productivities of the process. The values for the maximum biomass (63.88 mg/L.h) and lipid (18.9 mg/L.h) productivities as well for the calorific value (20.4 kJ/g) were obtained at a photoperiod of 24 t/d. It was qualitatively observed that the photoperiod significantly influenced the fatty acid profile of single-cell oil and, consequently, the quality of the produced biodiesel. Finally, the use of the photoperiods was also proven to be an effective strategy to improve the energy balance of the production process of microalgal biodiesel.

Keywords: Light/dark cycle, microalgae, photoperiods, lipid, biodiesel.

1 Introduction

It is commonly agreed that environmental deterioration and fossil fuel depletion are becoming two worldwide issues that threaten human development [1]. As a result, alternative sustainable and renewable sources of energy have been developed, such as the biofuels of the first, second, third, and fourth generation. Methyl esters of fatty acids, known as biodiesel, are nontoxic, biodegradable, and an excellent alternative to fossil diesel, since the combustion properties of this biofuel are similar to those of petroleum-based diesel [2].

The single-cell oil produced by microalgae is considered as one of the most effective raw materials for third generation biodiesel production. The advantages of biodiesel production from microalgae include the fast growth of cultures, high oil productivity, and low arable land demand [33]. Particularly, *Scenedesmus obliquus* is a robust green microalga that provides good productivity rates and has been commonly proposed as a promising candidate for biodiesel production [4, 5].

In order to competitively produce this biofuel, it is important to reduce the raw material costs of production. The main raw materials for the photosynthetic microalgae cultivation are nutrients, carbon dioxide, and light energy. The light energy can be provided by the sunlight, which is the most cost-effective energy source for microalgal production. However, it also has

certain disadvantages, including day/night cycles, influence of weather conditions, and seasonal changes. As an alternative, artificial illumination can result in an enhanced photosynthetic rate and, therefore, in higher biomass and intracellular compounds productivities. The continuous use of artificial light, however, results in an increase of electricity costs that will subsequently increase the final product costs [6, 7].

On the other hand, the modulation of light cycle appears as an alternative to reduce the demand for electrical energy in microalgal cultivations and then develop cheaper and more efficient processes. Under the appropriate light regimes, microalgae are able to tolerate residence time in the absence of light, reaching similar or higher productivity compared to cultures with continuous illumination [8, 9].

In addition, the light regime which microalgal cultures are submitted to is considered a determining factor in the cell productivity and chemical composition of biomass [10]. Several authors have previously reported that, besides reducing the operational costs of the process, the use of photoperiod can improve the photosynthetic rate as well as the productivity and quality of intracellular products [11-13].

In this regard, the aim of this work was to evaluate the artificial lighting strategies to produce microalgal biodiesel. The study focused on evaluating the influence of different photoperiods (long-term, frequency, and short photoperiods) on (i) productivities of the process, (ii) chemical composition of the biomass, and (iii) biodiesel quality, as well on (iv) energy balance.

2 Material and Methods

2.1 Microorganisms and culture media

Axenic cultures of *Scenedesmus obliquus* CPCC05 were obtained from the Canadian Phycological Culture Centre. Stock cultures were propagated and maintained in a synthetic BG11 medium (Braun-Grunow medium) [14]. The incubation conditions used were 30ºC, photon flux density of 30 µmol.m-2 s-1 and a photoperiod of 12 h.

2.2 Photobioreactor design

Measurements were carried out in a bubble column photobioreactor (Tecnal, Piracicaba-SP, Brazil). The system was built in 4 mm thick glass, an internal diameter of 7.5 cm, height of 75 cm, and a nominal working volume of 2.0 L. The dispersion system for the reactor consisted of a 1.5 cm diameter air diffuser located in the center of the column. The reactor was illuminated with 45 cool white LED lamps of 0.23 W each, located in a photoperiod chamber. The CO_2/air mixture

was adjusted to achieve the desired concentration of carbon dioxide in the airstream, through three rotameters that measured the flow rates of carbon dioxide, air, and the mixture of gases, respectively.

2.3 Obtaining the kinetic data in an experimental photobioreactor

The experiments were conducted in bioreactors operating in continuous mode, which after the residence time of batch culture (Table 1), a feed synthetic BG11 medium was added to the bioreactor at dilution rates showed at Table 1. These data were obtained through preliminary batch mode experiments. At the same time, equal volumes of cell suspension were withdrawn from the bioreactor. The steady-state was considered to have been established after at least 3 volume charges, with a variation of cell dry weight less than 5%.

[Insert Table 1]

The experimental conditions were the following: initial cell concentration of 100 mg/L, isothermal reactor operating at a temperature of 26°C, photon flux density of 150 μmol m−2 s−1, and continuous aeration of 1VVM (volume of air per volume of culture per minute) with the injection of air enriched with 15% carbon dioxide.

In the long-term photoperiods experiments, the light cycles evaluated were (h:h) 24:0, 22:2, 20:4, 18:6, and 12:12 (light:dark). In the light/dark cycle frequency experiments, the cells were exposed to 22 h of light and 2 h of dark (optimal condition previously defined), where these 2 h were divided into six frequencies: 2, 4, 8, 12, 24 and 48 times per day (t/d). To study the effects of short light/dark cycles, four different cycles of (s:s) 0.91:0.09, 0.83:0.17, 0.75:0.25, and 0.50:0.50 (light:dark) were set every one second.

The cell concentration was monitored every 24 h during the growth phase of the microorganism. The tests were carried out in duplicate and the kinetic data referred to the mean of four repetitions.

2.4 Kinetic parameters

Biomass data were used to calculate the biomass productivity [PX = Xmax.μmax, mg/L.h] and lipid productivity [PL = PX.LC, mg/L.h], where Xmax is the maximum biomass concentration (mg/L), μmax is the maximum specific growth rate (h-1) and LC is lipid content of the biomass (%).

2.5 Analytical methods

Cell concentration was evaluated gravimetrically by filtering a known volume of culture medium through a 0.45 µm filter (Millex FG, Billerica-MA, USA) and drying at 60°C. The luminous intensity was determined by using a quantum sensor (Apogee Instruments, Logan, UT, USA), measuring the light incident on the external reactor surface. The temperature was controlled by thermostats. The flow rates of carbon dioxide, air, and CO_2 enriched air were determined using rotameters (AFSG 100 Key Instruments, Trevose, PA, USA).

The chemical composition of microalgal biomass was performed based on the method described in AOAC [15], except to total lipid concentration of the biomass, which was determined gravimetrically by the modified Bligh and Dyer method [16]. The biomass calorific value was calculated by the Atwater System, using factors of 17 kJ/g for protein, 37 kJ/g for lipid and 17 kJ/g for total carbohydrate content [17].

The method of Hartman and Lago [18] was used to saponify and esterify the dried lipid extract to obtain the fatty acid methyl esters. Fatty acid composition was determined by using a VARIAN 3400CX gas chromatograph (Varian, Palo Alto, CA, USA. Fatty acid methyl esters were identified by comparison of the retention times with the authentic standards from FAME Mix-37 (P/N 47885-U, Sigma-Aldrich, St. Louis, MO USA) and quantified through area normalization by software T2100p Chromatography Station (Plus Edition) v9.04.

The fuel properties of biodiesel (ester content, EC; cetane number, CN; iodine value, II; degree of unsaturation, DU; saponification value, SV; long-chain saturated factor, LCSF; cold filter plugging point, CFPP; cloud point, CP; allylic position equivalents, APE; bis-allylic position equivalents, BAPE; oxidation stability, OS; higher heating value, HVV; kinematic viscosity, µ and kinematic density, ρ) were determined through the software BiodieselAnalyzer© 1.1, which estimates biodiesel properties based on the fatty acid profile of the parent oil, through a system of empirical equations [19].

2.6 Energy balance

The net energy ratio (NER) [$NER=\sum Eout/\sum Ein$] of a system was defined as the ratio of the total energy produced per day (energy content of the residual biomass, MJ/d) over the energy required for lighting of the photobioreactor per day (MJ/d), where Eout is the renewable energy output and Ein is the fossil fuel energy input.

To calculate the net energy balance (NEB) [NEB=∑inputs - ∑outputs] the inputs were considered as the energy required for lighting the photobioreactor per day and the outputs as the energy produced per day.

2.7 Statistical analysis

Analysis of variance (one-way ANOVA) and Tukey's test ($p<0.05$) were used to test the differences between the photoperiods. To elucidate the relationship between the production parameters of lipids and between the fatty acid and biodiesel properties under different lighting condition, multivariate analysis via principal component analysis (PCA) was performed. The analyses were performed with the software Statistica 7.0 (StatSoft, Tulsa, OK, USA).

3 Results and Discussion

The growth of microalgal culture depends on various abiotic factors, such as, temperature, level of nutrients, and available light. Among these factors, the light influences directly the photosynthesis mechanism being an important factor to reach optimal growth conditions for the culture [11]. In this sense, the Figure 1 shows the effect of long-term photoperiods (a), frequency photoperiods (b) and short photoperiods (c) on biomass and lipid productivity.

[Insert Figure 1]

As shown in Figure 1a, the biomass productivity is reduced as the dark period's increase. This is associated with the photolimitation condition that occurs when there is insufficient light to maintain the metabolism [20]. The maximum cell productivity (47.02 mg/L) was found in the photoperiod of 24:00 h (light: dark), followed by 22:02 h, which has a biomass productivity of 42.66 mg/L.h. Nevertheless, in these two conditions, no significant difference (Tukey's test $P<0.05$) was observed. These results show that *Scenedesmus obliquus* CPCC05 can store sufficient energy to sustain cell metabolism for periods of up to 2 h uninterrupted in the dark, without affecting the biomass productivity. Similar results were found by Jacob-Lopes [8] with *Aphanothece microscopica Nägeli* growth under different photoperiods, where this cyanobacterium proved to be able to maintain its biomass productivity, growth rate and carbon dioxide fixation rate for up to 2 h in the dark.

On the other hand, the cultures grown under other long-term photoperiods, with longer time in the absence of light showed evidence of photolimitation condition that occurs when there is insufficient light to maintain the metabolism (Figure 1a) [24]. Jacob-Lopes and

coworkers [8] also associate the low cell growth under conditions with long-term in the dark to the limited carbon source for cell growth, since the microalgae are unable to use inorganic carbon sources in the absence of light, and the organic carbon concentrations in the culture medium were insufficient for the energy maintenance of respiratory metabolism. On the other hand, for the other long-term photoperiods, the light regime significantly influenced the production of microalgal biomass.

The results showed in Figure 1a indicated that the photoperiod of 22:2 h was the condition that presented equilibrium between the electric energy saving and the biomass productivity. For this reason, in the following study this photoperiod was evaluated in different frequencies (Figure 1b), as a strategy to improve the performance of the process. An improvement can be seen in the productivity of the process, as it increases the number of frequencies per day. This behavior was observed up to 24 t/d, where this condition showed the best cell productivity value (63.88 mg/L.h), followed by 48 t/d (58.22 mg/L.h).

It was also observed that the photoperiod of 24 times per day had biomass productivity 35.8% higher than experiments with constant illumination. This can be associated to the photoinhibition phenomenon, where, when the cells are exposed to a constant illumination, there may be an excess of light energy. This effect is caused by a photo-oxidation reaction inside the cell due to excess light that cannot be absorbed by the photosynthetic apparatus [21].

The short light/dark cycles are very fast alternations between high light intensities and darkness, also called a flashing light effect. This light condition has been experimentally proven to be one of the most promising light regimes in microalgal cultivation [7]. For this reason, the effects of short light/dark cycle on biomass productivity are shown in figure 1c. The best results are evidenced at 0.91:0.09 s (light: dark), with biomass productivity of 67.9 mg/L.h. Moreover, the photoperiods of 0.91:0.09, 0.83.0.17, and 0.75:0.25 s (light:dark) presented results of biomass productivity superior to the culture with constant illumination. The improvement of cellular growth under short photoperiods could be as a result of an enhanced dark respiration rates following a period of photosynthesis in light. This mechanism is known as enhanced postillumination respiration [7, 22].

Changes in light quantity not only affect photosynthesis and the growth rate of the microorganism, but also influence the activity of cellular metabolism and chemical composition of the biomass. Lipids are intracellular products of microalgae and for this reason the lipid

productivity is the product of lipid content and biomass productivity. Thus, the best lipid producer has to combine biomass productivity and lipid content [2]. In this sense, the Figure 1 shows the lipid productivity, and the Figure 2 shows the lipid content of microalgal biomass in all the conditions tested.

The best results for lipid production are evidenced at a frequency photoperiod of 24 t/d, which presents a lipid content of 28.02%, and a lipid productivity of 18.89 mg/L.h. On the other hand, the worst light condition for lipid production was at a long-term photoperiod of 12:12 h, whereas that, besides the low cell growth, also has low lipid content, resulting in a lipid productivity of 0.004 g/L.h. This may be due to the fact that lipid/glucan biosynthesis and carbon fixation occur during the light period and, moreover, light will normally stimulate fatty acid synthesis in order to convert excess light to chemical energy in order to avoid photo-oxidative damage [23].

Figure 2 also shows the biochemical composition in terms of the content of total proteins, and carbohydrates for all light conditions tested. In the protein fraction, a small variation between the light conditions was verified. The results showed that the increase of protein content correspond with the decrease of lipid content. The highest value (62.3%) was found in the photoperiod of 12:12 h, and the lower (41.2) was at frequency photoperiod of 24 t/d. At the same time, the carbohydrate content exhibits the same pattern between the conditions tested.
[Insert Figure 2]

The calorific value is another parameter that must be considered to determine the feasibility of biofuel feedstock production from microalgae [24]. Figure 2 also presents the calorific value for all the photoperiods evaluated. The improvement in calorific value is linked to the increase in lipid content rather than any change in other components such as protein and carbohydrates. As expected, the higher calorific value was found with a frequency photoperiod of 24 t/d (20.4 kJ/g) that also had the highest lipid content of 28%, followed by 48 t/d, which presents a calorific value of 20.2 kJ/g and lipid content of 27.32%. In the other words, these photoperiods are more viable for biodiesel production, in quantitative terms.

However, the qualitative profile of the lipid fraction should also be considered to choose an ideal growing condition for bioenergy production. Table 2 shows the fatty acid (FA) composition of the oil extracts from the sixteen light/dark cycle evaluated here. Eleven majority

FAs were identified and, as expected, there was variability in FA composition for the different light conditions.

In the long-term photoperiods, the light:dark cycle of 24:0, 22:2, and 20:4 h showed a similar profile, which is predominantly polyunsaturated (42.34-50.9%). In comparison, the photoperiod of 18:6 showed a predominantly saturated profile (53.37%), followed by polyunsaturated FAs (28.13%). On the other hand, the light cycle of 12:12 h was the condition with the highest fraction of SFA (80.5%), followed by MUFA (18.8%). In terms of lipid content, this photoperiod showed the lowest value among the long-term photoperiods. This could be explained by the fact that lipids and fatty acids were oxidized when cells require energy in the dark during insufficient light for photosynthesis. As unsaturations are prone to oxidation, the polyunsaturated FAs are firstly degraded [25, 26].

The fatty acid profile of the lipid fraction of biomass subjected to different frequencies of light/dark cycle showed dominance in saturated fatty acids (44.73-51.60%), followed by saturated ones (27.93-42.34%). The dominant fatty acids were palmitic acid (C16:0), α-linolenic acid (C18:3n6) and linoleic acid (C18:2n6) for all the treatments. In this set of data, there were no pronounced differences for lighting conditions.

Finally, in terms of the fatty acid profile of short photoperiods, the lipid fraction of biomass indicated that this lipid profile was completely different from the other light conditions tested, where saturated fatty acids (51.6-85.7%) were the majority for all short light/dark cycles, followed by monounsaturated ones (8.9-32.7%).

To assess the potential of biodiesel as a complement or substitute traditional diesel fuel in engines, the properties of biodiesel, such as density, viscosity, flash point, cold filter plugging point, solidifying point, and heating value, were determined. A comparison of these properties of biodiesel from microalgal oils and US [27], European [28], and Brazilian [29] biodiesel standards is shown in Table 3.

[Insert Table 3]

Different light conditions have shown a significant effect on the fatty acid profile and, as a result, biodiesel properties were also affected. The Table 3 demonstrated that except for the parameters cetane number and viscosity, all the photoperiods tested comply with the limits established by the international standards.

CN is a prime indicator of fuel quality related to the ignition quality of a fuel in a diesel engine. The CN of a diesel fuel is determined by the ignition delay time. A higher CN value means better ignition properties and engine performance. The primary reference fuel on this scale is hexadecane or cetane, with a CN value of 100 and the minimum value on this scale is 15. The international standards requires a minimum CN of 45 (ANP 255), 47 (ASTM D6751), or 51 (EN14214). According to Ramos et al. [30], the longer the fatty acid carbon chains and the more saturated the fatty acids, the higher the cetane number. This explanation was confirmed by the light regimes of 24:0 h, 22:2 h, 20:4 h, 1 t/d, 8 t/d, 12 t/d, and 48 t/d, which showed the highest PUFAs values and consequently lower CN values (below the values established by the highest international standards).

The kinematic viscosity of biodiesel is another significant fuel property. The main problems associated with this parameter are observed for high-viscosity oils. This high-viscosity affects the atomization of a fuel on injection into the combustion chamber and, thereby, ultimately the formation of engine deposits. For this reason, high viscosity is the major fuel property why neat vegetable oils have been largely abandoned as alternative diesel fuel. Conversely, Table 3 showed that all conditions tested were lower than that of international standards established for kinematic viscosity. Thus, both the problem of low viscosity microalgae biodiesel and high viscosity of vegetable oils could be solved by blending. Blending has been extensively used and is considered a good and feasible method to improve the biodiesel quality [31-33].

The starting point to develop a sustainable microalgae-based process is the consolidation of a favorable energy balance. In this sense, the Table 4 shows the energy balance of the microalgal culture in different light regimes.

[Insert Table 4]

A process is considered technically feasible, if the NEB is positive and the NER is less than 1 [34]. The results shown in Table 3 indicated that the energy required to supply the artificial lighting of the photobioreactor was lower than that produced in all light conditions, except for the photoperiod of 12:12 h (light:dark) that presented a negative NEB and a NER of 0.00034.

Moreover, the modulation of photoperiods demonstrated to be an effective strategy to reduce the energy requirements and increased energy produced, resulting in higher NER and NEB values than those found in cultures under constant illumination. Among all the conditions

tested, the best values to NER (38.53) and NEB (30.4) were found at a frequency photoperiod of 24 t/d, followed by 48 t/d with an NER and an NEB of 34.65 and 27.26, respectively.

Finally, in order to organize the observed data and facilitate the interpretation, a principal component analysis (PCA) was used. PCA is a powerful statistical tool to analyze the interrelationships among a large number of variables and to explain these variables in a reduced number of information (principal components).

The first PCA was performed to examine the relationship between the feedstock production parameters. Figure 1a and b shows the weights (variables) and scores (treatments), respectively, from the two major principal components. Together, the principal component 1 (PC1) and principal component 2 (PC2) explained 93.14% of the overall variance. Not surprisingly, the lipid content was highly correlated with the calorific value. It was evident that both protein and carbohydrates did not influence any of the oil production parameters. As discussed herein above, the lipids are intracellular products and, therefore, the lipid productivity depends on both the lipid content as biomass productivity. This relationship is clearly shown in Figure 3a. As the parameters NER and NEB are mainly based on biomass productivity, they were clustered together on the top left-hand of the plot. The Figure 3b shows that the light regimes clustered at the left lower quadrant are the conditions with the best results in terms of single-cell oil production.

PCA was also carried out to find out the relationship between the fatty acid profile and biodiesel properties of different culture treatments (Fig. 4a and b). As shown in Figure 4a and b, PCA1 and PCA2 explained 72.19% of the observed variation. It was clearly shown that the SFA content is closely related to CN and OS of the biodiesel, while the PUFA content is related to IV of the biodiesel. The Figure 4b explained that the short photoperiods and 12:12 h (light:dark) are linked to higher CN, OS and SFA content, whereas the other long-term photoperiods were associated with higher PUFA content. In the frequencies' photoperiods there was a balance between PUFA and MUFA. The short photoperiods are more related with the saturated fatty acids e, consequently with higher values of CN and OS.

[Insert Figure 3]

[Insert Figure 4]

4. Conclusion

The productivities of the process, chemical composition, calorific value of biomass, and properties of biodiesel were significantly influenced by the photoperiod. The condition that presented better both quantitative and qualitative values for biodiesel production was the frequency photoperiod of 24 times per day. The modulation of photoperiods demonstrated to be an effective strategy to improve the energy balance of the process, turning it feasible for the use of artificial lighting for microalgal biodiesel production.

Funding

The authors are grateful to the Coordination for the Improvement of Higher Education Personnel (CAPES) (grant number 001) for the financial support.

Conflict of interest

The authors declare that there is no conflict of interest regarding the publication of the manuscript.

References

1. Chen T, Liu J, Guo B, Ma X, Sun P, Liu B, Chen F (2015) Light attenuates lipid accumulation while enhancing cell proliferation and starch synthesis in the glucose-fed oleaginous microalga *Chlorella zofingiensis*. Nat Sci Rep 5:14936-14946.

2. Su F, Li G, Fan Y, Yan Y (2016) Enhanced performance of lipase via microcapsulation and its application in biodiesel preparation. Nat Sci Rep 6:29670-29682.

3. Chisti Y (2007) Biodiesel from microalgae. Biotechnol Adv 25:294-206.

4. Chu FF, Chu PN, Shen XF, Lam PKS, Zeng RJ (2014) Effect of phosphorus on biodiesel production from *Scenedesmus obliquus* under nitrogen-deficiency stress. Bioresour Technol 152:241-246.

5. Abomohra AEF, Jin W, El-Sheekh M (2016) Enhancement of lipid extraction for improved biodiesel recovery from the biodiesel promising microalga *Scenedesmus obliquus.* Energy Convers Manage 108:23-29.

6. Blanken W, Cuaresma M, Wijffels RH, Janssen M (2013) Cultivation of microalgae on artificial light comes at a cost. Algal Res 2: 333-340.

7. Abu-Ghosh S, Fixler D, Dubinsky Z, Iluz D (2015) Flashing light in microalgae biotechnology. Bioresour Technol 203:357-363.

8. Jacob-Lopes E, Scoparo CHG, Lacerda LMCF, Franco TT (2009) Effect of light cycles (night/day) on CO_2 fixation and biomass production by microalgae in photobioreactors. Chem Eng Process 48:306-310.

9. Takache H, Pruvost J, Marec H (2015) Investigation of light/dark cycles effects on the photosynthetic growth of *Chlamydomonas reinhardtii* in conditions representative of photobioreactor cultivation. Algal Res 8:192-204.

10. Zhou Q, Zhang P, Zhan G, Peng M (2015) Biomass and pigments production in photosynthetic bacteria wastewater treatment: Effects of photoperiod. Bioresour Technol 190:196-200.

11. George B, Pancha I, Desai C, Chokshi K, Paliwal C, Ghosh T, Mishra S (2015) Effects of different media composition, light intensity and photoperiod on morphology and physiology of freshwater microalgae *Ankistrodesmus falcatus* -A potential strain for bio-fuel production. Bioresour Technol 171:367-374.

12. Krzeminska I, Pawlik-Skowronska B, Trzcinska M, Tys J (2014) Influence of photoperiods on the growth rate and biomass productivity of green microalgae. Bioprocess Biosyst Eng 37:735-741.

13. Mitra M, Patidar SK, George B, Shah F, Mishra S (2015) A euryhaline *Nannochloropsis gaditana* with potential for nutraceutical (EPA) and biodiesel production. Algal Res 8:161:167.

14. Rippka R, Derulles J, Watrerbury JB, Herdman M and Stainer RY (1979) Generic assignments, strain histories and properties of pure cultures of cyanobacteria. J Gen Microbiol 111:1-61.

15. AOAC (2000) Official Methods of Analysis of AOAC International. AOAC International, Gaithersburg, MD, USA

16. Bligh EG, Dyer JW (1959) A rapid method of total lipid extraction and purification. Can J Biochem Physiol 37:911-917.

17. Watt BK, Merrill AL (1963) Composition of foods. Agriculture Handbook No 8. Dept. of Agriculture, Washington.

18. Hartman L, Lago RCA (1973) Rapid preparation of fatty acids methyl esters. Lab Practice 22:475-476.

19. Talebi AF, Tabatabaei M, Chisti Y (2014) Biodiesel Analyzer: a user-friendly software for predicting the properties of prospective biodiesel. Biofuel Res J 2:55-57.

20. Xue C, Goh QY, Tan W, Hossain I, Chen WN, Lau R (2011) Lumostatic strategy for microalgae cultivation utilizing image analysis and chlorophyll a content as design parameters. Bioresour Technol 102:6005-6012.

21. Seyfabadi J, Ramezanpour Z, Khoeyi JA (2011) Protein, fatty acid, and pigment content of Chlorella vulgaris under different light regimes. J Appl Phycol 23:721-726.

22. Falkowsk PG, Raven JA (1997) Aquatic Photosynthesis. Princeton University Press, New Jersey.

23. Queiroz MI, Hornes MO, Silva-Manetti AG, Jacob-Lopes E (2011) Single-cell oil production by cyanobacterium *Aphanothece microscopica Nägeli* cultivated heterotrophically in fish processing wastewater. Appl Energy 88:3438-3443.

24. Sharma KK, Schuhmann H, Schenk PM (2012) High Lipid Induction in Microalgae for Biodiesel Production. Energies 5:1532-1553.

25. Illman AM, Scragg AH, Shales SW (2000) Increase in *Chlorella* strains calorific values when grown in low nitrogen medium. Enzyme Microb Technol 27:631-635.

26. Lim KC, Zaleha K (2013) Effect of photoperiod on the cellular fatty acid composition of three tropical marine microalgae. Malays Appl Biol 42:41-49.

27. ASTM-American Society for Testing and Materials (2002) ASTM 6751 - Standard Specification for Biodiesel Fuel (B100) Blend Stock for Distillate Fuels. ASTM, West Conshohocken.

28. EN-European Standard (2003) UNE-EN 14214 - Automotive Fuel - Fatty Acid Methyl Esters (FAME) for Diesel Engine - Requirements and Test Methods. European Standard, Pilsen.

29. ANP-National Petroleum Agency (2003) ANP 255 - Provisional Brazilian Biodiesel Standard. ANP, Brasília.

30. Ramos MJ, Fernández CM, Casas A, Rodríguez L, Pérez A (2009) Influence of fatty acid composition of raw materials on biodiesel properties. Bioresour Technol 100:261-268.

31. Geacai S, Iulian O, Nita I (2015) Measurement, correlation and prediction of biodiesel blends viscosity. Fuel 143:268-274.

32. Gülün M, Bilgin A (2016) Two-term power models for estimating kinematic viscosities of different biodiesel-diesel fuel blends. Fuel Process Technol 149:121-130.

33. Mandotra SK, Kumar P, Suseela MR, Nayaka S, Ramteke PW (2016) Evaluation of fatty acid profile and biodiesel properties of microalga *Scenedesmus abundans* under the influence of phosphorus, pH and light intensities. Bioresour Technol 201:222-229.

34. Santos AM, Deprá MC, Santos AM, Zepka LQ, Jacob-Lopes E (2015) Aeration Energy Requirements in Microalgal Heterotrophic Bioreactors Applied to Agroindustrial Wastewater Treatment. Cur Biotechnol 5:249-254.

Table 1. Dilution rates (D) and residence time of batch culture (RTBC) of different light conditions.

Light regime	D (h^{-1})	RTBC (h)
Long-term photoperiods		
24:00	0.033	72
22:02	0.033	48
20:04	0.024	72
18:06	0.012	72
12:12	0.005	72
Frequency photoperiods		
2 t/d	0.017	72
4 t/d	0.027	48
8 t/d	0.023	48
12 t/d	0.034	48
24 t/d	0.039	48
48 t/d	0.041	48
Short photoperiods		
0.91:0.09	0.035	48
0.83:0.17	0.025	48
0.75:0.25	0.022	48
0.50:0.50	0.022	72

Table 2. Fatty acid composition of single-cell oil in different light regimes.

	Methyl ester (%)											
	C8:0	C10:0	C14:0	C16:0	C16:1	C18:0	C18:1	C18:2	C18:3n6	C18:3n3	C22:2	Minorities
Long-term photoperiods												
24:00	ND	ND	0.95±0.00	33.83±0.41	9.98±0.29	2.47±0.00	12.26±0.15	23.04±0.51	1.31±0.45	20.49±0.45	ND	1.16±0.27
22:02	ND	ND	1.88±0.00	36.82±0.31	3.57±0.18	2.58±0.00	10.05±0.40	21.08±0.29	1.64±0.00	19.62±0.52	ND	2.87±0.33
20:04	ND	ND	0.95±0.00	29.05±0.68	5.13±0.13	1.35±0.00	10.62±0.14	23.89±0.46	0.60±0.00	25.60±0.40	ND	2.81±0.29
18:06	ND	ND	1.24±0.00	49.34±0.46	2.97±0.15	1.77±0.03	15.52±0.19	6.07±0.15	0.86±0.00	21.20±0.30	ND	1.02±0.07
12:12	35.70±0.71	5.70±0.03	ND	34.00±0.27	5.80±0.08	2.60±0.01	5.70±0.05	1.70±0.05	0.40±0.00	0.40±0.00	4.10±0.15	4.2±0.45
Frequency photoperiods												
1 t/d	ND	ND	1.88±0.00	36.82±0.21	3.57±0.00	2.58±0.00	10.05±0.14	21.08±0.21	1.64±0.00	19.62±0.40	ND	1.94±0.24
2 t/d	ND	ND	1.60±0.00	47.36±0.55	2.76±0.00	1.50±0.00	14.01±0.18	8.18±0.01	0.75±0.00	22.69±0.51	ND	1.14±0.19
4 t/d	ND	ND	1.22±0.00	43.50±0.10	1.31±0.00	2.26±0.00	23.28±0.20	5.98±0.04	0.58±0.00	21.37±0.34	ND	0.51±0.11
8 t/d	ND	ND	1.30±0.00	42.42±0.18	1.66±0.00	2.53±0.00	15.91±0.14	10.92±0.18	1.28±0.01	23.42±0.52	ND	0.57±0.05
12 t/d	ND	ND	1.30±0.00	42.17±0.34	1.72±0.00	1.93±0.02	13.01±0.40	12.15±0.10	1.38±0.00	25.75±0.51	ND	0.79±0.10
24 t/d	ND	2.76±0.00	2.07±0.00	34.26±0.44	3.02±0.20	5.64±0.03	16.69±0.30	19.05±0.21	2.59±0.20	10.89±0.09	ND	3.02±0.34
48 t/d	ND	2.30±0.00	1.56±0.00	39.28±0.09	2.54±0.00	3.09±0.04	14.49±0.70	23.25±0.30	1.49±0.00	16.40±0.15	ND	3.00±0.29
Short photoperiods												
0.91:0.09	39.20±0.50	4.80±0.10	ND	36.60±0.60	3.00±0.06	2.90±0.11	5.80±0.51	0.40±0.00	0.70±0.00	0.20±0.00	2.90±0.14	3.30±0.40
0.83:0.17	1.20±0.40	0.20±0.00	1.30±0.00	44.70±0.91	9.10±0.17	2.80±0.15	19.60±0.88	13.80±0.15	1.20±0.01	ND	0.30±0.20	1.70±0.22
0.75:0.25	31.90±0.70	3.40±0.11	0.91±0.00	28.64±0.38	6.61±0.31	1.35±0.19	11.93±0.11	6.58±0.78	0.60±0.00	0.61±0.00	3.40±0.35	4.00±0.39
0.50:0.50	33.10±0.32	4.10±0.03	ND	34.00±0.17	6.20±0.66	2.80±0.15	5.70±0.02	1.20±0.00	0.60±0.00	0.20±0.00	3.30±0.14	7.90±0.45

Table 3. Properties of microalgal biodiesel produced in different photoperiods and its comparison with the standards used in the US (ASTM 6751), Europe (EN 14214) and Brazil (ANP 255).

Light regime	CN	IV (gI_2100g^{-1})	DU (%)	SV	LCSF (%)	CFPP (ºC)	CP (°C)	APE	BAPE	OS (h)	HVV (MJ/kg)	μ (mm^2s^{-1})	ρ ($g\ cm^{-3}$)
Long-term photoperiods													
24:00	44.25	118.12	110.24	218.54	4.62	-1.96	12.80	100.26	65.00	5.27	41.06	1.29	0.91
22:02	48.32	108.11	97.62	207.20	4.97	-0.86	14.38	94.05	63.00	5.40	38.82	1.22	0.86
20:04	44.13	119.709	113.75	205.87	3.58	-5.23	10.29	108.62	75.00	5.00	38.77	1.20	0.86
18:06	52.37	88.13	74.63	210.75	5.82	1.81	20.96	71.66	50.07	6.79	39.20	1.26	0.87
12:12	61.18	22.13	23.50	274.89	5.30	0.17	12.89	14.70	3.00	120.52	36.13	0.75	0.85
Frequency photoperiods													
1 t/d	48.26	108.26	97.78	207.36	4.97	-0.86	14.38	94.21	63.08	5.39	38.85	1.23	0.86
2 t/d	51.36	93.12	79.13	209.84	5.49	0.77	19.92	76.37	54.18	6.37	39.05	1.25	0.87
4 t/d	52.29	90.55	78.55	207.02	5.48	0.74	17.89	77.24	47.98	6.96	38.91	1.26	0.86
8 t/d	49.77	101.43	87.41	207.60	5.51	0.83	17.32	85.75	58.92	5.97	38.99	1.25	0.87
12 t/d	47.78	109.32	93.03	209.34	5.18	-0.20	17.19	91.31	66.15	5.60	39.26	1.24	0.87
24 t/d	51.15	95.25	88.09	207.66	6.25	3.16	18.06	87.21	49.33	6.27	38.65	1.23	0.86
48 t/d	46.58	106.24	98.75	225.65	6.82	4.95	15.67	96.82	61.17	5.52	42.02	1.34	0.93
Short photoperiods													
0.91:0.09	61.00	19.56	20.00	285.69	5.81	1.78	14.26	14.50	4.80	93.31	36.99	0.75	0.87
0.83:0.17	60.33	56.27	59.90	204.46	6.27	3.22	18.52	50.60	16.80	10.45	37.62	1.25	0.83
0.75:0.25	57.73	40.49	42.74	265.73	5.19	-0.17	10.07	33.03	11.80	19.44	36.77	0.83	0.86
0.50:0.50	59.22	32.18	30.7	270.71	7.15	5.99	12.89	22.90	11.20	61.56	37.02	0.83	0.87
International standards													
ANP 255	min. 45	-	-	-	-	max. 19	-	-	-	-	-	-	-
ASTM 6751	min. 47	-	-	-	-	-	-	-	-	min. 3	-	1.9-6.0	-
EN 14214	min. 51	max. 120	-	-	-	-	-	-	-	min. 6	-	3.5-5.0	-

Table 4. Analysis of the net energy ratio (NER) and net energy balance (NEB) of the microalgal culture in different light regimes

Light regime	Energy requeriments (MJ/d)	Energy produced (MJ/d)	NER	NEB
Long-term photoperiods				
24:00	0.89	21.84	24.53	-20.95
22:02	0.81	21.44	26.47	-20.63
20:04	0.74	8.58	11.60	-7.84
18:06	0.66	6.50	9.84	-5.84
12:12	0.44	0.00015	0	0.43
Frequency photoperiods				
1 t/d	0.81	21.44	26.47	-20.63
2 t/d	0.81	13.34	16.46	-12.53
4 t/d	0.81	16.65	20.55	-15.84
8 t/d	0.81	18.26	22.54	-17.45
12 t/d	0.81	23.61	29.15	-22.8
24 t/d	0.81	31.21	38.53	-30.4
48 t/d	0.81	28.07	34.65	-27.26
Short photoperiods				
0.91:0.09	0.81	28.13	34.72	-27.32
0.83:0.17	0.74	14.25	19.25	-13.51
0.75:0.25	0.66	12.03	18.22	-11.37
0.50:0.50	0.44	10.91	24.79	-10.47

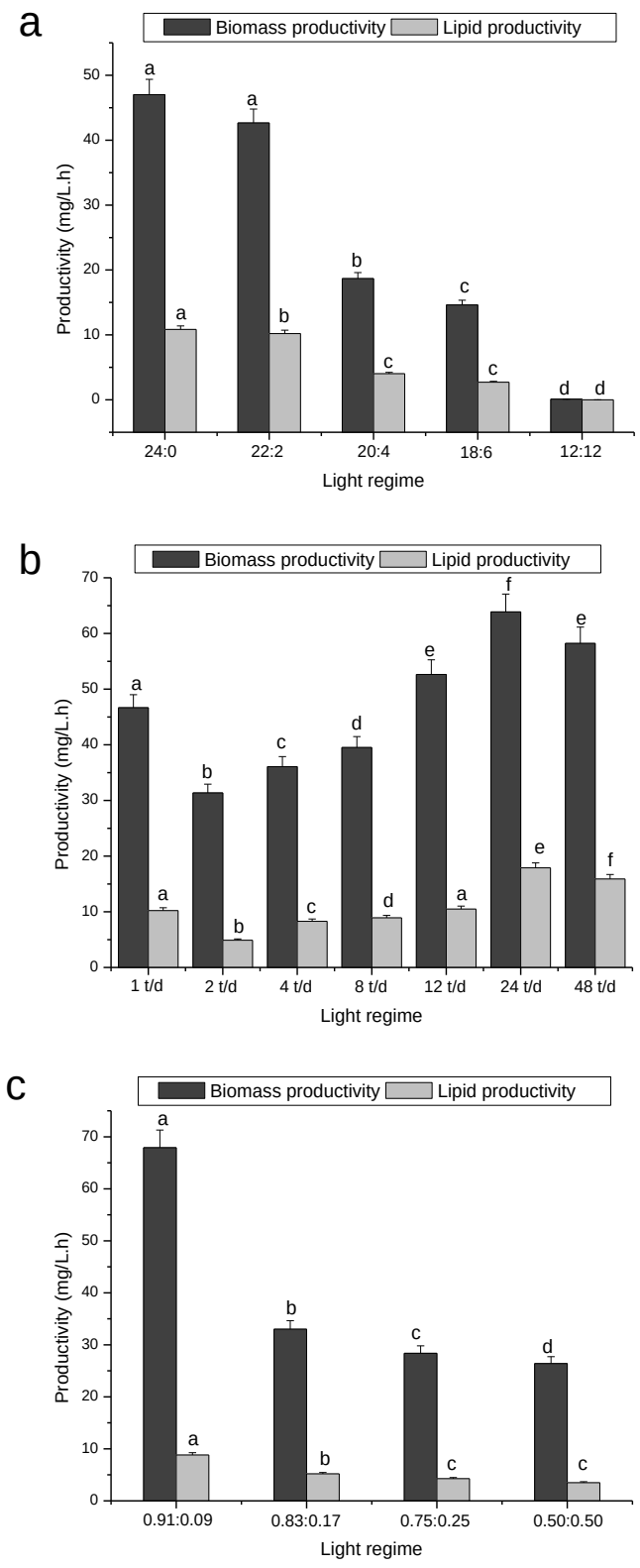

Figure 1. Effects of long-term photoperiods (a), frequency photoperiods (b) and short photoperiods (c) on the biomass and lipid productivity. Same letters indicate that data did not differ statistically (Tukey test, $p \leq 0.05$).

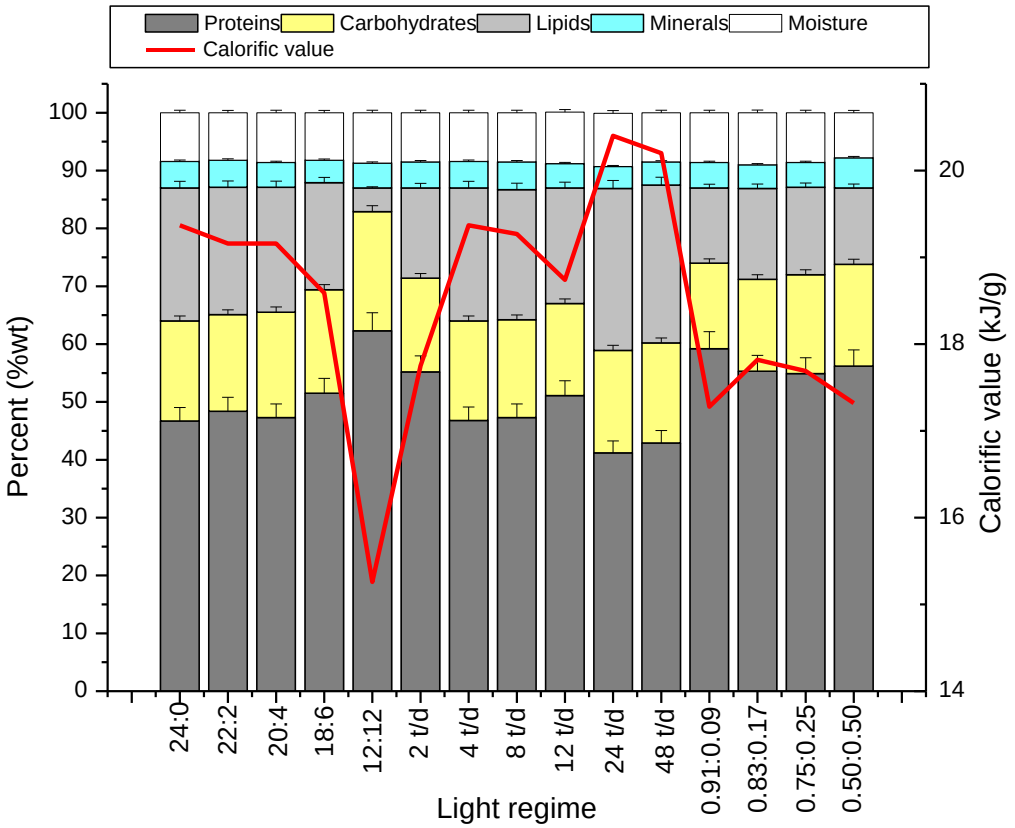

Figure 2. Biochemical composition and energy value of the microalgal biomass in different photoperiods.

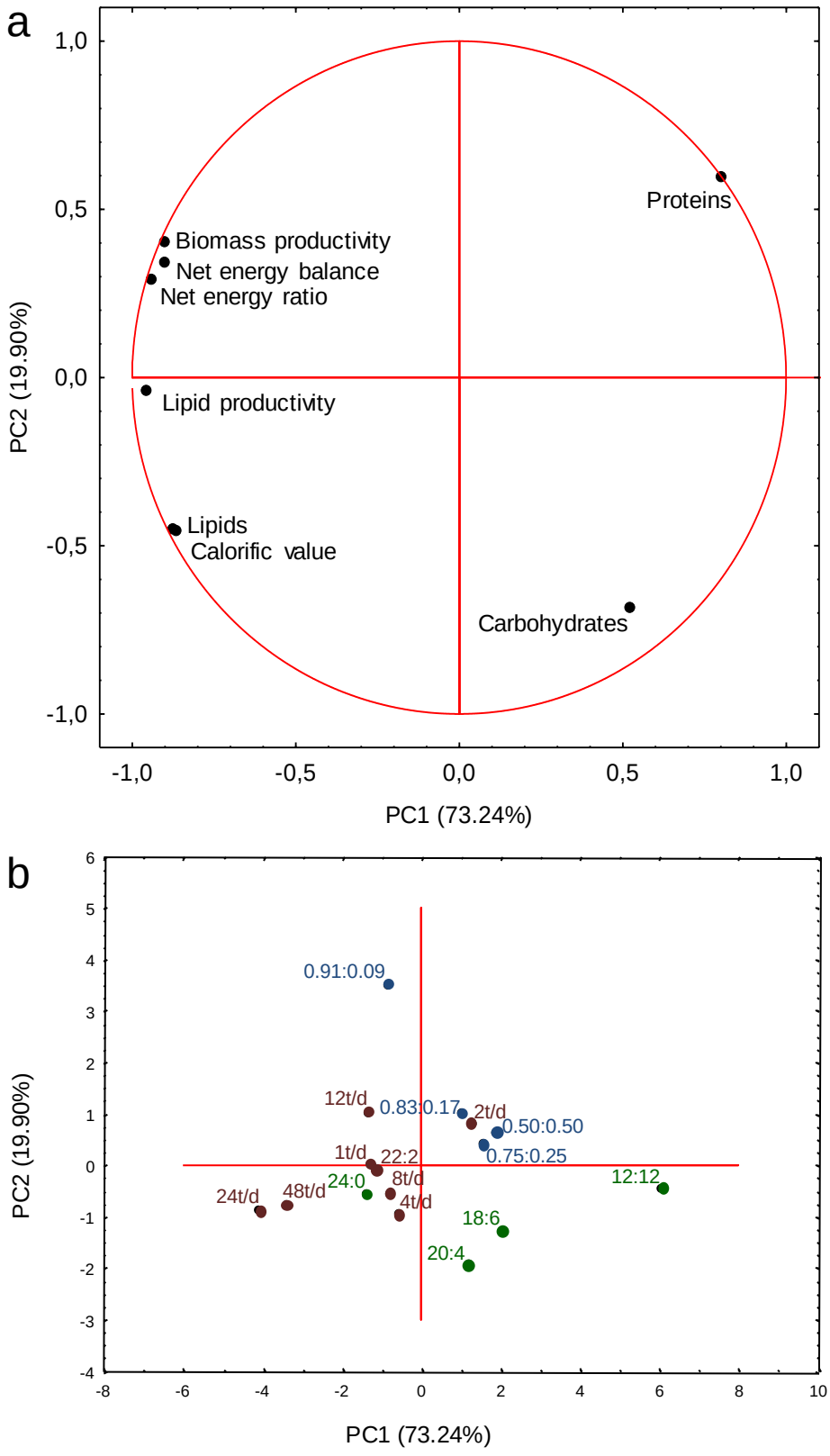

Figure 3. PCA of chemical composition, calorific value, productivities and energy balance (a), under different light conditions (b).

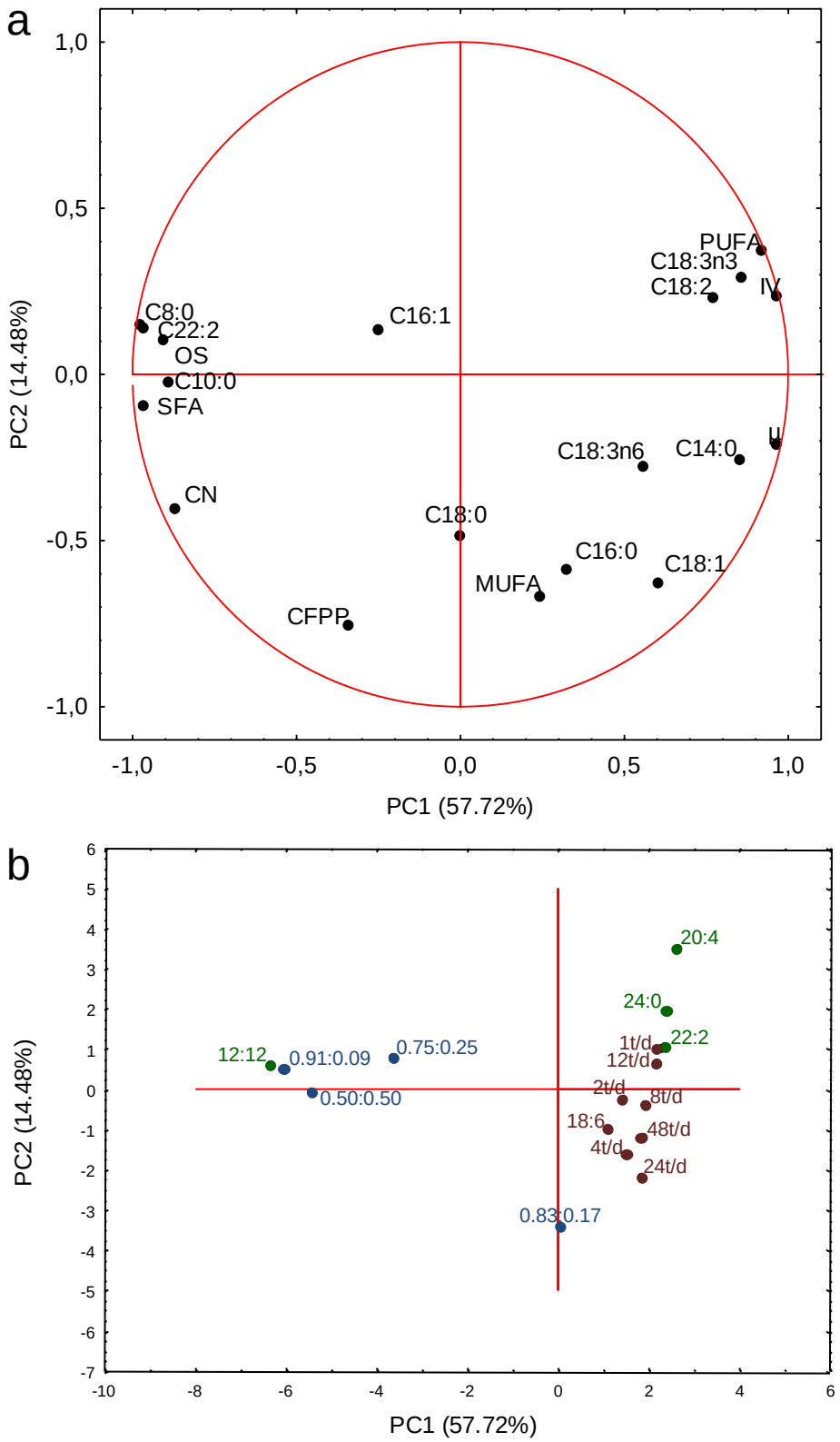

Figure 4. PCA of fatty acid profile and fuel properties (a), under different light conditions (b).

CAPÍTULO 6

Artigo 1: Esterified carotenoids as new food components in cyanobacteria

Publicado na revista Food Chemistry, v. 287, p. 295–302 (2019)

Food Chemistry 287 (2019) 295–302

Contents lists available at ScienceDirect

Food Chemistry

journal homepage: www.elsevier.com/locate/foodchem

Esterified carotenoids as new food components in cyanobacteria

Mariana Manzoni Maroneze[a], Eduardo Jacob-Lopes[a], Leila Queiroz Zepka[a], María Roca[b], Antonio Pérez-Gálvez[b,*]

[a] Department of Food Science and Technology, Federal University of Santa Maria (UFSM), 97105-900 Santa Maria, RS, Brazil
[b] Food Phytochemistry Department, Instituto de la Grasa (CSIC), University Campus, Building 46, 41013 Sevilla, Spain

ARTICLE INFO

Chemical compounds studied in this article:
9-Cis-violaxanthin (PubChem CID: 5282218)
9-Cis-neoxanthin (PubChem CID: 101052392)
Zeaxanthin (PubChem CID: 5280899)
Zeinoxanthin (PubChem CID: 5281234)
Echinenone (PubChem CID 5281236)
α-Carotene (PubChem CID: 6419725)
β-Carotene (PubChem CID: 5280489)

Keywords:
Aphanotece
Cyanobacteria
Carotenoid esters
Esterification
Mass spectrometry
Phormidium

ABSTRACT

Among the nutritional properties of microalgae, this study is focused in the presence of carotenoid esters in prokaryote microalgae, an event that has not been shown so far. Three carotenoid esters that accumulate in non-stressful culture conditions are identified in *Aphanotece microscopica* Nägeli and *Phormidum autumnale* Gomont, what may provide an extra value to the quality attributes of the carotenoid profile in cyanobacteria as functional foods. In addition, new data on the carotenoid characterization added quality criteria for the identification of the esterified metabolites, enabling the monitoring of these food components. Specifically, the metabolomic approach applied to the food composition analysis, has allowed to differentiate between the esters of zeinoxanthin and β-cryptoxanthin, which were undifferentiated to date during the MS characterization of carotenoids in other food sources. We propose a new qualifier product ion specific for zeinoxanthin ester, which it is not present in the MS^2 spectrum of β-cryptoxanthin esters.

1. Introduction

Most of microalgae biotechnology companies concentrate investments and technology in low-volume high-value food products, which can be successfully allocated in lines of business with high projected returns and growing demands. This is the case of the microalgae market for production of secondary metabolites, a cluster of healthy food components with attractive selling prices and significant applications in the development of functional food products. Microalgae carotenoids represent a model of success in terms of economic viability that competes in a global market value of $1.4 billion with an estimated annual growth rate of 2.3% (Liu et al., 2016). Indeed, the alternative chemical synthesis of carotenoids presents a limited use for human consumption due to safety concerns, so that natural sources of carotenoids are the production platform for the nutraceutical market (Gong & Bassi, 2016). Microalgae present several advantages as carotenoid sources in comparison with higher plants, including faster growth rate, greater specific carotenoid content and higher versatility to different cultivation conditions. Consequently, a large group of food industries produce carotenoids from microalgae, with astaxanthin in the pool position followed by β-carotene and lutein, with promising market values in the range of $230-$447 million (Panis & Rosales Carreon, 2016).

Several strategies are applied to improve the carotenoid production in microalgae, from genetic modifications to the implementation of new technologies, as well as diverse environmental growing settings. Hence, for secondary carotenoids (astaxanthin, canthaxanthin, zeaxanthin or fucoxanthin) and some primary carotenoids (β-carotene) the nutrient-stressed, high light and high salt conditions are factors that promote the quantities of carotenoids accumulated in the eukaryote microalgae (Lemoine & Schoefs, 2010). Biologically, the high accumulation of specific carotenoids is a strategy to store energy and carbon supplies for future stressful conditions, and to enhance the cell resistance to oxidative stress (Lemoine & Schoefs, 2010). This spectacular carotenogenesis induced in eukaryote microalgae by stressful environment implies morphological and metabolic modifications in the cells, which have been intensely studied in eukaryote microalgae considering the economic value of those metabolites and their industrial applications. The most extensively studied taxa are *Dunaliella salina* to produce β-carotene and *Haematococcus pluvialis* for the extraction of astaxanthin.

An interesting biological consequence of the intense

* Corresponding author.
E-mail addresses: jacoblopes@pq.cnpq.br (E. Jacob-Lopes), zepkaleila@yahoo.com.br (L. Queiroz Zepka), mroca@ig.csic.es (M. Roca), aperez@ig.csic.es (A. Pérez-Gálvez).

https://doi.org/10.1016/j.foodchem.2019.02.102
Received 9 October 2018; Received in revised form 1 February 2019; Accepted 20 February 2019
Available online 28 February 2019
0308-8146/

carotenogenesis in eukaryote microalgae is the activation of the esterification process of the secondary carotenoids with fatty acids. In this sense, only a significant accumulation of esterified carotenoids has been described for different Chlorophyte species, *Haematococcus pluvialis*, *Chlamydomonas nivalis*, and *Chlorella zofingiensis* (Lemoine & Schoefs, 2010). The esterification of carotenoids is one incompletely comprehended metabolic process, frequently associated with the ripening of carotenogenic fruits such as peppers (Breithaupt & Schwack, 2000) or oranges (Giuffrida, Dugo, Salvo, Saitta, & Dugo, 2010), flowers and cereals (Ziegler et al., 2015). This reaction proceeds only with xanthophylls that carry at least one hydroxyl group, which reacts with the carboxylic group of the fatty acid, yielding an ester bond. During the carotenogenic process, the chloroplasts are transformed into chromoplasts, where the esterified carotenoids are accumulated in the corresponding plastoglobules. The accumulation of esterified carotenoids is well-documented in fruits and vegetables and recent reviews compile the current available information (Bunea, Socaciu, & Pintea, 2014; Mercadante, Rodrigues, Petry, & Mariutti, 2017).

From the nutritional point of view, the *ester* condition is considered a positive extra attribute that enhances several characteristics of the xanthophylls, and a growing number of evidences are becoming available to support this point. Thus, it has been shown that xanthophyll esters are more stable to UV-radiation and thermal treatment than the free forms in model systems (Bunea et al., 2014), and they present an increased quenching ability that results in higher antioxidant activity in both *in vivo* eukaryote microalgae organisms (Kobayashi, 2000) and *in vitro* systems (Sun et al., 2011). Additionally, bioavailability of carotenoid esters is relatively higher than that of the free carotenoid (Mariutti & Mercadante, 2018). However, the *ester* attribute is lost during intestinal digestion/cellular absorption (Pérez-Gálvez & Mínguez-Mosquera, 2005) and only the free forms have been observed in plasma (Wingerath, Stahl, & Sies, 1995). Consequently, it could be assumed that the extra value of the *ester* feature is to increase their bioavailability. Anyhow, a significant re-esterification process has been recently discovery in human tissues (Ríos et al., 2017). Nevertheless, the added benefits of xanthophylls in their ester form could be still functional during the gastrointestinal transit. Thus, esterified astaxanthin from *Haematococcus pluvialis* has been shown to protect from oxidative stress caused by ethanol-induced gastric ulcers in rat (Kamath, Srikanta, Dharmesh, Sarada, & Ravishankar, 2008) and in murine gastric ulcer models (Murata, Oyagi, Takahira, Tsuruma, Shimazawa, Ishibashi, & Hara, 2012) and attention has been focused in the possible modulation of carcinogenesis in the gastrointestinal tract (Amaro et al., 2013).

Despite these progresses in knowledge, the esterification of eukaryote microalgae carotenoids has been exclusively investigated in Chlorophyte, as a process resulting from stress factors (Lemoine & Schoefs, 2010) and referred to both astaxanthin and fucoxanthin esters. The search of the accumulation of xanthophyll esters beyond astaxanthin has recently started to be accomplished, describing the presence of zeaxanthin esters in the *Coelastrella* sp. KGU-Y002 (Saeki, Aburai, Aratani, Miyashita, & Abe, 2017) and in other eukaryote microalgae classes. This is the case of *Nannochloropsis gaditana* (Simionato et al., 2013) from the Scenedesmaceae family that accumulates violaxanthin, antheraxanthin, zeaxanthin and vaucheriaxanthin esters. Therefore, this scenario opens the door to the optimization process to increase the accumulation of xanthophyll esters as added-value food components.

However, the acquisition of successful approaches to enhance the metabolism of microalgae lipids requires the application of high-resolution analytical tools to obtain a clear picture of the food components. The hypothesis of this study was to determine the presence of carotenoid esters in prokaryote microalgae, as valuable components that have not been detected so far. Briefly, we used axenic cultures of *Aphanotece microscopica* Nägeli and *Phormidum autumnale* Gomont, which were grown under non-stressing conditions. We isolated the pigment fraction and the extracts were analyzed by HPLC-high resolution-MS^n applying a data processing protocol dedicated to metabolomics of carotenoids (Pérez-Gálvez, Sánchez-García, Garrido-Fernández, & Ríos, 2018). With these metabolomic tools we were able to identify three carotenoid esters that accumulated in non-stressful culture conditions what may provide an extra value to the quality attributes of the carotenoid profile in cyanobacteria as functional foods for production of added-value products.

2. Materials and methods

2.1. Microorganisms and cultivation conditions

Axenic cultures of *Aphanothece microscopica* Nägeli (rsman92) were originally isolated from the Patos Lagoon Estuary, at the state of Rio Grande do Sul, Brazil (32°01′s − 52°05′w). The strain is within the collection of the Cyanobacteria and Phycotoxins Laboratory of the Institute of Oceanography from the Federal University of Rio Grande - FURG (www.cianobacterias.furg.br). Axenic cultures of *Phormidium autumnale* were originally isolated from the Cuatro Cienegas desert, Mexico (26°59′ N, 102°03′ W). The strains were propagated and maintained in synthetic BG-11 medium (Rippka, Deruelles, Waterbury, Herdman, & Stanier, 1979).

2.2. Microalgal biomass production

The biomass production was carried in a bubble column photobioreactor, operating in intermittent regime, fed with 2.0 L of BG11 medium (Rippka et al., 1979). The experimental conditions were as follows: initial concentration of inoculum of 100 mg/L, temperature of 26 °C, aeration of 1 vol of air per volume of medium per minute, a photon flux density of 25 μmol m^{-2} s^{-1}, a light cycle of 24:0h (light:dark), and a residence time of 168 h.

2.3. Reagents

All the chemical compounds used for the BG-11 medium, sodium chloride, ammonium acetate (98%) and tetrabutylammonium acetate were supplied by Sigma-Aldrich Chemical Co. (Madrid, Spain). Acetone and diethyl ether (analysis grade) were supplied by Teknokroma (Barcelona, Spain). *N,N*-dimethylformamide (DMF) and hexane (analysis grade) and methanol, methyl *tert*-butyl ether and water (HPLC grade) were supplied by Panreac (Barcelona, Spain). The deionised water used was obtained from a Milli-Q 50 system (Millipore Corp., Milford, MA, USA). Solutions of carotenoid standards α-carotene, β-cryptoxanthin and β-cryptoxanthin esters, echinenone, myxoxanthophyll, neoxanthin and violaxanthin isolated from natural sources were obtained following the procedures described by Britton et al. (1995), while zeaxanthin and β-carotene standards were obtained from Extrasynthese (Genay Cedex, France). Aliquots of the carotenoid standard solutions were analysed with the same experimental conditions and the UV–visible and bbCID MS^n spectra were acquired and compared with those obtained from the microalgae extracts, so that direct experimental criteria were applied for identification of known carotenoids. Standards of zeinoxanthin and β-cryptoxanthin epoxides were not available, so that identification was performed according to literature data.

2.4. Extraction of pigments

Microalgae biomass aliquots (5 mL) were filtered under vacuum through a 47-mm diameter glass microfiber filter (GF/F; Whatman), and immediately frozen at −80 °C (Wright et al., 1991). The filtered microalgae was mixed with liquid nitrogen and grinded into powder in a mortar. Then, this powder was mixed with 10 mL of extraction solvent, DMF: deionised water (9:1) under stirring at 4 °C for 15 min and centrifuged (10,000 rpm, 5 min). The organic layer was accumulated in

a decanting funnel, while the solid residue was re-extracted with 10 mL hexane, mixed in an ultrasonic bath (5 min, 720 W), vortexed (5 min), and after the addition of 10 mL NaCl solution (10% w/v) the mixture was centrifuged (10,000 rpm, 5 min). The supernatant was added to the funnel and the pellet was re-suspended with 10 mL diethyl ether, mixed in an ultrasonic bath (5 min, 720 W), vortexed (5 min), and finally centrifuged (10,000 rpm, 5 min) after the addition of 10 mL NaCl solution (10% w/v). The combined solvent fractions in the funnel were extracted with diethyl ether and NaCl solution (10% w/v). The upper phase was isolated and concentrated to dryness in a rotary evaporator. The residue was dissolved in acetone. Samples were stored at −20 °C until analysis.

2.5. Pigments identification by HPLC-PDA-APCI(+)-hrTOF-MS^n

The chromatographic separation was performed using a liquid chromatograph Dionex Ultimate 3000RS U-HPLC (Thermo Fisher Scientific, Waltham, MA, USA). For carotenoid pigments a C_{30} 3 µm particle size reversed-phase YMC analytical column (250 × 4.6 mm, YMC Europe, Dinslaken, Germany) was used. The elution gradient applied for this group of pigments was based on the method published by Breithaupt, Wirt, and Bamedi (2002), and it has been recently modified (Ríos, Roca, & Pérez-Gálvez, 2015). The injection volume was 30 µL with 1 mL/min as the flow rate. UV–visible spectra were recorded by a PDA detector at the 300–700 nm wavelength range. A split post-column of 0.4 mL/min was introduced directly on the mass spectrometer ion source. Mass spectrometry was performed using a micrOTOF-QIITM High Resolution Time-of-Flight mass spectrometer (UHR-qTOF) with Qq-TOF geometry (Bruker Daltonik, Bremen, Germany). The instrument equipped with an APCI source was operated in positive ion mode using a scan range of *m/z* 50–1200 Da. The full scan mode was applied for initial characterizations, while extracted ion chromatogram mode was employed during the study of the MS^n of the new carotenoids. The mass spectra acquisition was a broad-band collision induced dissociation mode (bbCID), providing at the same time MS and MS^2 spectra. The software used for the instrument control was Hyphenation Star PP (version 3.2, Bruker Daltonik, Bremen, Germany) and DataAnalysis (version 4.1, Bruker Daltonik, Bremen, Germany) for evaluation of MS spectra. The software TargetAnalysis™ 1.2 allowed the automated peak detection on the extracted ion chromatograms and the identification according to mass accuracy and in combination with the isotopic pattern in the SigmaFit™ algorithm (Ríos et al., 2015). The tolerance limits were set at 5 ppm for mass accuracy and 50 for SigmaFit values. The SmartFormula3D™ software module allowed the interpretation of the MS^2 spectra (Ríos et al., 2015) as well as for checking the consistency of the product ions with the same criteria for mass accuracy and isotopic pattern established for the corresponding protonated molecule. *In silico* MS^2 spectra were obtained for target compounds with the MassFrontier™ software (Thermo Scientific™ version 4.0, Waltham, USA) to perform the evaluation of experimental MS^2 and the acquisition of both analogue and diverging theoretical product ions when different structural isomers were possible for a single bbCID spectrum.

3. Results and discussion

3.1. Carotenoid profile

Table 1 shows the chromatographic and spectrometric parameters that have allowed the identification of the carotenoid profile in the cyanobacteria: the maxima wavelength value of each UV–visible spectrum, exact mass (Da), error mass (ppm) and the mSigma matching factor between the theoretical and experimental isotopic patterns (Pérez-Gálvez et al., 2018) that fulfil the established tolerance limits, as well as the main experimental characteristic product ion(s), which have been described in literature (Van Breemen, Dong, & Pajkovic, 2012; Rivera, Christou, & Canela-Garayoa, 2014). These product ions

Table 1
Carotenoids identified in *Aphanotece microscopica* Nagëli (A) and *Phormidium autumnale* Gomont (P) by HPLC-PDA-APCI(+)-hrTOF-MS^n.

Peak	Carotenoid	Strains	t_R (min)	Wavelength maxima (nm)	$[M+H]^+$ (*m/z*)	Mass error (ppm)	mSigma	Main product ions (*m/z*)
1	*cis*-violaxanthin	A, P	5.9	412, 434, 463	599.4126[a]	4.3	29.5	581.4002 $[M+H-18]^+$, 477.3559 $[M+H-3\text{-hydroxy-ring}]^+$
2	*cis*-neoxanthin	A	6.3	412, 434, 462	599.4113[a]	2.2	32.9	583.4400 $[M+H-18]^+$
3	*all-trans*-zeaxanthin	A, P	17.2	425, 450, 476	569.4368	2.6	18.1	551.3379 $[M+H-18]^+$, 477.3571 $[M+H-92]^+$
4	5,6-epoxy-β-cryptoxanthin	A	20.0	420, 444, 470	569.4373	3.5	32.1	551.3251 $[M+H-18]^+$
5	*all-trans*-zeinoxanthin	P	26.0	420, 448, 472	553.4386	3.3	19.0	535.4295 $[M+H-18]^+$, 461.3349 $[M+H-92]^+$, 377.2892 $[M+H-9,10C]^+$, 337.2524 $[M+H-12,13C]^+$
6	2′-linolenoyl-myxol ester	A	26.5	446, 470, 502	829.6506[b]	3.4	14.6	607.4155 $[M+H-C_{15}H_{26}\text{-}18]^+$, 567.4214 $[M+H\text{-}FA]^+$[c], 493.3881 $[M+H\text{-}FA\text{-}56]^+$, 475.3568 $[M+H\text{-}FA\text{-}92]^+$
7	*all-trans*-echinenone	A, P	27.7	461	551.4257	1.8	10.4	533.4121 $[M+H-18]^+$, 495.3632, 459.3641 $[M+H-92]^+$
8	*cis*-5,8-epoxy-β-cryptoxanthin	A	28.3	402, 426, 450	569.4325	4.9	32.1	551.3237 $[M+H-18]^+$
9	*cis*-echinenone	A, P	29.4	455	551.4236	2.0	13.0	533.4153 $[M+H-18]^+$, 495.3641, 459.3690 $[M+H-92]^+$
10	myristoyl-zeinoxanthin ester	P	31.2	420, 448, 472	763.6385	1.0	14.2	731.6136 $[M+H\text{-}CH_4O]^+$, 535.4298 $[M+H\text{-}FA]^+$ 507.4211 $[M+H\text{-}14,15C]^+$, 443.3657 $[M+H\text{-}FA\text{-}92]^+$, 399.3046 $[M+H\text{-}FA\text{-}7,8C]^+$
11	myristoyl-β-cryptoxanthin ester	A	32.1	424, 450, 472	763.6389	1.0	16.4	731.6130 $[M+H\text{-}\ CH_4O]^+$, 535.4305 $[M+H\text{-}FA]^+$, 507.4202 $[M+H\text{-}14,15C]^+$, 443.3663 $[M+H\text{-}FA\text{-}92]^+$
12	9-*cis*-α-carotene	A, P	32.3	330, 420, 444, 472	537.4443	2.2	18.5	453.3683 $[M+H-84]^+$
13	*all-trans*-β-carotene	A, P	36.6	424, 451, 477	537.4436	3.6	16.6	457.33770 $[M+H-80]^+$, 413.3107 $[M+H-124]^+$
14	9-*cis*-β-carotene	A, P	38.0	340, 420, 446, 472	537.4455	0.0	28.2	457.3765 $[M+H-80]^+$, 413.3155 $[M+H-124]^+$

[a] Protonated ion arising from the $M^{+\cdot}$ radical ion.
[b] $[M+H-18]^+$.
[c] FA means fatty acid.

Table 2
Carotenoids quantified (percent area at 450 nm) in *Aphanotece microscopica* Nagëli and *Phormidium autumnale* Gomont by HPLC-PDA.

Peak	Carotenoid	*Aphanotece microscopica*	*Phormidium autumnale*
1	*cis*-violaxanthin	0.82	0.67
2	*cis*-neoxanthin	0.69	0.66
3	*all-trans*-zeaxanthin	4.35	3.70
4	5,6-epoxy-β-cryptoxanthin	1.37	–
5	*all-trans*-zeinoxanthin	–	0.41
6	2′-linolenoyl-myxol ester	0.91	–
7	*all-trans*-echinenone	7.96	6.00
8	*cis*-5,8-epoxy-β-cryptoxanthin	0.72	–
9	*cis*-echinenone	10.1	9.52
10	myristoyl-zeinoxanthin ester	–	0.79
11	myristoyl- β-cryptoxanthin ester	1.46	–
12	9-*cis*-α-carotene	0.70	0.22
13	*all-trans*- β-carotene	67.5	69.4
14	9-*cis*-β-carotene	3.42	8.63

correspond with the loss of water $[M+H\text{-}18]^+$, toluene $[M+H\text{-}92]^+$, $[M+H\text{-}124]^+$, $[M+H\text{-}40]^+$, $[M+H\text{-}56]^+$, $[M+H\text{-}80]^+$, $[M+H\text{-}84]^+$, or in-chain losses. Table 2 contains the percent area values for the identified carotenoids in both cyanobacteria species that present the typical carotenoid pattern of the cyanobacteria phylum, rich in β-carotene, echinenone and zeaxanthin and absence of lutein. Specifically, the carotenoid profile is dominated by the group of carotenes that account more than 70% of the total carotenoids in both species. Echinenone (*trans* and *cis* isomers) is the first signifying xanthophyll (15–18%) followed by zeaxanthin (around 4%). Other minor xanthophylls (neoxanthin, violaxanthin, zeinoxanthin, 5,6-epoxy-β-cryptoxanthin and 5,8-epoxy-β-cryptoxanthin) have been also identified in both strains previously (Patias et al., 2017). The most known species of *Aphanotece* is *Aphanotece halophytica* (Berland, Le Campion, & Campos, 1989) with a similar carotenoid content as the one described here for *Aphanotece microscopica* Nägeli.

3.2. Esterified carotenoids

In addition to the carotenoids identified in Table 1, the HPLC chromatogram of the pigments extracted from cyanobacteria (Fig. 1) showed three signals with the characteristic UV–visible pattern of carotenoids (peaks 6, 10, 11) that eluted at the apolar region of the chromatogram. Recently, it has been summarized the main MS^2 characteristic product ions formed using APCI in positive mode for xanthophyll esters: loss of toluene (92 Da) as the featured neutral loss from the polyene chain, the backbone of the xanthophyll and the loss of the fatty acid (Mercadante et al., 2017).

The first unknown pigment (peak 6, at 26.5 min.) was exclusively observed in *Aphanotece microscopica* and exhibits the maximum absorbance value at 472 nm wavelength in the UV–Visible spectrum (Fig. 1), which is limited to few carotenoids. Specifically, in the carotenoid pigment profile of this cyanobacteria (Patias et al., 2017), the only carotenoid identified with similar absorbance spectrum is myxoxanthophyll. In this carotenoid kind, which it is exclusive of cyanobacteria, the carotenoid (myxol) is bonded to different glycosides at the hydroxyl group of the *C*2′ of the ψ-end group (Takaichi, Mochimaru, & Maoka, 2006). Particularly, in *Aphanotece microscopica*, the accurate mass from the $[M+H\text{-}18]^+$ protonated molecule was observed at m/z = 829.6506 Da corresponding to the elemental composition $C_{58}H_{86}O_2$. Four characteristic product ions were obtained in the bbCID spectrum of this pigment (Table 1, Fig. 2, Fig S1). The product ion at m/z = 567.4214 Da ($C_{40}H_{55}O_2$) arises from the release of the fatty acid (280 Da, Fig. 2a) and the product ion at m/z = 475.3568 Da ($C_{33}H_{47}O_2$) could be assigned to the combined release of both the fatty acid and one in-chain unit of toluene (Fig. 2b), features that match with the characteristic MS^2 profile of an esterified xanthophyll. Two additional product ions were new fragmentations. The product ion at m/z = 607.4155 Da corresponds to an atypical fragmentation of the fatty acid that generates a compound with $C_{42}H_{55}O_3$ as elemental composition (Fig. 2c). Finally, the neutral loss of 354 Da ($C_{21}H_{38}O_4$) agreed with the fragmentation at the 12,13-carbon bond remaining the charge in the originally esterified 2′ carbon atom (Fig. 2d). These experimental product ions were predicted *in silico* by the MassFrontier™ software, and they fulfilled the quality criteria for the mass error and mSigma value. The combination of all the MS data obtained for the peak 6, allowed us to tentatively identify this carotenoid as 2′-linolenoyl-myxol-ester. Esterification at the 3-hydroxy-β-ring was discarded by the *in silico* prediction of the fragmentation pattern of the 3-linolenoyl-myxol-ester that did not include the product ion observed at m/z = 493.3881 Da (Fig. 2d) that it is exclusive of the unimolecular decomposition profile of the 2′-linolenoyl-myxol-ester. This carotenoid has not been previously identified, and even the detection of the free form (myxol) is scarce (Takaichi et al., 2006). The presence of similar structures has been reported in few species of bacteria (*Rhodococus* and *Gordonia*), the so-called glucosyl mycoloyl esters (Takaichi, Maoka, Akimoto, Carmona, & Yamaoka, 2008).

In *Phomidium autumnale*, the peak 10 at 31.2 min showed a UV–visible spectrum with three maxima at 420, 448 and 472 nm (Fig. 1) and the HPLC-APCI(+)-hrTOF-MS^n analysis determined an experimental monoisotopic mass at m/z = 763.6385 Da corresponding with the elemental composition $C_{54}H_{82}O_2$. The fragmentation of the protonated molecular ion yielded different product ions (Table 1, Fig. S2), which contain information about the significant structural features of this compound. The main product ion was observed at m/z = 535.4298 Da ($C_{40}H_{56}$) that corresponds with the loss of myristic acid (228 Da) from a monohydroxylated xanthophyll (the fragmentation mechanism is depicted in Fig. 3a). Other characteristic product ion was observed at m/z = 443.3657 Da with the elemental composition $C_{33}H_{47}$ generated after the loss of the fatty acid and elimination of one in-chain unit of toluene (Fig. 3b). The other three product ions, which have not been reported before, were created *in silico* by the predictive software MassFrontier™, and then targeted in the experimental mass spectrum with the extracted ion chromatogram function. These product ions as well as the former ones fulfill the criteria for exact mass, elemental composition and isotope pattern described in the Section 2.4. Hence, the product ion at m/z = 507.4211 Da and elemental composition $C_{35}H_{55}O_2$ corresponds with the fragmentation at the 14,15-carbon bond, remaining the 3-hydroxy- β-ring in its ester form (Fig. 3c). The formation of the product ion at m/z = 731.6136 Da ($C_{53}H_{79}O$) that preserves the myristic acid but the decyclization process involves the 3,4- and 4,5-carbon bonds (Fig. 3d). Considering the structural features of these product ions; that free zeinoxanthin has been identified in the pigment profile of *P. autumnale* (Rodrigues, Menezes, Mercadante, Jacob-Lopes, & Zepka, 2015) (Table 1); the UV–visible wavelength maxima and the chromatographic behavior (Table 1), this peak is assigned as myristoyl-zeinoxanthin ester. Although it has been proposed that the esters of zeinoxanthin and β-cryptoxanthin show the same MS behavior (Petry & Mercadante, 2016) the *in silico* fragmentation of the myristoyl-zeinoxanthin ester with the MassFrontier™ software predicted a product ion at m/z = 399.3041 Da ($C_{30}H_{39}$) that was also experimentally observed. This product ion is produced from the elimination of the fatty acid moiety and fragmentation at the polyene chain at 7,8-carbon bond (Fig. 3e). In the experimental MS acquired the signal at m/z = 399.3046 Da was consistent with the elemental composition and formulae of the *in silico* product ion, which fulfil the filtering rules applied to mass error and isotopic pattern. As this product ion is not generated in the simulated fragmentation pattern of the myristoyl- β-cryptoxanthin ester, we propose the product ion at m/z = 399.3046 Da to distinguish by MS the identified zeinoxanthin ester from its β-

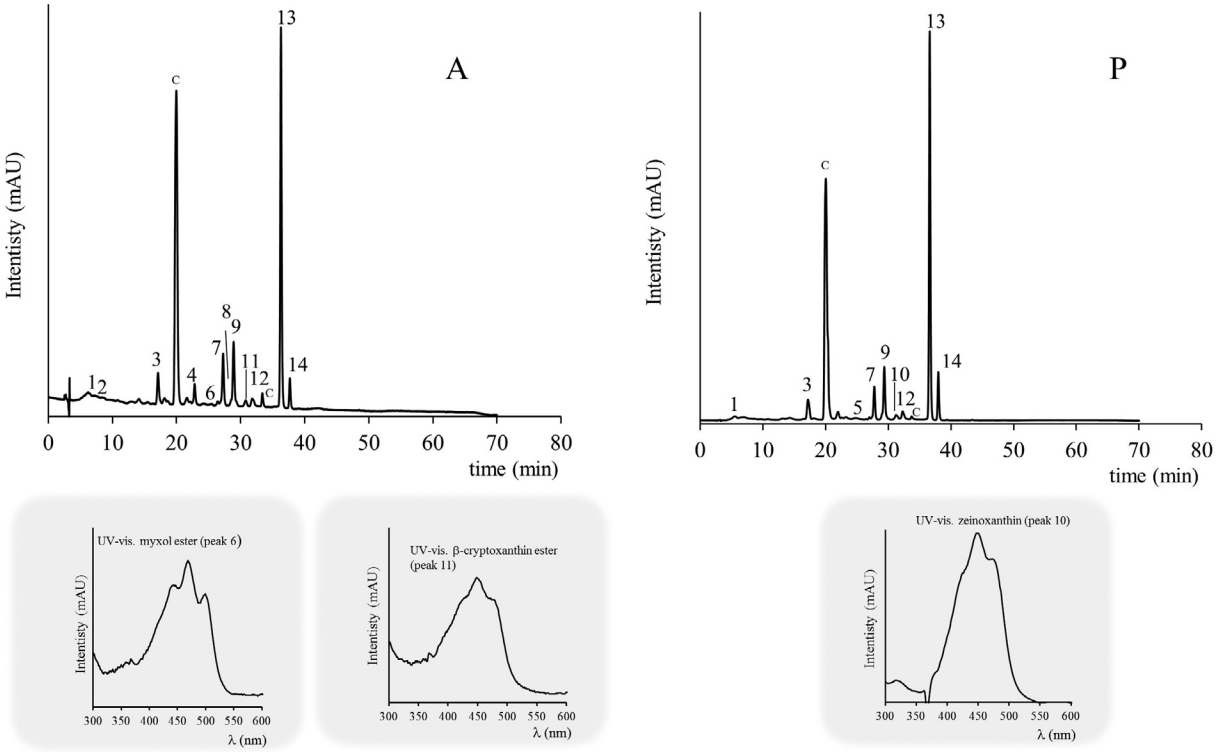

Fig. 1. Chromatogram traces at 450 nm of *Aphanotece microscopica* Nagëli (A) and *Phormidium autumnale* (P) extracts. UV–visible spectra of the esterified carotenoids. Peak number identification is detailed in Table 1. "C" means chlorophyll pigment.

cryptoxanthin ester isomer. The former esterified pigment is a scarce carotenoid, not present in typical esterifying/carotenogenic organisms. Indeed, myristoyl-zeinoxanthin ester has only been described in very low amounts in Arazá fruits (Garzón et al., 2012) and more recently in tangor fruits (Petry & Mercadante, 2016). The MS^2 fingerprint described for this carotenoid (Petry & Mercadante, 2016) contains two typical product ions, one corresponding with the fatty acid elimination, the corresponding one arising from the loss of toluene from the polyene chain coupled with the loss of fatty acid, coincident with the data obtained in Table 1.

Concurrently, the chromatographic profile of *A. microscopica* presents at 32.1 min a signal with a similar UV–visible pattern to the myristoyl-zeinoxanthin ester (Fig. 1, peak 11). In fact, this carotenoid showed a MS protonated molecule at m/z = 763.6389 Da corresponding with the same elemental composition as myristoyl zeinoxanthin ester ($C_{54}H_{82}O_2$). In this case, the bbCID spectrum of the

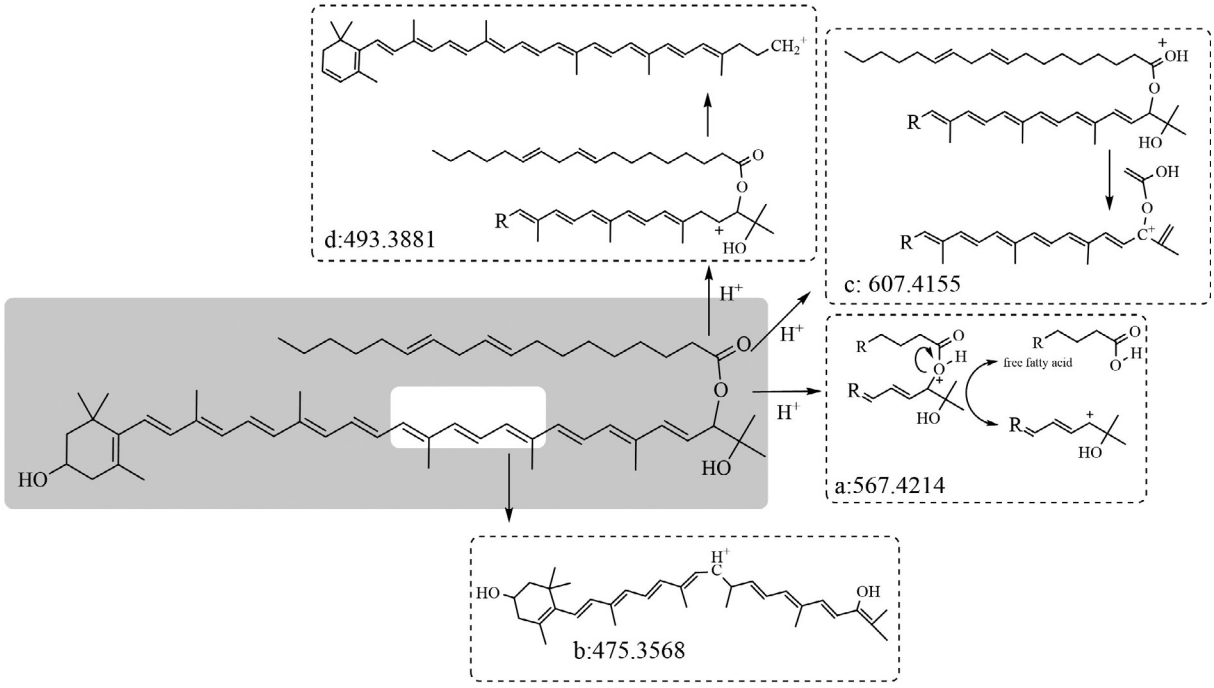

Fig. 2. Experimental product ions acquired by APCI(+)-bbCID of 2′-linolenoyl-myxol ester.

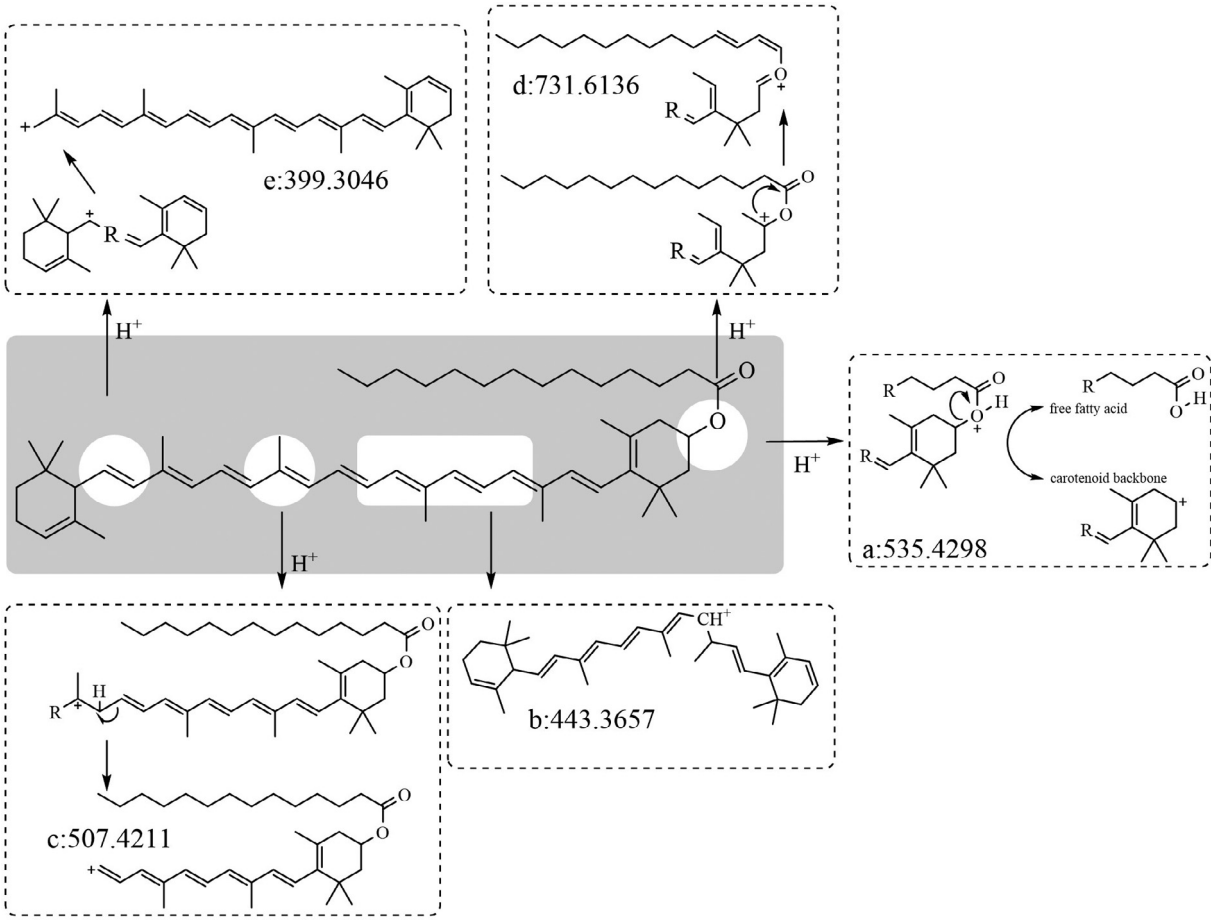

Fig. 3. Experimental product ions acquired by APCI(+)-bbCID of myristoyl-zeinoxanthin ester.

protonated ion at m/z = 763.6389 Da did not show the signal at m/z = 399.3046 Da. Otherwise, two typical product ions were determined (Fig. S3), one corresponding with release of the fatty acid (observed at m/z = 535.4305 Da, $C_{40}H_{56}$, Fig. 4a) and the characteristic loss of the myristic acid in combination with the in-chain yield of toluene (observed at m/z = 443.3663 Da, $C_{33}H_{47}$, Fig. 4b). An additional product ion was observed at m/z = 507.4202 Da that corresponds with the fragmentation at the 15,16-carbon bond remaining the 3-hydroxy–ring in its ester configuration (Fig. 4c). Additionally, the formation of the product ion at m/z = 731.6130 Da ($C_{53}H_{79}O$) that preserves the myristic acid but the decyclization process involves the 3,4- and 4,5-carbon bonds (Fig. 4d) was also observed. With these data, this signal was assigned as myristoyl- β-cryptoxanthin ester. This pigment is a common carotenoid in vegetables and fruits rich in esterified carotenoids such as chili, tangerine, clementine or pepper (Breithaupt & Bamedi, 2001) and recently it has been found as the main monoester in peach fruit (jam and juice) (Giuffrida et al., 2013) or in Physalys fruits (Wen et al., 2017).

As stated before, the esterification of carotenoids in eukaryote microalgae is associated with environmental stress conditions, when the vegetative cell is transformed into red cysts (Lemoine & Schoefs, 2010). As a reaction to the stressful conditions, the eukaryote microalgae synthetize new carotenoids with the aim of protecting the cellular tissues from oxidative reactions. A hypothesis is that, in similarity with eukaryote microalgae, cyanobacteria could respond to the environmental stress not only increasing the quantity of secondary carotenoids but also esterifying them. The presence of a fatty acid could facilitate the integration of the carotenoid in the different membranes, as carotenes and xanthophylls affect the viscosity of the membranes (Zakar, Laczko-Dobos, Toth, & Gombos, 2016), allowing the acclimation of cyanobacteria to different temperatures. In fact, Zakar et al. (2017) have pointed out the cooperative roles between xanthophylls and polyunsaturated lipids, providing evidence for the interdependence of lipid and carotenoid contents in the thylakoid membranes. Further investigations will be required to analyze the behavior of *Aphanotece* and *Phormidium* under different stress conditions with the aim to potentiate the esterification of carotenoids and go into detail about the physiological meaning.

4. Conclusion

The novelty of this study is the identification in cyanobacteria by first time of esterified carotenoids as a result of the use of an exhaustive extraction procedure of the pigment profile, and through the application of high resolution metabolomic tools. Specifically, we observed myristoyl-zeinoxanthin and myristoyl- β-cryptoxanthin esters, which were identified previously in several fruits, and 2′-linolenoyl-myxol-ester, which it is a new MS^n identification as myxoxanthophylls are unique in cyanobacteria. The identification of esterified carotenoids in cyanobacteria generates new possibilities for the food industry (previous authorizations) as it will be possible to utilize cyanobacteria as a new bio-factories for esterified carotenoids. At the end, the *ester* condition is a valuable character for the design of new food formulae, as it has been shown that esterified carotenoids are more stable, possess higher antioxidant characteristic and indeed their bioavailability is higher. The next development should be establishing the optimal stressing conditions to maximize the reaction of esterification affecting the secondary carotenoids. However, this would not be a handicap considering that microalgae show a high biosynthetic plasticity for secondary metabolites (carotenoids) in comparison with higher plants,

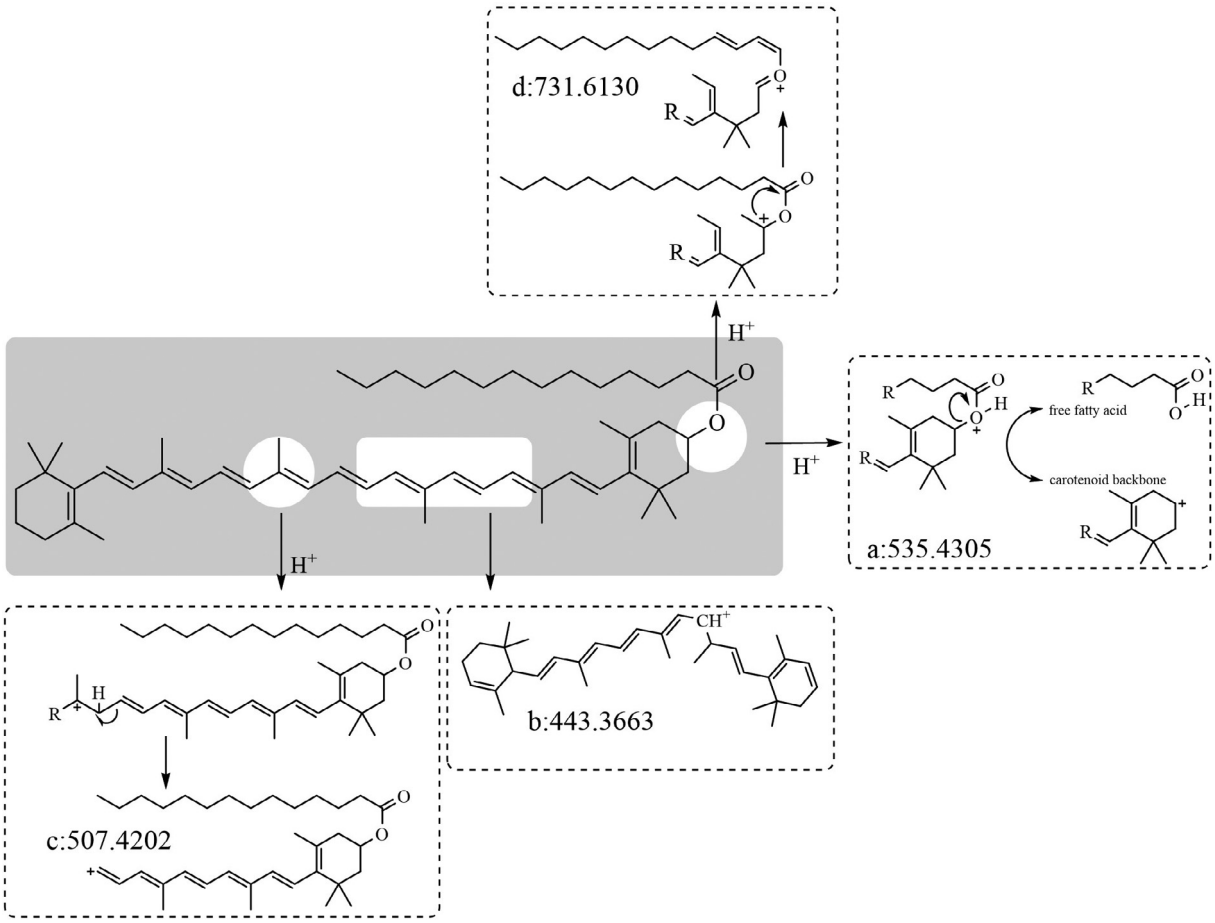

Fig. 4. Experimental product ions acquired by APCI(+)-bbCID of myristoyl-β-cryptoxanthin ester.

and the food industry has taken the most of this feature previously with other microalgae strains. Finally, the application of accurate hyphenated techniques and powerful post-processing software to the analysis of food has allowed to propose a new qualifier product ion to distinguish between the esters of zeinoxanthin and β-cryptoxanthin (with different pro-vitamin A values), a problem not determined so far in the characterization of esterified carotenoids in fruits.

Acknowledgements

The authors would like to thank to Sergio Alcañiz for his technical assistance.

Conflict of interest statement

The authors declare that they have no conflict of interest.

Funding

This work was supported by the Comisión Interministerial de Ciencia y Tecnología (CICYT-EU, Spanish and European Government, grant number AGL 2015-63890-R). MM was supported with a fellowship from CAPES.

Appendix A. Supplementary material

Supplementary data to this article can be found online at https://doi.org/10.1016/j.foodchem.2019.02.102.

References

Amaro, H. M., Barros, R., Guedes, A. C., Sousa-Pinto, I., & Macata, F. X. (2013). Microalgal compounds modulate carcinogenesis in the gastrointestinal tract. *Trends in Biotechnology, 31*, 92–98. https://doi.org/10.1016/j.tibtech.2012.11.004.

Berland, B., Le Campion, T., & Campos, H. (1989). Interaction de lasalinité et de la température sur la morphologie, la croissance et lacomposition cellulaire d'une cyanobactérie halotolerante (Aphanothece sp.). *Botanica Marina, 32*, 317–329. https://doi.org/10.1515/botm.1989.32.4.317.

Breithaupt, D. E., & Bamedi, A. (2001). Carotenoid esters in vegetable and fruits: A screening with emphasis on beta-cryptoxanthin esters. *Journal of Agricultural and Food Chemistry, 49*, 2064–2070. https://doi.org/10.1021/jf001276t.

Breithaupt, D. E., & Schwack, W. (2000). Determination of free and bound carotenoids in paprika (*Capsicum annuum* L.) by LC/MS. *European Food Research and Technology, 211*, 52–55. https://doi.org/10.1007/s002170050588.

Breithaupt, D. E., Wirt, U., & Bamedi, A. (2002). Differentiation between lutein monoester regioisomers and detection of lutein diesters from marigold flowers (*Tagetes erecta*, L.) and several fruits by liquid chromatography-mass spectrometry. *Journal of Agricultural and Food Chemistry, 50*, 66–70. https://doi.org/10.1021/jf010970l.

Britton, G., Liaaen-Jensen, S., & Pfander, H. (1995). Carotenoids. Volume 1A: Isolation and analysis. Birkhäuser Verlag, Basel.

Bunea, A., Socaciu, C., & Pintea, A. (2014). Xanthophyll esters in fruits and vegetables. *Notulae Botanicae Horti. Agrobotanici, 42*, 310–324. https://doi.org/10.15835/nbha4229700.

Garzón, G. A., Narváez-Cuenca, C. E., Kopec, R. E., Barry, A. M., Riedl, K. M., & Schwartz, S. J. (2012). Determination of carotenoids, total phenolic content, and antioxidant activity of Arazá *(Eugenia stipitata* McVaugh), an Amazonian fruit. *Journal of Agricultural Food Chemistry, 60*, 4709–4717. https://doi.org/10.1021/jf205347f.

Giuffrida, D., Dugo, P., Salvo, A., Saitta, M., & Dugo, G. (2010). Free carotenoid and carotenoid ester composition in native orange juices of different varieties. *Fruits, 65*, 277–284. https://doi.org/10.1051/fruits/2010023.

Giuffrida, D., Torre, G., Dugo, P., & Dugo, G. (2013). Determination of the carotenoid profile in peach fruits, juice and jam. *Fruits, 68*, 39–44. https://doi.org/10.1051/fruits/2012049.

Gong, M., & Bassi, A. (2016). Carotenoids from microalgae: A review of recent developments. *Biotechnology Advances, 34*, 1396–1412. https://doi.org/10.1016/j.biotechadv.2016.10.005.

Kamath, B. S., Srikanta, B. M., Dharmesh, S. M., Sarada, R., & Ravishankar, G. A. (2008).

Ulcer preventive and antioxidative properties of astaxanthin from *Haematococcus pluvialis*. *European Journal of Pharmacology, 590*, 387–395. https://doi.org/10.1016/j.ejphar.2008.06.042.

Kobayashi, M. (2000). *In vivo* antioxidant role of astaxanthin under oxidative stress in the green alga *Haematococcus pluvialis*. *Applied Microbiology and Biotechnology, 54*, 550–555. https://doi.org/10.1007/s002530000416.

Lemoine, Y., & Schoefs, B. (2010). Secondary ketocarotenoid astaxanthin biosynthesis in algae: A multifunctional response to stress. *Photosynthesis Research, 106*, 155–177. https://doi.org/10.1007/s11120-010-9583-3.

Liu, J., Sun, Z., & Gerken, H. (2016). Recent Advances in Microalgal Biotechnology, OMICS Group eBooks, Foster City, 2016.

Mariutti, L. R. B., & Mercadante, A. Z. (2018). Carotenoid esters analysis and occurrence: What do we know so far? *Archives of Biochemistry and Biophysics, 648*, 36–43. https://doi.org/10.1016/j.abb.2018.04.005.

Mercadante, A. Z., Rodrigues, D. B., Petry, F. C., & Mariutti, L. R. B. (2017). Carotenoid esters in foods – A review and practical directions on analysis and occurrence. *Food Research International, 99*, 830–850. https://doi.org/10.1016/j.foodres.2016.12.018.

Murata, K., Oyagi, A., Takahira, D., Tsuruma, K., Shimazawa, M., Ishibashi, T., & Hara, H. (2012). Protective effects of astaxanthin from Paracoccus carotinifaciens on murine gastric ulcer models, Phytotherapy Research, 26, 1126–1132. https://doi.org/ 10.1002/ptr.3681.

Panis, G., & Rosales Carreon, J. (2016). Commercial astaxanthin production derived by green alga *Haematococcus pluvialis*: A microalgae process model and a techno-economic assessment all through production line. *Algal Research, 18*, 175–190. https://doi.org/10.1016/j.algal.2016.06.007.

Patias, L. D., Fernandes, A. S., Petry, F. C., Mercadante, A. Z., Jacob-Lopes, E., & Zepka, L. Q. (2017). Carotenoid profile of three microalgae/cyanobacteria species with peroxyl radical scavenger capacity. *Food Research International, 100*, 260–266. https://doi.org/10.1016/j.foodres.2017.06.069.

Pérez-Gálvez, A., & Mínguez-Mosquera, M. I. (2005). Esterification of xanthophylls and its effect on chemical behavior and bioavailability of carotenoids in the human. *Nutrition Research, 25*, 631–640. https://doi.org/10.1016/j.nutres.2005.07.002.

Pérez-Gálvez, A., Sánchez-García, A., Garrido-Fernández, J., & Ríos, J. J. (2018). MS tools for a systematic approach in survey for carotenoids and their common metabolites. *Archives of Biochemistry and Biophysics, 650*, 85–92. https://doi.org/10.1016/j.abb.2018.05.010.

Petry, F. C., & Mercadante, A. Z. (2016). Composition by LC-MS/MS of new carotenoid esters in mango and citrus. *Journal of Agricultural and Food Chemistry, 64*, 8207–8224. https://doi.org/10.1021/acs.jafc.6b03226.

Ríos, J. J., Roca, M., & Pérez-Gálvez, A. (2015). Systematic HPLC/ESI-high resolution-qTOF-MS methodology for metabolomic studies in nonfluorescent chlorophyll catabolites pathway. *Journal of Analytical Methods in Chemistry, 2015*, 490627. https://doi.org/10.1155/2015/490627.

Ríos, J. J., Xavier, A. A. O., Díaz-Salido, E., Arenilla-Vélez, I., Jarén-Galán, M., Garrido-Fernández, J., ... Pérez-Gálvez, A. (2017). Xanthophyll esters are found in human colostrum. *Molecular Nutrition and Food Research, 61*, 1700296. https://doi.org/10.1016/j.foodres.2016.12.018.

Rippka, R., Deruelles, J., Waterbury, J. B., Herdman, M., & Stanier, R. Y. (1979). Generic assignments, strain histories and properties of pure cultures of cyanobacteria. *Journal of General Microbiology, 111*, 1–61. https://doi.org/10.1099/00221287-111-1-1.

Rivera, S. M., Christou, P., & Canela-Garayoa, R. (2014). Identification of carotenoids using mass spectrometry. *Mass Spectrometry Reviews, 33*, 353–372. https://doi.org/10.1002/mas.21390.

Rodrigues, D. B., Menezes, C. R., Mercadante, A. Z., Jacob-Lopes, E., & Zepka, L. Q. (2015). Bioactive pigments from microalgae *Phormidium autumnale*. *Food Research International, 77*, 273–279. https://doi.org/10.1016/j.foodres.2017.06.069.

Saeki, K., Aburai, N., Aratani, S., Miyashita, H., & Abe, K. (2017). Salt-stress and plant hormone-like responses for selective reactions of esterified xanthophylls in the aerial microalga Coelastrella sp. KGU-Y002. *Journal of Applied Phycology, 29*, 115–122. https://doi.org/10.1007/s10811-016-0911-7.

Simionato, D., Block, M. A., La Rocca, N., Jouhet, J., Maréchal, E., Finazzi, G., & Moroinotto, T. (2013). The response of *Nannochloropsis gaditana* to nitrogen starvation includes de novo biosynthesis of triacylglycerols, a decrease of chloroplast galactolipids, and reorganization of the photosynthetic apparatus. *Eukaryotic Cell, 12*, 665–676. https://doi.org/10.1128/EC.00363-12.

Sun, Z., Liu, J., Zeng, X., Huanqfu, J., Jiang, Y., Chang, M., & Chen, F. (2011). Astaxanthin is responsible for antiglycoxidative properties of microalga *Chlorella zofigiensis*. *Food Chemistry, 126*, 1629–1635. https://doi.org/10.1016/j.foodchem.2010.12.043.

Takaichi, S., Maoka, T., Akimoto, N., Carmona, M. L., & Yamaoka, Y. (2008). Carotenoids in a corynebacterineae, Gordonia terrae AIST-1: Carotenoid glucosyl mycoloyl esters. *Bioscience, Biotechnology and Biochemistry, 72*, 2615–2622. https://doi.org/10.1271/bbb.80299.

Takaichi, S., Mochimaru, M., & Maoka, T. (2006). Presence of free myxol and 4-hydroxymyxol and absence of myxol glycosides in anabaena variabilis ATCC 29413, and proposal of a biosynthetic pathway of carotenoids. *Plant and Cell Physiology, 47*, 211–216. https://doi.org/10.1093/pcp/pci236.

Van Breemen, R. B., Dong, L., & Pajkovic, N. D. (2012). Atmospheric pressure chemical ionization tandem mass spectrometry of carotenoids. *International Journal of Mass Spectrometry, 312*, 163–172. https://doi.org/10.1016/j.ijms.2011.07.030.

Wen, X., Hempel, J., Schweiggert, R. M., Ni, Y., & Carle, R. (2017). Carotenoids and carotenoid esters of red and yellow Physalis *(Physalis alkekengi* L. and *P. pubescens* L.) fruits and calyces. *Journal of Agricultural Food Chemistry, 65*, 6140–6151. https://doi.org/10.1021/acs.jafc.7b02514.

Wingerath, T., Stahl, W., & Sies, H. (1995). β-Cryptoxanthin selectively increases in human chylomicrons upon ingestion of tangerine concentrate rich in β-cryptoxanthin esters. *Archives of Biochemistry and Biophysics, 324*, 385–390. https://doi.org/10.1006/abbi.1995.0052.

Wright, S. W., Jeffrey, S. W., Mantoura, F. C., Llewellyn, C. A., Bjørnland, T., Repeta, D., & Welschmeyer, N. (1991). Improved HPLC method for the analysis of chlorophylls and carotenoids from marine phytoplankton. *Marine Ecology Progress Series, 77*, 183–196. https://doi.org/10.3354/meps077183.

Zakar, T., Laczko-Dobos, H., Toth, T. N., & Gombos, Z. (2016). Carotenoids assist in cyanobacterial photosystem II assembly and function. *Frontier in Plant Science, 7*, 295. https://doi.org/10.3389/fpls.2016.00295.

Zakar, T., Herman, E., Vajravel, S., Kovacs, L., Knoppová, J., Komenda, J., ... Laczko-Dobos, H. (2017). Lipid and carotenoid cooperation-driven adaptation to light and temperature stress in Synechocystis sp. PCC6803. *Biochimica et Biophysica Acta, 1868*, 337–350. https://doi.org/10.1016/j.bbabio.2017.02.002.

Ziegler, J. U., Wahl, S., Würschum, T., Longin, C. F. H., Carle, R., & Schweiggert, R. M. (2015). Lutein and lutein esters in whole grain flours made from 75 genotypes of 5 Triticum species grown at multiple sites. *Journal of Agricultural Food Chemistry, 63*, 5061–5071. https://doi.org/10.1021/acs.jafc.5b01477.

CAPÍTULO 7

Manuscrito 2: Systematic high-through approach reveals new 2 carotenoid metabolism in cyanobacteria

Submetido no periódico Marine Drugs

marine drugs

MDPI

Article

Systematic high-through approach reveals new carotenoid metabolism in cyanobacteria

Mariana Manzoni Maroneze[1], Belén Caballero-Guerrero[2], Leila Queiroz Zepka[1], Eduardo Jacob-Lopes[1], Antonio Pérez-Gálvez[3], and María Roca[3,*]

[1] Department of Food Science and Technology, Federal University of Santa Maria (UFSM), 97105-900 Santa Maria, RS, Brazil; mariana_maroneze@hotmail.com (M.M), zepkaleila@yahoo.com.br (L.Q.), ejacoblopes@gmail.com (E.J.)

[2] Microbiology Service, Instituto de la Grasa (CSIC), University Campus, Building 46, 41013, Sevilla, Spain; cabaguer@cica.es.

[3] Food Phytochemistry Department, Instituto de la Grasa (CSIC), University Campus, Building 46, 41013, Sevilla, Spain; aperez@cica.es.

* Correspondence: mroca@ig.csic.es; Tel.: +34-954-611-550

Received: date; Accepted: date; Published: date

Abstract: Cyanobacteria and microalgae are characterised by a rich and varied chlorophyll and carotenoid profile, biodiversity that facilitates the adaptation to different environments. Specialised and expert-curated analyses have delineated the main biosynthetic routes so far. However, an unspoiled enhancement for the advance in that knowledge is the application of metabolomic approach. We propose a systematic workflow, to gain insights in the metabolism of photosynthetic pigments in phytoplankton. The pipeline methodology includes a specific extraction method combined with an ultrahigh-performance liquid chromatography method coupled with high-resolution tandem mass spectrometry in broad-band Collision Induced Dissociation mode to acquire, simultaneously, MS and MS^n spectra. Following an untargeted strategy, two unprecedented carotenoid structures have been unraveled in cyanobacteria. Hence, the goodness of the comprehensive analytical approach has allowed to show that cyanobacteria synthetize, by first time, carotenoids with 5,6-epoxy-groups and that the α-branch of the carotenoid biosynthetic pathway is also active. An *in silico* search has retrieved putative sequences of the carotenogenic enzymes implied in the corresponding biosynthetic pathways in the analysed cyanobacteria species. In conclusion, high-through metabolomics studies are a powerful tool to introduce insights of unknown or poorly understood chlorophyll and carotenoid metabolism in phytoplankton species.

Keywords: 2′-dehydrodeoxomyxol; 5,6-epoxy-groups; *Aphanotece;* carotenoids; chlorophylls; cyanobacteria*; Desertifilum*; mass spectrometry; metabolomics; microalgae.

1. Introduction

Cyanobacteria and microalgae are of great interest as microscopic factories to produce through sustainable procedures several metabolites with high-economic potential in different areas, such as biofuels, single-cell proteins and high-value compounds, including long-chain polyunsaturated fatty acids, and pigments. The microalgal biodiversity and ecology represent an opportunity to face several of the challenges that current society is claiming regarding environmental concerns and demands of alternative sources of natural primary metabolites. This heterogeneous collection of prospects is feasible because microalgae and cyanobacteria are characterised by their high physiological plasticity that facilitates the adaptation to changing environmental conditions, and their metabolic diversity that makes them capable of producing a wide range of metabolites. Phytoplankton exhibits a diverse profile of chlorophylls and carotenoids as many of them are unique between different groups and they are not biosynthesised in terrestrial plants. This richness in lipophilic pigments means that the synthetic pathways are highly complex and far away to be

accomplished [1]. For example, cyanobacteria, in exclusivity, accumulate myxoxanthophylls, as well as synthetise β-carotene, and its biosynthetic derivatives, echinenone and zeaxanthin (Figure 1, filled blue squares). However, the β-branch does not progress further and consequently cyanobacteria species lack carotenoids with the 5,6-epoxy-group arrangement (as antheraxanthin or violaxanthin) [2-3]. On the contrary, in Chlorophyta, as many other eukaryotic microalgae, through the β-branch, besides β-carotene, violaxanthin and its derivative, neoxanthin (Figure 1, filled green squares) are typically biosynthesized. The α-carotene branch (Figure 1) is restricted to certain phyla of eukaryotic photosynthetic organisms: Rhodophyta, Cryptophyta, Chlorarachniophyta, Chlorophyta and terrestrial plants [4-5], being lutein an important carotenoid in Chlorophyta species. Recent reviews have compiled the present knowledge in their metabolism [1, 6-8]. However, the exhaustive characterization of the pigment profile in microalgae and cyanobacteria deserves further attention, in fact, due to their importance, the term *pigmentome* or pigment fingerprint has been coined as a metabolic snapshot in defined conditions [9].

Phytoplankton could be a complex material for extraction of lipophilic material as some species contain cell walls with chemical and mechanical properties that difficult the efficiency of extraction, being cyanobacteria and certain chlorophyte species considered recalcitrant [10]. Multiple protocols have been assayed for chlorophyll and carotenoid extraction from microalgae [7, 11-12]. In addition, for those studies exclusively dealing with carotenoid pigments, an alkaline hydrolysis step is almost required as this process is particularly effective for removing colourless contaminating lipid material, and chlorophylls [13], yielding a clean extract that provides improved UV-visible signals. On the contrary, this step avoids the detection of esterified carotenoids and may induce certain structural modifications in some carotenoids, so that the alkaline hydrolysis is not appropriate in all circumstances. Consequently, there is still a constant need for optimization of the pigment extraction methods [14-15]

The arrangement of double bonds in chlorophylls and carotenoids made the spectroscopy the straightforward method for analysis, being HPLC-DAD, the most widespread analytical system applied. However, an accurate analysis requires the application of mass spectrometry detection system [16]. In addition, microalgae and cyanobacteria pigment profiles are highly complex, and conventional LC-MS-based methods exhibit low separation efficiency, long analysis time, and low mass accuracy, with the possibility of inaccurate identification [17]. Consequently, modern analytical methods are based in high-resolution MS (HRMS) and when it is possible, they include tandem mass spectrometry [16,18]. Pigments in microalgae have been identified implementing different ionizations techniques (ESI or APCI) in combination with diverse mass analysers (TOF, ion trap or ion cyclotron) [18,19]. Additional approaches with the traveling wave ion mobility mass spectrometer (TWIM-MS) have gained further identification criterion by collision cross section (CCS) [20]. Anyhow, the basis of the LC-MS-based metabolomics studies is the data analysis [21]. The application of potent analytical methodologies (as HRMS) produce large-scale of high-dimensional data that demand a complex processing to understand and decipher the meaning of the metabolomics study. In this sense, two approaches can be considered, targeted, when the study is focused on already known metabolites or untargeted analysis, when the objective is to detect as many compounds as possible, independently whether the structure is known or not. For both approaches multiple software packages have been developed and exploited, all of them applying strict criteria of mass accuracy and isotopic pattern and based on features as m/z values or retention times [21]. Additional information can be gained through the utilization of fragmentation prediction bioinformatics tools, in the two existing versions: rule-based, which uses several chemical rules to predict fragmentations, or combinatorial-based, which applies a combinatorial fragmentation procedure, breaking bonds methodologically [22].

Altogether means that the advancement of analytical techniques, allow the detection of minor metabolites, but implies the combination of different methodologies that require the use of an appropriate workflow to optimize the acquisition of results within a biological context. Multiple workflows have been proposed, untargeted [23] or specific for a group of metabolites [24] in plants.

However, limited workflows have been described specifically for phytoplankton [25-26], and even less for lipophilic pigments [19].

Therefore, the aim of this manuscript was to advance in the knowledge of the metabolism of photosynthetic pigments in phytoplankton through a complete workflow that allows high-throughput screening. Thus, the workflow includes a protocol for the exhaustive extraction of chlorophyll and carotenoid pigments from different microalgae and cyanobacteria. Subsequently, a HPLC-MS platform was used for the reliable detection and identification of chlorophylls and carotenoids in the extracts of phytoplankton with the implementation of a post-processing routine with software tools that automatically perform the process of matching the experimental and the theoretical values of the selected orthogonal data that increase accuracy of the identification. Additionally, the experimental tandem MS spectra obtained in bbCID mode were dissected with the aid of predictive software to detect characteristic product ions that assist in the structural elucidation of unknown carotenoids. With this approach we have provided insights of unexpected pathways in the metabolism of carotenoids in cyanobacteria.

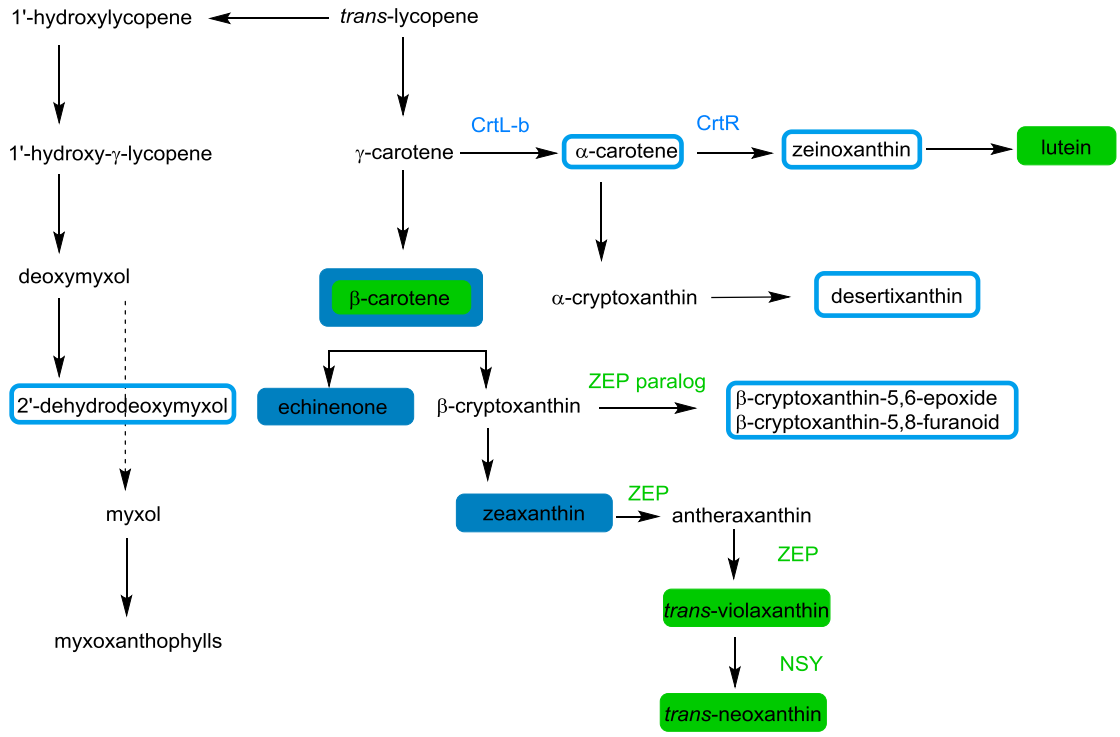

Figure 1. Proposed biosynthetic pathways of carotenoids in phytoplankton, based on Huang et al. [1]. The typical carotenoid pattern in Chlorophyta is highlighted with filled green squares while the common carotenoid profile in cyanobacteria is filled squared in blue. The new or unusual carotenoids identified in the research have been highlighted in open blue squares. The *in silico* blast proteins are reproduced in green letters for proteins exclusively identified in microalgae and in blue letters for cyanobacterial proteins.

2. Results

2.1. Re-identification of Phormidium autumnale Gomont as Desertifilum sp.

The cyanobacteria strain originally isolated from the Mexico desert was initially eco and morphologically identified as *Phormidium autumnale* Gomont [27]. Since then, several species of the recent genus *Desertifilum* have been identified [28-30], being all of them phylogenetically close to *Phormidium*. Taking advantage of the molecular tools, the 16S rRNA sequence of the tentative *Phormidium autumnale* Gomont was blast against the database at NCBI. Results showed a 99% identity with *Desertifilum tharense*, 99% with *Desertifilum salkalinema*, and 99% with *Desertifilum dzianense*. Consequently, we can conclude that the original strain identified as *Phormidium autumnale* Gomont

belongs to the genus *Desertifilum*. However, as it has been revealed [30], the 16S rRNA gene sequences of the different strains of this cyanobacterium share high sequence similarity (>98%). In base to our results, it is not possible to define the species and further molecular analysis will be developed to determine the *Desertifilum* species.

2.2. Targeted high-throughput workflow allows accurate identification of photosynthetic pigments from microalgae and cyanobacteria

The proposed systematic workflow (Figure 2) starts with an extraction methodology developed for the combined isolation of chlorophylls and carotenoids, from microalgae and cyanobacteria, without alkaline hydrolysis. The protocol means an exhaustive process including sequential extraction steps with different solvents which are aimed to comprise the wide range of polarities of photosynthetic pigments (from the apolar carotenoid esters and carotenes, to the more polar free xanthophylls and chlorophyll derivatives). Subsequently, the protocol combines different mechanical procedures as grinding, sonication, vortexing, stirring and centrifugation with the objective of achieving a complete extraction of pigments, independently of the cellular complexity of the microalgae or cyanobacteria species. The chlorophyll and carotenoid contents in microalgae and cyanobacteria are determined by environmental factors, such as light, temperature, composition of the culture medium, in addition to genetic factors. Consequently, it is difficult to establish a constant qualitative/quantitative profile of pigments for each species. Thus, we have obtained with the built extraction protocol a total amount of chlorophyll pigments in the 15-20 mg/g range for both chlorophytes and in the 8-12 mg/g range for both cyanobacteria (Table 1). For carotenoids, both chlorophytes species showed similar amounts, around 2.2 mg/g, while *Aphanotece microscopica* and *Desertifilum* sp. accumulated different carotenoid amounts, 1.9 mg/g and 2.6 mg/g, respectively. These figures are very close to previous published data for *Chlorella* and *Scenedesmus* spp. [31], even although the extraction protocol was different from that applied in this study. However, the figures for the cyanobacteria are higher with the improved protocol, in comparison with data from literature [31-32].

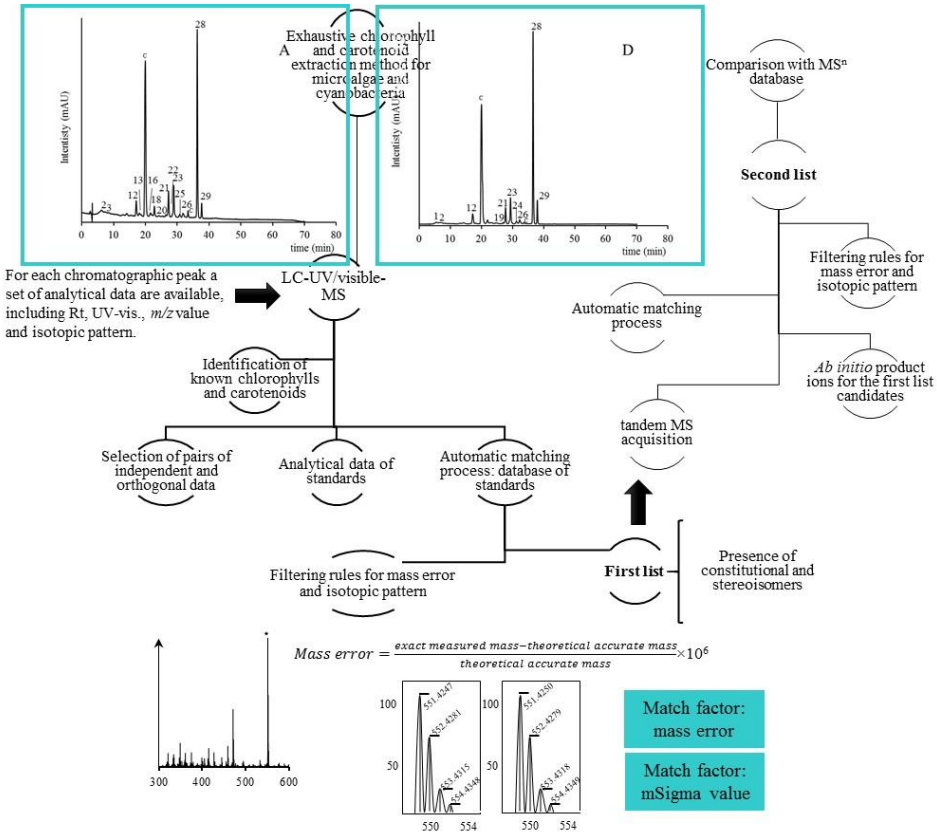

Figure 2. Diagram of the holistic analytical methodology proposed to accurately identify lipophyllic pigments in microalgae and cyanobacteria. Peak numbers in the HPLC trace at 450 nm in A

(*Aphanotece* extract) and D (*Desertifilum* extract) correspond to table 1. In both HPLC traces c means chlorophyll pigment.

Following, a targeted analysis was applied through the HPLC-PDA-ESI/APCI(+)-HRTOF analysis to identify known structures (Table S1). The identification of the chlorophyll and carotenoid profile in the microalgae and cyanobacteria species analysed in this study was based in a complete set of independent and complementary physicochemical properties, which were organised in pairs (retention time and UV-visible characteristics, accurate mass and tandem MS features, accurate mass and isotopic pattern) and compared with the same analytical pairs of data relative to authentic compounds examined with the same experimental conditions (Figure 2). During the processing of this analytical information, filtering rules were applied to those matched pairs of theoretical and experimental data to discard false positives and increase the confidence level of the identification. Finally, complementary data regarding chromatographic behaviour, UV-Visible characteristics and intensity of mass signals were required for the differentiation of possible geometrical isomers (Tables 1 and 2). In the chlorophyll fraction, chlorophyll *a* and *b* and some derivatives were identified in the chlorophyte species, while only chlorophyll derivatives of the series a were detected for cyanobacteria, as it was expected. Relative amounts of pheophytin *a* were quantified along the different species, being this catabolite an intermediate product of the chlorophyll degradation pathway [33]. In relation with the carotenoid fraction, two dissimilar profiles were observed, as it was foreseeable. *Chlorella* and *Scenedesmus*, member species of the class Chlorophyceae, showed lutein, β-carotene, neoxanthin and violaxanthin (including luteoxanthin) as the main carotenoids [10]. In minor amounts, other secondary carotenoids were also identified as diadinoxanthin, diatoxanthin and α-carotene. Diadinoxanthin and diatoxanthin are specific markers for chromophyte algae species, while they are present in the marine phytoplankton including diatoms, dinoflagellates and prymnesiophytes [34]. Regarding the Cyanophycea species analysed in this study, *Aphanotece* and *Desertifilum*, they contain significant amounts of β-carotene, zeaxanthin and echinenone [10], showing the typical carotenoid pattern in this taxonomic group. However, unexpectedly, unusual carotenoids were identified in cyanobacteria, α-carotene and xanthophylls with an 5,6-epoxy-arrangement (violaxanthin and neoxanthin) exclusively in *Aphanotece*. In addition, different esterified carotenoids were observed in both species as it has been recently described [35] in physiological culture conditions.

Table 1. Carotenoids identified by HPLC-PDA-APCI(+)-qQ-TOF and quantified by HPLC-PDA in the species analysed in the study.

peak	carotenoid	t_R (min)	Content (μg/g dry weight)			
			Chlorella	*Scenedesmus*	*Aphanotece*	*Desertifilum*
1	desertixanthin	5.6				+
2	*cis*-violaxanthin	5.9	85.28±19.09	58.56±0.45	+	+
3	*cis*-neoxanthin	6.3	298.44±15.72	414.64±5.79	+	
4	*cis*-mutatoxanthin	8.0	58.24±8.06	49.68±3.70		
5	*cis*-luteoxanthin	8.6	57.08±16.57	76.24±3.22		
6	diadinoxanthin	10.0	+	+		
7	*trans*-diatoxanthin	11.4		+		
8	*cis*-anteraxanthin	12.0	+			
9	*all-trans*-lutein	14.5	1242.28±113.36	1128.8±32.52		
10	*cis*-lutein	15.9	171.44±8.51	173.32±0.94		
11	chlorophyll *b*	16.1	3981.98±165.09	3621.54±33.57		

12	*cis*-zeaxanthin	16.6			161.52±14.54	109.4±8.4
13	*all-trans*-zeaxanthin	17.2			20.60±1.23	
14	13²-hydroxy-chlorophyll *a*	18.5			115,35±9.35	
15	chlorophyll *a*	19.9	11334.48±243.42	10171.32±611.95	8128,82±424.79	6410.84±18.95
16	5,6-epoxy-β-cryptoxanthin	20.0			+	
17	chlorophyll *a´*	22.0			151.52±2.72	
18	2-dehydrodeoxymyxol	23.6			70.14±1.16	
19	*all-trans*-zeinoxanthin	26.0				+
20	2´-linolenoyl-myxol ester	26.5			+	
21	*all-trans*-echinenone	27.7			403.7±16.93	330.77±32.54
22	*cis*-5,8-furanoid-β-cryptoxanthin	28.3			20.41±0.25	
23	*cis*-echinenone	29.4			595.83±36.28	402.65±21.3
24	myristoyl-β-zeinoxanthin ester	31.2				+
25	myristoyl-β-cryptoxanthin ester	32.1			+	
26	*9-cis*-α-carotene	32.3	+	+	+	11.03±0.65
27	pheophytin *a*	33.2		6284.58±848.21	3201.06±26.53	1710.01±15.13
28	*all-trans*-β-carotene	36.6	347.04±4.61	433.94±5.79	1276.18±70.98	1286.78±211.99
29	9-*cis*-β-carotene	38.0			139.05+3.82	104.38±5.36
	Total chlorophylls		15316.46±65.23	20077.44±462.85	11596.75±745.68	8120.85±25.54
	Total carotenoids		2259.80±128.95	2335.18±158.34	2687.43±153.68	2245.01±52.67

+ means presence but under the LOQ.

2.3. Untargeted high-throughput workflow allows identification of unusual carotenoids

Alternatively, experimental data from the second list (Figure 2) that did not match with the analytical information obtained from both the available standards and from literature were reviewed in order to detect possible unexpected or even unknown structures. Thus, in the MS spectra of *Aphanotece*, two signals corresponding to uncommon carotenoids in cyanobacteria were observed at *m*/*z* = 569.4373 Da (peak 16) and at *m*/*z* = 569.4325 Da (peak 22). The filtering rules of mass error and isotopic pattern were below the established threshold values of the same elemental composition for both signals $C_{40}H_{56}O_2$ (Figure S2). An examination of the second dimension (second list in Figure 2) of the analytical data provided characteristic product ions observed at *m*/*z* = 551.4225 Da and at *m*/*z* = 551.4237 Da, corresponding to the loss of 18 Da from the protonated molecular ion, the typical fragment that points to the presence of a hydroxyl group in the compound [36]; at *m*/*z* = 477.3725 Da and at *m*/*z* = 477.3720 Da corresponding to the loss of in-chain 92 Da units, a characteristic fragment showing the existence of a conjugated double bond system in the structure [36]; at *m*/*z* = 493.3820 Da and at *m*/*z* = 493.3847 Da, which arise from a decyclization process [37]; at *m*/*z* = 221.1540 Da and at *m*/*z* = 221.1531 Da that denotes the presence of epoxide or furanoid groups fused to a hydroxylated end ring [38] (Table 2). The consistency of these product ions was checked with the SmartFormula™

algorithm and they satisfied the filtering rules applied to mass error and isotopic pattern. We propose, in based to the structural information obtained from the selected pairs of analytical information that these signals correspond to 5,6-epoxy-β-cryptoxanthin (peak 16, Figure 2 HPLC trace A) and cis-5,8-furanoid- β -cryptoxanthin (peak 22, Figure 2 HPLC trace A). The first carotenoid has been associated with several classes of algae [39], although never in cyanobacteria, and it is not currently related with any specific taxonomic group [10]. Diversely, cis-5,8-furanoid- β -cryptoxanthin has not been identified, to the best of our knowledge, in phytoplankton, although it is widely distributed in tropical fruits [38,40].

Table 2. Characterization by HPLC-PDA-APCI(+)-Qq-TOF-MS in bbCID mode of unusual and unknown carotenoids in microalgal extracts.

p [1]	Carotenoid	EC [2]	Product ions (m/z)		
			Loss of in-chain units	Fragmentation of the polyene chain and end units	Decyclization process
1	desertixanthin	$C_{40}H_{54}O_2$	487.4097 $[M+H-80]^+$; 475.3553 $[M+H-92]^+$	549.4093 $[M+H-18]^+$; 443.3345 [M+H-ring]$^+$; 361.2550 [M+H-(10,11 carbon-carbon bond)]$^+$	525.3741 [M+H-2,4 carbon-carbon bond]$^+$; 507.3622 [M+H-C_3H_6-18] 483.3619 [M+H-(3′,4′ carbon-carbon bond, 1′,6′ carbon-carbon bond)]$^+$; 469.3470 [M+H-(4′,5′ carbon-carbon bond, 1′,6′ carbon-carbon bond)]$^+$
16	5,6-epoxy-β-cryptoxanthin	$C_{40}H_{56}O_2$	477.3725 $[M+H-92]^+$	551.4225 $[M+H-18]^+$ 221.1540 $[M+H-348]^+$	493.3820 [M+H-18-(1,2 carbon-carbon bond, 4,5 carbon-carbon bond)]$^+$
18	2′-dehydrodeoxymyxol	$C_{40}H_{54}O_2$	475.3567 $[M+H-92]^+$	549.4058 $[M+H-18]^+$; 533.4137 $[M+H-18-16]^+$; 453.3530 [M+H-(4,5 carbon-carbon bond)]$^+$	509.3786 [M+H-(1′,2′ carbon-carbon bond)]$^+$; 493.3812 [M+H-18-(2,3 carbon-carbon bond, 1,6 carbon-carbon bond)]$^+$
22	cis-5,8-furanoid-β-cryptoxanthin	$C_{40}H_{56}O_2$	477.3720 $[M+H-92]^+$	551.4237 $[M+H-18]^+$ 221.1531 $[M+H-348]^+$	493.3847 [M+H-18-(1,2 carbon-carbon bond, 4,5 carbon-carbon bond)]$^+$

[1] p means peaks as in Table 1. [2] EC means Elemental Composition.

In addition, the pigment profile of *Aphanothece* presented a characteristic UV-visible carotenoid spectrum (Figure 3a, peak 20) at 23.6 min with the MS signal of the protonated molecular ion at *m*/*z* = 567.4172 Da that fits with the elemental composition $C_{40}H_{54}O_2$ and fulfills the filtering rules for mass error and isotopic pattern (Table 2 and Table S2). The maxima absorbance wavelengths in the UV-visible spectrum, which were located at 446, 472 and 504 nm, resemble the UV-visible spectra of myxoxanthophyll-type pigments, a characteristic xanthophyll of the cyanobacteria. The product ions observed in the tandem MS spectrum (Table 2 and Figure 3a) arise from different fragmentations represented in Figure 3b. The product ions were detected at *m*/*z* = 549.4058 Da, showing the presence of an hydroxyl group, at *m*/*z* = 533.4137 Da, arising from the consecutive loss of the hydroxyl and keto groups predicted by the MassFrontier™ software; at *m*/*z* = 453.3530 Da, which involves a complete

acyclic end unit with keto and hydroxyl functional groups predicted by the MassFrontier™ software, and at *m/z* = 509.3786 Da that arise from the fragmentation at the acyclic end unit in a similar fashion as the characteristic fragmentation of a type β end ring [38]; at *m/z* = 493.3812 Da, yielded after the decyclization process in combination with the loss of water; and finally at *m/z* = 475.3567 Da, a product ion generated by the elimination of an in-chain 92 Da unit and characteristic of the polyene system [36]. The chromatographic characteristics and MS spectroscopic behaviour of this carotenoid agree with the structure proposed in Figure 2b, which correspond with the 2′-dehydrodeoxymyxol. All the product ions were predicted by the software Mass Frontier™, and all of them satisfied the requirements for exact mass, elemental composition and isotope pattern described in Materials and Methods.

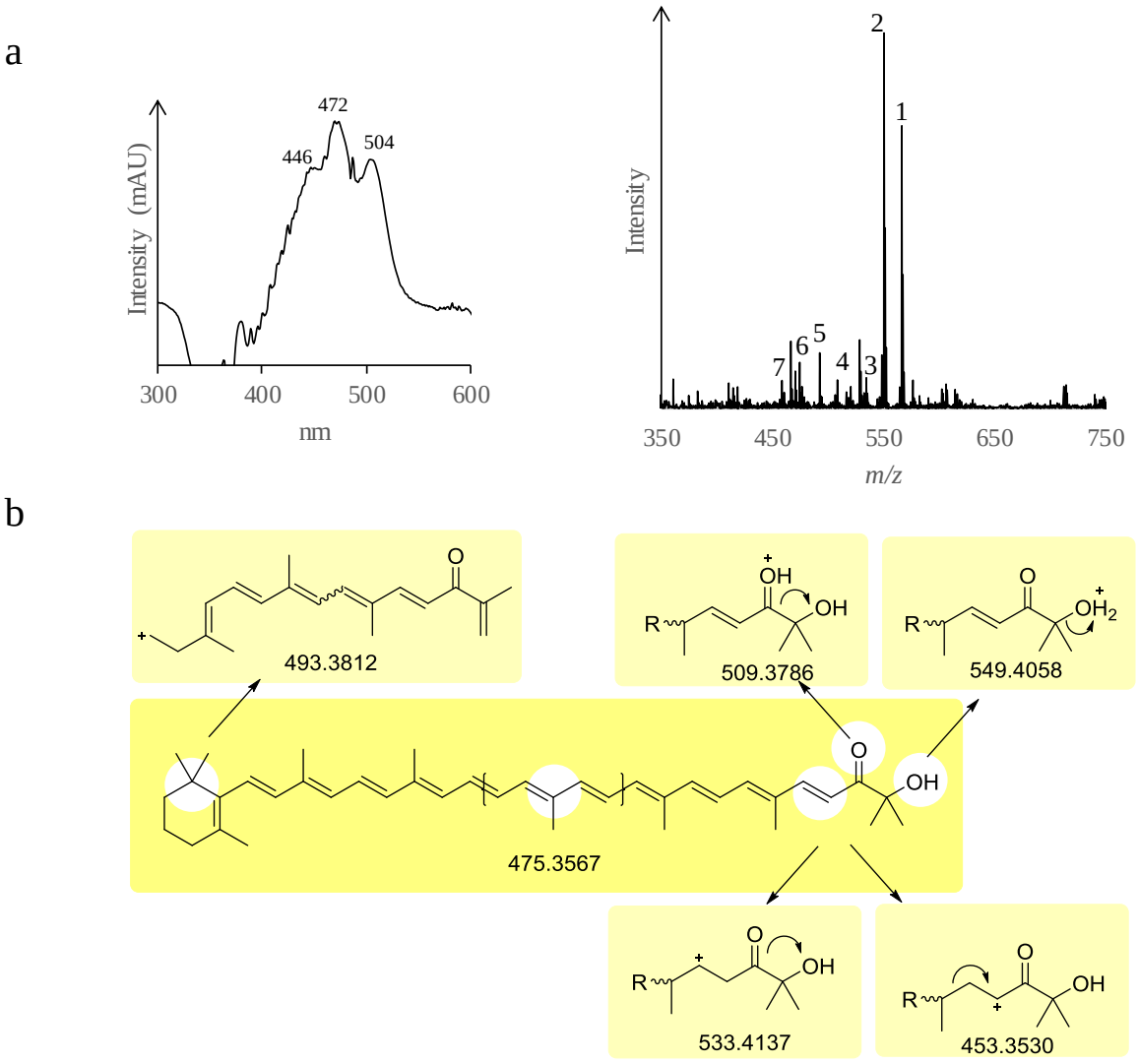

Figure 3. Characterization of 2′-dehydrodeoxymyxol: a) UV-visible and bbCID-mode MS spectra. Product ions are: 1, 567.4172 Da; 2, 549.4058 Da; 3, 533.4137 Da; 4, 509.3786 Da; 5, 493.3812 Da; 6, 475.3567 Da; 7, 453.3530 Da, described in table 2. b) Proposed fragmentation scheme showing the location of the protonation processes in the parent compound that yield the corresponding product ions.

In parallel, the data analysis of *Desertifilum* sp. revealed a protonated molecular ion at *m/z* = 567.4204 Da that fits with the elemental composition $C_{40}H_{54}O_2$ (Table 2, peak 1). This MS signal is associated with a characteristic carotenoid-type UV-visible spectrum, which shows three maxima located at 400, 416 and 440 nm (Figure 4a). The retention time and spectroscopic characteristics resemble to those of flavoxanthin/chysanthemaxanthin [4]. The MS spectrum acquired in bbCID

mode of the molecular ion (Figure 4a) showed diverse signals detailed in Table 2. The product ion at *m*/*z* = 549.4093 Da corresponds to the loss of a hydroxyl group [36], while the product ions observed at *m*/*z* = 483.3619 Da, 469.3470 Da and 443.3345 Da are produced from decyclization and in-chain elimination reactions (Table 2) compatible with a dehydrated hydroxyl β cyclic end unit (Figure 3b). These fragmentations are yielded in a similar fashion as those denoted previously for hydroxyl-β-rings substituents [37]. In addition, the signal at *m*/*z* = 361.2550 Da could be assigned with a fragmentation at the 10,11 carbon-carbon bond and shows the presence of an epoxide group fused with a β cyclic end unit [38]. Additional product ions produced from the elimination of in-chain units (*m*/*z* = 487.4097 Da and 475.3553 Da) are also characteristic of the typical polyene structure of the carotenoids [36] (Figure 4b). To check the consistency, the structure of this carotenoid was fragmented *in silico* by the Mass Frontier™ software to predict all the product ions obtained experimentally. Indeed, the software predicted the presence of two additional product ions that subsequently were annotated in the experimental tandem MS of this carotenoid. These product ions observed at *m*/*z* = 525.3741 Da and 507.3622 Da, supports the presence of a 5,8-furanoid-ring, because the fragmentation mechanism is consistent with the presence this structural arrangement (Figure 4b). The combination of all the experimental data, both spectroscopic and chromatographic ones, allows the proposal of the structure depicted in Figure 4b as the most plausible. Chemically, the compound is the 5,8-furanoid-5,8-dihydro-2′-3′-didehydro-beta, epsilon-3-ol. Tentatively, we proposed the name desertixanthin, in honor to the species in which it is described.

3. Discussion

We have shown that recent progresses in the hyphenated HPLC systems with hybrid mass spectrometers, and potent post-processing software allows the identification of uncommon and unknown pigments in phytoplankton improving the previous analytical procedures. However, the significance of the enhancement in the measurement of independent and complementary physicochemical properties for the identification of pigments is aimed to gain biological meaning from metabolic processes where pigments participate.

In this sense, and as it was noted above, cyanobacteria species does not accumulate carotenoids with a 5,6-epoxy-group arrangement [2,3]. In fact, the ability to synthesize 5,6-epoxy-xanthophylls has been proposed as progress in the evolution from cyanobacteria to algae [3] because violaxanthin (a xanthophyll containing two 5,6-epoxide groups) is considered the central intermediate metabolite in the synthesis of other significant photoprotective xanthophylls. However, the application of an exhaustive extraction method, the use of more accurate and hybrid detection hardware, and the assistance of recent metabolomic tools greatly improved the fingerprint or *pigmentome* for a metabolic status, with the detection of minor components in microalgae and cyanobacteria. Table 1 shows the unusual detection of epoxy-xanthophylls (violaxanthin, neoxanthin, 5,6-epoxy-β-cryptoxanthin and 5,8-furanoid-β-cryptoxanthin) in cyanobacteria. Anyhow, the content of epoxy-xanthophylls is much higher in green microalgae (Table 1) that represent the typical species where the xanthophyll-cycle fully works [34]. The plastid zeaxanthin epoxidase (ZEP) is the responsible for the occurrence of the 5,6-epoxy-arrangement in terrestrial plants, green algae and recently in red algae [3]. ZEP synthetizes antheraxanthin from zeaxanthin and subsequently violaxanthin (Figure 1). Interestingly, Dautermann and Lohr [3] have retrieved several sequences in eight different cyanobacteria species through an *in silico* analysis that have been putatively assigned as ZEPs. In fact, following a similar approach and using one of their identified ZEP (Gloeocapsa sp. PCC7428), we have identified several positive matches for the sequence of ZEP in *Phormidium, Aphanotece* and *Desertifilum* spp. (Table 3). In this line, neoxanthin synthase (NSY) catalyses the formation of the allenic group in neoxanthin from violaxanthin, a pathway that has been observed in terrestrial plants [41]. However, Lohr, [42], found homologues for NSY in different genome banks (GenBank and Genome Portal of the Joint Genome Institute) for three cyanobacteria species (*Synechococcus, Synechocystis* and *Gloeobacter*). Specifically, in *Phormidium, Aphanotece* and *Desertifilum* spp. (Table 3), we have also identified several putative sequences for NSY using *Nostoc cycadae* [43] for query. The present data obtained using high-resolution MS (and MS^n) in combination with powerful post-processing software constitutes the

experimental support to show that certain carotenoid biosynthetic reactions, initially not considered in cyanobacteria, are active.

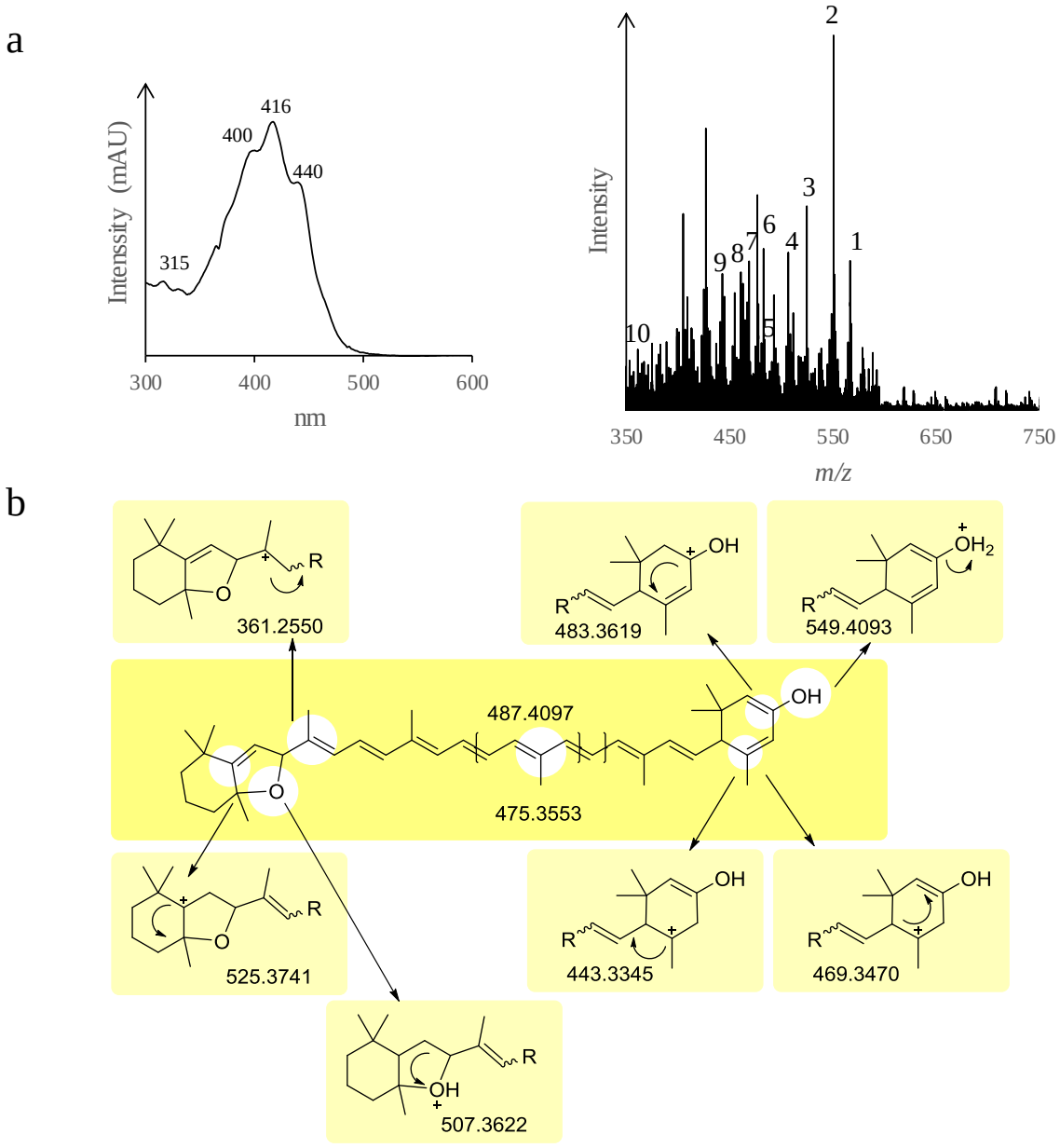

Figure 4. Characterization of desertixanthin: a) UV-visible and bbCID-mode MS spectra. Product ions are: 1, 567.4207 Da; 2, 549.4093 Da; 3, 525.3741 Da; 4, 507.3622 Da; 5, 487.4097 Da; 6, 483.3619 Da; 7, 475.3553 Da; 8, 469.3470 Da; 9, 443.3345 Da; 10, 361.2550 Da, described in table 2. b) Proposed fragmentation scheme showing the location of the protonation processes in the parent compound that yield the corresponding product ions.

The α-carotene branch (Figure 1) is limited to certain phyla of eukaryotic photosynthetic organisms [4,5. However, in cyanobacteria, this pathway is exceptionally active only in two peculiar genera: *Acaryochloris* and *Prochlorococcus*, which plenty accumulate α-carotene and its derivatives [44-46]. Recently, Takaichi et al. [47] have reconfirmed the presence of α-carotene in these genera in addition to low amounts of zeinoxanthin, and the presence of singular chlorophylls. *Acaryochloris* contains the unusual chlorophyll *d* as the major photosynthetic pigment and *Prochlorococcus* accumulates the uncommon DV-Chls *a* and *b* instead of the usual MV-chlorophylls, although the relationship with the α-carotene pathway is unknown. We have included in the automatic matching process (Figure 2) those unusual chlorophylls in the targeted screening, but the search has been

unsuccessful both in *Aphanotece* and *Desertifilum*. Another difference with *Acaryochloris* and *Prochlorococcus* is that their carotenoid profile is rich in α-carotene and zeaxanthin but low contents of β-carotene and zeinoxanthin are observed [47]. However, *Aphanotece* and *Desertifilum* presented the typical carotenoid profile of a cyanobacteria, rich in β-carotene and zeaxanthin, while α-carotene and zeinoxanthin are minor carotenoids. A biosynthetic pathway for α-carotene in cyanobacteria has been proposed [47], including the open reading frame and identities of the corresponding biosynthetic genes. Following this scheme, the *in silico* search of homologous of CrtL-b and CrtR in *Phormidium, Aphanotece* and *Desertifilum* spp. (Table 3) gave positive results in comparison with the functional proteins previously identified in *Prochlorococcus* and *Synechocystis* [46,48-49]. As it has been predicted [47], further search among cyanobacteria species for α-carotene synthesis would produce positive matches. Our systematic workflow seems to be a useful tool for future targeted metabolomics with that aim.

Table 3: *In silico* identification of specific carotenogenic genes/enzymes in *Aphanotece*, *Phormidium* or *Desertifilum* sp. cyanobacteria. Data were compiled from BLASTP searches.

Gene/ enzyme	Query sequence for BLASTP		Cyanobacteria specie	e-value	Identity (%)	Accession number
	Accession number	Cyanobacteria specie				
ZEP	WP_015191032.1	*Gloeocapsa* sp. PCC7428[a]	*Aphanothece hegewaldii*	0.0	74.35%	WP_073593680.1
			Phormidium tenue	0.0	69.87%	WP_069967261.1
			Phormidium ambiguum	0.0	67.18%	WP_106456341.1
			Desertifilum sp. IPPAS B-1220	3e-175	62.44%	WP_073607122.1
NSY	WP_031293851.1	*Leptolyngbya* sp. strain Heron Island[b]	*Phormidium tenue*	5e-158	56.23%	WP_073608653.1
			Aphanothece minutissima	1e-120	50.50%	WP_106220476.1
CrtL-b	CAE19523.1	*Prochlorococcus marinus* CCMP1986 [c]	*Aphanothece minutissima*	4e-134	50.87%	WP_106220476.1
			Phormidium tenue	8e-125	45.11%	WP_073608653.1
CrtR	BAA17468.1	*Synechocystis* sp-PCC 6803 [d]	*Aphanothece sacrum*	3e-175	81.23%	WP_124976402.1
			Aphanothece hegewaldii	1e-174	78.60%	WP_106457299.1
			Phormidium ambiguum	1e-163	72.00%	WP_073592421.1
			Desertifilum sp. IPPAS B-1220	3e-153	72.26%	WP_069966993.1
			Phormidium sp. HE10JO	1e-151	69.59%	WP_087709186.1
			Phormidium sp. OSCR	2e-151	69.59%	KPQ34345.1
			Phormidium willei	7e-151	69.59%	WP_068788347.1
			Phormidium sp. SL48-SHIP	8e-151	69.59%	TAN89557.1
			Phormidium tenue	5e-147	66.44%	WP_073610059.1
			Aphanothece minutissima	7e-122	59.67%	WP_106220774.1

Following with the unexpected results obtained with the systematic approach, myxoxanthophyll, a xanthophyll (myxol) glycoside (rhamnose or hexose) ester [50] is not observed in the carotenoid profile although it is a characteristic and widely distributed carotenoid in

cyanobacteria. However, Takaichi et al, [51] described the first cyanobacteria species that accumulates free myxol (or 3-hydroxy-deoxymyxol) but not the myxol glycosides. Interestingly, this strain accumulated a novel derivative from myxol, the 4-hydroxy-myxol. This divergence over the general distributed myxoxantophyll pathway in cyanobacteria is like the one observed here for *Aphanotece* and *Desertifilum*. However, in these species there is not even synthesis of myxol, either free or esterified, so that it should be assumed that the 2′-dehydrodeoxymyxol identified in this work arises from the precursor deoxomyxol or plectionoxanthin through the activity of a desaturase-type enzyme. In fact, Hertzberg et al. [52] found a species of *Phormidium* (*P. persicinum*), which is highly phylogenetically related with *Desertifilum*, that also lacks glycosidic carotenoids, while the rest of *Phormidium* species exhibited myxolglycosides. However, with the analytical tools available in those years the detection of minor carotenoids was hardly possibly. Probably, although the general pattern in cyanobacteria is the synthesis and accumulation of myxolglycosides, the continuous development of more precise and accurate analytical tools will reveal alternative pathways to the common one in certain cyanobacteria species.

Finally, although the tentative carotenoid structure, desertixanthin, displays common ring configurations in the biosynthetic pathway of carotenoids, the combination of a dehydrated ε-ring and a furanoid-β ring constitutes an exceptional rearrangement. Similar carotenoid precursors have been identified in algal species. For example, α-cryptoxanthin has been described in red microalgae [53] while 5,6-epoxy-α-cryptoxanthin accumulated in green chlorophyte algae [54]. In this sense, our tentatively identified carotenoid is highly related with two already known carotenoids, considering the structural arrangements, polarity and even spectroscopic characteristics: flavoxanthin/chrysanthemaxanthin and flavochrome, The first carotenoid (flavoxanthin or chrysanthemaxanthin, both epimers at the C8 atom) is the 5,8-furanoid-5,8-dihydro-beta,epsilon-carotene-3,3′-diol [55-56], usually present in minor amounts in several terrestrial plants, lichens and even algae [57-58]. Flavochrome, 5,8-furanoid-5,8-dihydro-beta, epsilon-carotene, was initially identified in calendula flowers [59] and since then its accumulation has been described in other species of plants, lichens and even in animals. However, to the best of our knowledge, no biosynthetic pathway has been proposed for any of the previous carotenoids. Considering the tentative structure proposed for desertixanthin, the starting branch in cyanobacteria should be α-carotene, including a subsequent 5,8-furanoid arrangement at the β-ring and a hydroxylation at the C3′atom of the ε-ring. Even, the configuration 2',3'-didehydro- in the ε-ring is present in several algal carotenoids as the anhydromicromonal, anhydromicromonol and anhydroprasinoxanthin (*Mantoniella squamata*) or anhydrouriolide (*Micromonas pusilla*). Chemically, all the functional groups that characterize desertixanthin are present in carotenoids described in living organisms in the nature, but it is necessary further characterizations in cyanobacteria to get insights of the precursors and to establish a plausible biosynthetic pathway. Indeed, all these structural arrangements are examples of the biosynthetic plasticity of phytoplankton in the carotenoid pathway and, consequently, point to the great potential of these organisms for carotenoid production.

4. Materials and Methods

4.1 Microorganisms and cultivation conditions

Axenic cultures of *Scenedesmus obliquus* (CPCC05) and *Chlorella vulgaris* (CPCC90) were obtained from the Canadian Phycological Culture Centre. Axenic cultures of *Aphanothece microscopica* Nägeli (RSMan92) was obtained from the collection of the Cyanobacteria and Phycotoxins Laboratory of the Institute of Oceanography from the Federal University of Rio Grande (www.cianobacterias.furg.br). Axenic cultures of tentative *Phormidium autumnale* Gomont were originally isolated from the Cuatro Cienegas desert, in Mexico (26º59' N, 102º03' W). All the strains were cultivated in a bubble column photobioreactor using synthetic BG-11 medium [60] at pH 7.6 and 26 °C under constant photon flux density of 25 μmol.m^{-2} s^{-1} through a photoperiod of 24:0 h light:dark.

4.2 DNA isolation and sequencing

Total DNA from tentative *Phormidium autumnale* Gomont strain to be used in PCR and sequencing was extracted from isolated colonies by the small-scale fast chloroform method as previously described [61]. A fragment of the 16S rRNA gene (1400pb aprox.) was amplified with the primer pair 7 for ((5´AGAGTTTGATYMTGGCTCAG3`) and 1510r (5´TACGGYTACCTTGTTACGACTT3´) [62]. The resulting amplicon were purified using a Sureclean Plus Kit (Bioline meridian bioscience, London, UK) and sequenced with the same both primers at STAB vida Lda. (Caparica, Portugal). The resulting sequences were edited by Chromas and the consensus sequence was compared with those available in GenBank using the BLAST tool available at the Nacional Center for Biotechnology Information web site (http://blast.ncbi.nlm.nih.gov/Blast.cgi). Finally, our strain was identified as *Desertifilum* sp. with a 100% of similarity, and it was deposited in the GenBank with the accession number MK307822.

4.3 In silico analyses of ZEP, NSY, CrtL-b and crtR homologues from Aphanotece microscopica and Desertifilum sp.

Sequence data from *Aphanotece* and *Desertifilum* spp. were searched for ZEP, NSY, CrtL-b and crtR candidates with the BLASTP tool using the amino acid sequence of the corresponding genes in the cyanobacteria where they have been identified as input (Table 3).

4.4 Reagents

All the chemical compounds used for the BG-11 medium, sodium chloride, ammonium acetate (98%) and tetrabutylammonium acetate were supplied by Sigma-Aldrich Chemical Co. (Madrid, Spain). Analysis grade solvents, acetone and diethyl ether were supplied by Teknokroma (Barcelona, Spain) and *N*,*N*-dimethylformamide (DMF) and hexane by Panreac. HPLC grade solvents, methanol, methyl *tert*-butyl ether and water were supplied by Panreac (Barcelona, Spain), while acetone was supplied by Merck. Deionised water used was produced in a Milli-Q 50 system (Millipore Corp., Milford, MA, USA). Chlorophyll *a* and *b* were purchased from Wako (Neuss, Germany) and Sigma-Aldrich (Madrid, Spain), respectively. Chlorophyllide *a* was obtained by enzymatic de-esterification of the corresponding parent chlorophyll *a*, using partially purified chlorophyllase from orange peel [63]. 13²-Hydroxy chlorophyll *a* was produced by oxidizing chlorophyll *a* with SeO_2 in pyridine at 70 ºC for 3 h [64]. Pheophytin *a* was obtained from chlorophyll *a* dissolved in diethyl ether by acidification with two or three drops of 5 M HCl [65]. Standards of lutein, zeaxanthin, β-carotene were obtained from Extrasynthese (Genay Cedex, France), while standards of diadinoxanthin, diatoxanthin and antheraxanthin were obtained from DHI lab (Hørsholm Denmark). Other carotenoid standards (α-carotene, β-cryptoxanthin, echinenone, myxoxanthophyll, neoxanthin, violaxanthin, luteoxanthin and mutatoxanthin) were obtained following the procedures described by Britton et al. [66]. All the standards were analysed with the same experimental conditions as the microalgae extracts, allowing the comparison of the UV-visible and bbCID MS^n between them. Standards of zeinoxanthin and β-cryptoxanthin epoxides were not available, and the identification was performed according to previous results.

4.5 Extraction of photosynthetic pigments

Aliquots of microalgae or cyanobacteria biomass (5 mL) were filtered through a 47-mm diameter glass microfiber filter (GF/F; Whatman), and directly frozen at -80 °C [67]. The filter was grinded with liquid nitrogen into powder and mixed with 10 mL of DMF:water (9:1) under stirring at 4 °C for 15 min and spinning (10000 rpm, 5 min). Next, the solvent phase was collected in a separation funnel whereas the solid residue was re-extracted with 10 mL hexane, ultrasonicated (5 min, 720 W) and vortexed (5 min). Then, 10 mL NaCl solution (10% w/v) was added to the mixture, centrifuged (10000 rpm, 5 min) and the supernatant was mixed in the funnel. Finally, the pellet was dissolved with 10 mL diethyl ether, ultrasonicated (5 min, 720 W) and vortexed (5 min). After the addition of 10 mL NaCl solution (10% w/v) the mixture is centrifuged (10000 rpm, 5 min). All the mixed solvent layers were extracted in the funnel with diethyl ether and NaCl solution (10% w/v). The upper phase was concentrated to dryness in a rotary evaporator and the residue was dissolved in acetone. Samples were stored at -20 °C until analysis within one week.

4.6 Identification of photosynthetic pigments by HPLC-ESI/APCI-HRTOF-MS^n

A liquid chromatograph Dionex Ultimate 3000RS U-HPLC (Thermo Fisher Scientific, Waltham, MA, USA) was used to achieve chromatographic separation of photosynthetic pigments. For chlorophyll pigments, a 3 μm particle C_{18} column was used (200×4.6 mm i.d., Teknokroma, Barcelona, Spain) with the elution gradient previously described by [64]. However, the column assayed for carotenoids pigments was a C_{30} with 3 μm particle size (250 mm×4.6 mm i.d., YMC, Schermbeck, Germany), applying the elution gradient described by Breithaupt et al. [68] and recently modified [69]. The PDA detector recorded the UV-visible spectra from the 300 nm to 700 nm wavelength range. For both group of pigments, the injection volume was 30 μL and the flow rate was set at 1 mL/min, while a split post-column of 0.4 mL/min was introduced directly on the mass spectrometer ion source. The mass spectrometry equipment was a micrOTOF-QIITM High Resolution Time-of-Flight mass spectrometer (UHR-qTOF) with Qq-TOF geometry (Bruker Daltonics, Bremen, Germany). The analysis was developed with an ESI interface (for chlorophyll compounds) or an APCI source (for carotenoid compounds). In all cases, the instrument was operated in positive ion mode scanning the *m*/*z* values in the 50-1200 Da range. The mass spectra acquisition mode was broad-band Collision Induced Dissociation mode (bbCID), allowing to study at the same time MS and MS/MS spectra. The control of the instrument was done using the software Bruker Compass HyStar (Bruker Daltonics version 3.2) and Bruker Compass DataAnalysis (Bruker Daltonics version 4.1) for data evaluation. For the automated peak detection on the EICs, the software TargetAnalysis™ (Bruker Daltonics version 1.2) was used. The corresponding identifications were carried out according to mass accuracy, with a tolerance limit at 5 ppm and in combination with the isotopic pattern calculated by SigmaFit™ algorithm with a limit of 50 [64]. The interpretation of the MS/MS spectra and the consistency of the product ions (with identical criteria for mass accuracy and isotopic pattern established for the corresponding protonated molecule) was developed with the SmartFormula3D™ module [64]. The software MassFrontier™ (Thermo Scientific™ version 4.0, Waltham, USA) allowed the acquisition of the *in silico* MS^2 spectra of target compounds to compare the theoretical product ions with the corresponding experimental MS^2. This software enables the evaluation of different product ions when different isomers respond to the same bbCID spectrum.

4.7 Quantification of photosynthetic pigments by HPLC-UV-visible detection

The identified pigments were quantified by reversed-phase HPLC using a Hewlett-Packard HP 1100 liquid chromatograph with the same columns and gradients as for MS analysis. The on-line UV-visible spectra were recorded from 350 nm to 800 nm wavelength range with a photodiode–array detector, and sequential detection was performed at 410, 430, 450 and 666 nm. Data were collected and processed with the software HP ChemStation (Rev.A.05.04). Quantification of pigments was achieved with the corresponding calibration curves (amount versus integrated peak area). The calibration equations were obtained by least-squares linear regression analysis over a concentration range according to the observed levels of the pigments in the samples. Triplicate injections were made for five different volumes of each standard solution.

4.8 Statistical analysis

Normality of data (mean values of three independent measurements) was checked with the Shapiro-Wilk test, and one-way analysis of the variance was performed using Statistica software (StatSoft, Inc., 2001). Post-hoc comparison for investigation of the statistically significant differences was made with the Tukey, setting the significance value a $P<0.05$.

Supplementary Materials: The following are available online at www.mdpi.com/xxx/s1, Table S1: Carotenoids identified by HPLC-PDA-APCI(+)-Q-TOF in the species analysed in the study, Table S2: Characterization by HPLC-PDA-APCI(+)-Qq-TOF-MS in bbCID mode of unusual and unknown carotenoids in microalgal extracts.

Author Contributions: conceptualization, L.Q.Z., E.J. and M.R.; methodology, B.C. and M.R.; software, A.P.; validation, M.M.M and B.C.; formal analysis, M.M.M., B.C., A.P. and M.R.; investigation, M.M.M. and B.C.; resources, L.Q.Z. and E.J.; data curation, A.P. and M.R.; writing—original draft preparation, M.R.; writing—

review and editing, L.Q.Z., E.J., A.P. and M.R.; supervision, M.R.; project administration, M.R.; funding acquisition, M.R.

Funding: This work was supported by the Comisión Interministerial de Ciencia y Tecnología (CICYT-EU, Spanish and European Government, grant number RTI2018-095415-B-I00). MM was supported with a fellowship from CAPES. The APC was partially funded by CSIC.

Acknowledgments: The authors would like to thank to Jose Luis Ruiz-Barba for his scientific assistance.

Conflicts of Interest: The authors declare no conflict of interest.

References

1. Huang, J.J.; Lin, S.; Xu, W.; Cheung, P.C.K. Occurrence and biosynthesis of carotenoids in phytoplankton. *Biotechnol. Adv.* **2017**, *35*, 597-618. DOI: 10.1016/j.biotechadv.2017.05.001.
2. Goodwin, T.W. *The biochemistry of the carotenoids*, 2nd ed. Chapman and Hall: London, New York, **1980**.
3. Dautermann, O.; Lohr, M. A functional zeaxanthin epoxidase from red algae shedding light on the evolution of light-harvesting carotenoids and the xanthophyll cycle in photosynthetic eukaryotes. *Plant J.* **2017**, *92*, 879-891. DOI: 10.1111/tpj.13725.
4. Britton, G., Liaaen-Jensen, S. and Pfander, H. *Carotenoids: Handbook*, Basel: Boston: Birkhäuser Verlag. 2004.
5. Takaichi, S. Carotenoids in algae: distributions, biosynthesis and functions. *Mar Drugs* **2011**, *9*, 1101–1118. DOI: 10.3390/md9061101.
6. Brzezowski, P.; Richter, A.S.; Grimm, B. Regulation and function of tetrapyrrole biosynthesis in plants and algae. *Biochim. Biophys. Acta*. **2015**, *1847*, 968-985. DOI: 10.1016/j.bbabio.2015.05.007.
7. Gong, M.; Bassi, A. Carotenoids from microalgae: A review of recent developments. *Biotechnol. Adv*. **2016**, *34*, 1396–1412.
8. Liang, M.H.; Zhu, J.; Jiang, J.G. Carotenoids biosynthesis and cleavage related genes from bacteria to plants. *Crit. Rev. Food Sci. Nutr.* **2018**, 58, 2314-2333. DOI: 10.1080/10408398.2017.1322552.
9. Serive, B.; Nicolau, E.; Bérard, J.B.; Kaas, R.; Pasquet, V.; Picot, L.; Cadoret, J.P. Community analysis of pigment patterns from 37 microalgae strains reveals new carotenoids and porphyrins characteristic of distinct strains and taxonomic groups. *PLoS One* **2017**, *12*, e0171872. DOI: 10.1371/journal.pone.0171872.
10. Jeffrey, S.W.; Wright, S.W.; Zapata, M. Microalgal classes and their signature pigments. In *Phytoplankton pigments,* Roy, S., Llewellyn, C.A., Egeland, E.S., Johnsen, G., Eds. Cambridge University Press: United Kingdom, 2011; pp. 3-77.
11. Hosikian A.; Lim S.; Halim, R.; Danquah, M.K. Chlorophyll Extraction from Microalgae: A Review on the Process Engineering Aspects. *Int. J. Chem. Eng.* **2010**, 1-11. DOI: 10.1155/2010/391632.
12. Kumar, J.S.P.; Garlapati, V.K.; Dash, A.; Scholz, P.; Banerjee, R. Sustainable green solvents and techniques for lipid extraction from microalgae: A review. *Algal Res.* **2017**, *21*, 138–147. DOI: 10.3389/fenrg.2014.00061.
13. Scotter, M.J. Overview of EU regulations and safety assessment for food colours. In *Colour additives for foods and beverages*, Scotter, M.J., Eds.; Woodhead Publ.: Cambridge, UK., 2015; pp. 61–74.
14. Cerón-García, M.C.; González-López, C.V.; Camacho-Rodríguez, J.; López-Rosales, L.; García-Camacho, F.; Molina-Grima, E. Maximizing carotenoid extraction from microalgae used as food additives and determined by liquid chromatography (HPLC). *Food Chem*. **2018**, *15*, 316-324. DOI: 10.1016/j.foodchem.2018.02.154.
15. Poojary, M.M.; Barba, F.J.; Aliakbarian, B.; Donsì, F.; Pataro, G.; Dias, D.A.; Juliano, P. Innovative Alternative Technologies to Extract Carotenoids from Microalgae and Seaweeds. *Mar Drugs*. **2016**, *4*, E214. DOI: 10.3390/md14110214.
16. Juin, C.; Bonnet, A.; Nicolau, E.; Bérard, J.B.; Devillers, R.; Thiéry, V.; Cadoret, J.P.; Picot, L. UPLC-MSE Profiling of Phytoplankton Metabolites: Application to the Identification of Pigments and Structural Analysis of Metabolites in *Porphyridium purpureum*. *Mar. Drugs*. **2015**, *13*, 2541-2558. DOI: 10.3390/md13042541.
17. Sommella, E.; Conte, G.M.; Salviati, E.; Pepe, G.; Bertamino, A.; Ostacolo, C.; Sansone, F.; Prete, F.; Aquino, R.P.; Campiglia, P. Fast Profiling of Natural Pigments in Different Spirulina (Arthrospira platensis) Dietary Supplements by DI-FT-ICR and Evaluation of their Antioxidant Potential by Pre-Column DPPH-UHPLC Assay. *Molecules* **2018**, *23*, 1152. DOI: 10.3390/molecules23051152.
18. Gavalás-Olea, A.; Garrido, J.L.; Riobo, P.; Alvarez, S.; Vaz, B. Mass Spectrometry of Algal Chlorophyll *c* Compounds. *Curr. Org. Chem.* **2018**, *22*, 836-841.

19. Pacini, T.; Fu, W.; Gudmundsson, S.; Chiaravalle, A.E.; Brynjolfson, S.; Palsson, B.O.; Astarita, G.; Paglia, G. Multidimensional Analytical Approach Based on UHPLC-UV-Ion Mobility-MS for the Screening of Natural Pigments. *Anal. Chem.* **2015**, *87*, 2593–2599. DOI: 10.1021/ac504707n.
20. Sun, P.; Wong, C.C.; Li, Y.; He, Y.; Mao, X.; Wu, T.; Ren, Y.; Chen, F. A novel strategy for isolation and purification of fucoxanthinol and fucoxanthin from the diatom *Nitzschia laevis*. *Food Chem*. **2019**, *30*, 566-572. DOI: 10.1016/j.foodchem.2018.10.133.
21. Li, Z.; Lu, Y.; Guo, Y.; Cao, H.; Wang, Q.; Shui, W. Comprehensive evaluation of untargeted metabolomics data processing software in feature detection, quantification and discriminating marker selection. *Anal Chim Acta*. **2018**, *31*, 50-57. DOI: 10.1016/j.aca.2018.05.001.
22. Allen, F.; Greiner, R.; Wishart, D. Competitive fragmentation modeling of ESI-MS/MS spectra for putative metabolite identification. *Metabolomics* **2015**, *11*, 98–110.
23. Kang, K.B.; Ernst, M.; van der Hooft, J.J.J.; da Silva, R.R.; Park, J.; Medema, M.H.; Sung, S.H.; Dorrestein, P.C. Comprehensive mass spectrometry-guided plant specialized metabolite phenotyping reveals metabolic diversity in the cosmopolitan plant family Rhamnaceae. *Plant J.* **2019**, doi: 10.1111/tpj.14292.
24. Kaufmann, A.; Butcher, P.; Maden, K.; Walker, S.; Widmer, M. High-resolution mass spectrometry-based multi-residue method covering relevant steroids, stilbenes and resorcylic acid lactones in a variety of animal-based matrices. *Anal. Chim. Acta*. **2019**, *1054*, 59-73. DOI: 10.1016/j.aca.2018.12.012.
25. Saito, M.A.; Dorsk, A.; Post, A.F.; McIlvin, M.R.; Rappé, M.S.; DiTullio, G.R.; Moran, D.M. Needles in the blue sea: Sub-species specificity in targeted protein biomarker analyses within the vast oceanic microbial metaproteome. *Proteomics* **2015,** *15*, 3521-3531. DOI: 10.1002/pmic.201400630.
26. Sharma, S.K.; Nelson, D.R.; Abdrabu, R.; Khraiwesh, B.; Jijakli, K.; Arnoux, M.; O'Connor, M.J.; Bahmani, T.; Cai, H.; Khapli, S.; Jagannathan, R.; Salehi-Ashtiani, K. An integrative Raman microscopy-based workflow for rapid in situ analysis of microalgal lipid bodies. *Biotechnol. Biofuel*. **2015**, *8*, 164. DOI: 10.1186/s13068-015-0349-1.
27. Francisco, E.C.; Franco, T.T.; Wagner, R.; Jacob-Lopes, E. Assessment of different carbohydrates as exogenous carbon source in cultivation of cyanobacteria. *Bioprocess Biosyst. Eng*. **2014**, *37*, 1497-505. DOI: 10.1007/s00449-013-1121-1.
28. Cai, F.; Chen, Y.; ZHU, M.; Li, X.; Li, R. *Desertifilum salkalinema* sp. nov. (Oscillatoriales, Cyanobacteria) from an alkaline pool in China. *Phytotaxa* **2017**, *292*, 262–270. DOI: 10.11646/phytotaxa.292.3.6.
29. Dadheech, P.K.; Abed, R.M.M.; Mahmoud, H.; Mohan, M.K.; Krienitz, L. Polyphasic characterization of cyanobacteria isolated from desert crusts, and the description of *Desertifilum tharense* gen. et sp. nov. (Oscillatoriales). *Phycologia* **2012**, *51*, 260-270. DOI: 10.5507/fot.2014.010.
30. Cellamare, M., Duval, C., Drelin, Y.; Djediat, C.; Touibi, N.; Agoguë, H.; Leboulanger, C.; Ader, M.; Bernard. C. Characterization of phototrophic microorganisms and description of new cyanobacteria isolated from the saline-alkaline crater-lake Dziani Dzaha (Mayotte, Indian Ocean). *FEMS Microbiol. Ecol.* **2018**, *94*, fiy108. DOI: 10.1093/femsec/fiy108.
31. Paliwal, C.; Ghosh, T.; George, B.; Pancha, Y.; Maurya, R.; Chokshi, K.; Ghosh, A.; Mishra, S. Microalgal carotenoids: Potential nutraceutical compounds with chemotaxonomic importance. *Algal Res.* **2016**, *15*, 24-31. DOI: 10.1016/j.algal.2016.01.017.
32. Rodrigues, D.B.; Menezes, C.R.; Mercadante, A.Z.; Jacob-Lopes, E.; Zepka, L.Q. Bioactive pigments from microalgae *Phormidium autumnale*. *Food Res. Int*. **2015**, *77*, 273–279. DOI: 10.1016/j.foodres.2015.04.027.
33. Guyer, L.; Salinger, K.; Krügel, U.; Hörtensteiner, S. Catalytic and structural properties of pheophytinase, the phytol esterase involved in chlorophyll breakdown. *J. Exp. Bot.* **2018**, *69*, 879-889.
34. Brunet, C.; Johnsen, G.; Lavaud, G.; Roy, S. (2011) Pigments and photoacclimation processes. In *Phytoplankton pigments,* Roy, S., Llewellyn, C.A., Egeland, E.S., Johnsen, G., Eds.; Cambridge University Press: United Kingdom, pp. 445-471.
35. Maroneze, M.M.; Jacob-Lopes, E.; Zepka, L.Q.; Roca, M.; Pérez-Gálvez, A. Esterified carotenoids as new food components in cyanobacteria. *Food Chem*. **2019**, *287*, 295–302. DOI: 10.1016/j.foodchem.2019.02.102.
36. van Breemen, R.B.; Huan, C.R.; Tan, Y.; Sander, L.C.; Schilling, A.B. Liquid chromatography/mass spectrometry of carotenoids using atmospheric pressure chemical ionization. *J. Mass Spectrom.* **1996,** *31*, 975-981. DOI: 10.1002/(SICI)1096-9888(199609)31:9<975::AID-JMS380>3.0.CO;2-S C.
37. van Breemen, R.B.; Dong, L.; Pajkovic, N.D. Atmospheric pressure chemical ionization tandem mass spectrometry of carotenoids. *Int. J. Mass Spectrom*. **2012,** *312*, 163-172. DOI: 10.1016/j.ijms.2011.07.030.

590 38. de Rosso, V.V.; Mercandante, A.Z. Identification and quantification of carotenoids by HPLC-PDA-MS/MS
591 from Amazoniam fruits. *J. Agric. Food Chem.* **2007**, *55*, 5062-5072. DOI: 10.1021/jf0705421.
592 39. Young, A.; Britton, G. *Carotenoids in photosynthesis,* Chapman and Hall: London, UK, 1993.
593 40. Turcsi, E.; Murillo, E.; Kurtán, T.; Szappanos, A.; Illyés, T.; Gulyás-Fekete, G.; Agócs, A.; Avar, P.; Deli, J.
594 Isolation of β-Cryptoxanthin-epoxides, Precursors of Cryptocapsin and 3′-Deoxycapsanthin, from Red
595 Mamey (*Pouteria sapota). J. Agric. Food Chem*. **2015,** *63*, 6059–6065. DOI: 10.1021/acs.jafc.5b01936.
596 41. Bouvier, F.; D'Harlingue, A.; Backhaus, R.A.; Kumagai, M.H.; Camara, B. Identification of neoxanthin
597 synthase as a carotenoid cyclase paralog. *Eur. J. Biochem*. **2000**, *267*, 6346-6352. DOI: 10.1046/j.1432-
598 1327.2000.01722.x.
599 42. Lohr, M. Carotenoid metabolism in phytoplankton. In *Phytoplankton pigments*, Roy, S., Llewellyn, C.A.,
600 Egeland, E.S., Johnsen, G., Eds.; Cambridge University Press: United Kingdom, 2011; pp. 113-161.
601 43. Kanesaki, Y.; Hirose, M.; Hirose, Y.; Fujisawa, T.; Nakamura, Y.; Watanabe, S.; Matsunaga, S.; Uchida, H.;
602 Murakami, A. Draft Genome Sequence of the Nitrogen-Fixing and Hormogonia-Inducing Cyanobacterium
603 *Nostoc cycadae* Strain WK-1, Isolated from the Coralloid Roots of *Cycas revolute*. *Genome Announc*. **2018**, *15*.
604 DOI: 10.1128/genomeA.00021-18.
605 44. Goericke, R.; Repeta, D.J. The pigments of *Prochlorococcus marinus*: the presence of divinyl chlorophyll *a*
606 and *b* in a marine prokaryote. *Limnol. Oceanogr*. **1992**, *37*, 425–433.
607 45. Miyashita, H.; Adachi, K.; Kurano, N.; Ikemoto, H.; Chihara, M.; Miyachi, S. Pigment composition of a
608 novel oxygenic photosynthetic prokaryote containing chlorophyll *d* as the major chlorophyll. *Plant Cell*
609 *Physiol.* **1997**, *38*, 274–281.
610 46. Stickforth, P.; Steiger, S.; Hess, W.R.; Sandmann, G. A novel type of lycopene e-cyclase in the marine
611 cyanobacterium *Prochlorococcus marinus* MED4. *Arch. Microbiol*. **2003,** *179*, 409–415. DOI: 10.1007/s00203-
612 003-0545-4.
613 47. Takaichi, S.; Mochimaru, M.; Uchida, H.; Murakami, A.; Hirose, E.; Maoka, T.; Tsuchiya, T.; Mimuro, M.
614 Opposite Chilarity of α-Carotene in Unusual Cyanobacteria with Unique Chlorophylls, *Acaryochloris* and
615 *Prochlorococcus. Plant Cell Physiol*. **2012,** *53*, 1881–1888. DOI: 10.1093/pcp/pcs126.
616 48. Masamoto, K.; Misawa, N.; Kaneko, T.; Kikuno, R.; Toh, H. β-Carotene hydroxylase gene from the
617 cyanobacterium *Synechocystis* sp. PCC6803. *Plant Cell Physiol.* **1998**, *39*, 560–564.
618 49. Lagarde, D.; Vermaas, W. The zeaxanthin biosynthesis enzyme β-carotene hydroxylase is involved in
619 myxoxanthophyll synthesis in *Synechocystis* sp. PCC 6803. *FEBS Lett*. **1999**, *454*, 247–251. DOI:
620 10.1016/S0014-5793(99)00817-0.
621 50. Takaichi, S.; Mochimaru, M. Carotenoids and carotenogenesis in cyanobacteria: unique ketocarotenoids
622 and carotenoid glycosides. *Cell. Mol. Life Sci.* **2007,** *64*, 2607–2619. DOI: 10.1007/s00018-007-7190-z.
623 51. Takaichi, S.; Mochimaru, M.; Maoka, T. Presence of free myxol and 4-hydroxymyxol and absence of myxol
624 glycosides in *Anabaena variabilis* ATCC 29413, and proposal of a biosynthetic pathway of carotenoids. *Plant*
625 *Cell Physiol.* **2006,** *47*, 211-216. DOI: 10.1093/pcp/pci236.
626 52. Hertzberg, S.; Liaaen-Jensen S.; Sielgelman, H. W. The carotenoids of blue-green algae. *Phytochem*. **1971**, *10*,
627 3121- 3127. DOI: 10.1016/S0031-9422(00)97362-X.
628 53. Bjørnland, T.; Aguilar-Martinez, M. Carotenoids in red algae. *Phytochem*. **1976**, *15*, 291-296. DOI:
629 10.1016/S0031-9422(00)89006-8.
630 54. Nybraaten, G.; Jensen, S. L. Algal Carotenoids. XI. New Carotenoid Epoxides from *Trentepohlia iolithus*. *Acta*
631 *Chem. Scand. Ser. B*, **1974**, *28*, 483- 485.
632 55. Cadosch, H.; Vögeli, U.; Rüedi, P.; Eugster, C.H. On the Carotenoids Flavoxanthin and
633 Chrysanthemaxanthin: 1H-NMR., 13C-NMR. and Mass Spectra, Absolute Configuration. *Helv. Chim. Acta.*
634 **1978**, *61*, 783-794. DOI: 10.1002/hlca.19780610226
635 56. Kull, D.; Pfander, H. Isolation and Identification of Carotenoids from the Petals of Rape (*Brassica napus*). *J.*
636 *Agric. Food Chem*. **1995**, *43*, 2854–2857. DOI: 10.1021/jf00059a016.
637 57. Strain, H.H.; Manning, W.M.; Hardin, G. Xanthophylls and carotenes of diatoms, brown algae,
638 dinoflagellates, and sea-anemones. *Biol. Bull*. **1944,** *86*, 169-191. DOI: 10.2307/1538339.
639 58. Hegazi, M.M.; Pérez-Ruzafa, A.; Almela, A.; Candela, M.E. Separation and identification of chlorophylls
640 and carotenoids from *Caulerpa prolifera, Jania rubens* and *Padina pavonica* by reversed phase high-
641 performance liquid chromatography. *J. Chromatogr. A,* **1998**, *829*, 153–159. DOI: 10.1016/S0021-
642 9673(98)00803-6.

59. Goodwin, T.W. Studies in Carotenogenesis. 13. The carotenoids of the flower petals of *Calendula officinalis*. *Biochem. J.* **1954**, *58*, 90-94.
60. Rippka, R.; Deruelles, J.; Waterbury, J.B.; Herdman, M.; Stanier, R.Y. Generic Assignments, Strain Histories and Properties of Pure Cultures of Cyanobacteria. *J. Gen. Microbiol.* **1979**, *111*, 1-61. DOI: 10.1099/00221287-111-1-1.
61. Ruiz-Barba, J.L.; Maldonado, A.; Jiménez-Díaz, R. Small-scale total DNA extraction from bacteria and yeast for PCR applications. *Anal. Biochem*. **2005,** *347*, 333-335. DOI: 10.1016/j.ab.2005.09.028.
62. Lane, D.J. 16/23S rRNA sequencing. In *Nucleic Acid Techniques in Bacterial Systematics*, Stackebrandt, E., Goodfellow, M., Eds.; Wiley: Chichester, UK, 1991; pp. 115–175.
63. Roca, M.; León, L.; de la Rosa, R. Pigment metabolism of "Sikita" olive (*Olea europaea* L.) A new cultivar obtained by cross-breeding A new cultivar obtained by cross-breeding. *J. Agric. Food Chem*. **2011**, *59*, 2049-2055. DOI: DOI: 10.1021/jf104374t.
64. Chen, K.; Ríos, J.J.; Pérez, A.; Roca, M. Development of an accurate and high-throughput methodology for structural comprehension of chlorophylls derivatives. (I) Phytylated derivatives. *J. Chromatograph. A*. **2015**, *1406*, 99-108. DOI: 10.1016/j.chroma.2015.05.072.
65. Sievers, G.; Hynninen, P. Thin-layer chromatography of chlorophylls and their derivatives on cellulose layer. *J. Chromatog.* **1977**, *134*, 359–364. DOI: 10.1016/S0021-9673(00)88534-9.
66. Britton, G.; Liaaen-Jensen, S.; Pfander, H. (1995). Carotenoids. Volume 1A: Isolation and analysis. Basel: Birkhäuser Verlag.
67. Wright, S. W.; Jeffrey, S.W.; Mantoura, F.C.; Llewellyn, C.A.; Bjørnland, T.; Repeta, D.; Welschmeyer, N. Improved HPLC method for the analysis of chlorophylls and carotenoids from marine phytoplankton. *Marine Ecol. Progr. Ser.* **1991,** *77*, 183–196. DOI: 10.3354/meps077183.
68. Breithaupt, D.E.; Wirt, U.; Bamedi, A. Differentiation between lutein monoester regioisomers and detection of lutein diesters from marigold flowers (*Tagetes erecta,* L.) and several fruits by liquid chromatography-mass spectrometry. *J. Agric. Food Chem*. **2002**, *50*, 66–70. DOI: 10.1021/jf010970l.
69. Ríos, J.J.; Xavier, A.A.O.; Díaz-Salido, E.; Arenilla-Vélez, I.; Jarén-Galán, M.; Garrido-Fernández, J.; Pérez-Gálvez, A. Xanthophyll esters are found in human colostrum. *Mol. Nutr. Food Res*. **2017**, *61*, 1700296. DOI: 10.1002/mnfr.201700296.

CONCLUSÃO

Apesar de a área de desenvolvimento de sistemas de produção de microalgas ter evoluído muito nos últimos anos, até o momento, não há um sistema livre de limitações. Os principais problemas o custo de construção e operação e dificuldade de aumento de escala, sendo que ambos são intimamente relacionados ao aporte de energia luminosa às células.

O biorreator e câmara de fotoperíodo de bancada depositado no INPI possibilita o cultivo de microalgas sob ciclos de iluminação e intensidade luminosa variáveis. Tal invenção viabiliza estudos sobre estratégias de iluminação em cultivos microalgais a nível laboratorial nas mais diversas áreas do conhecimento, como ciência de alimentos, engenharias, química e biologia.

O uso de fotoperíodos demonstrou ser uma estratégia de iluminação artificial eficiente melhorar substancialmente o balanço de energia do processo de produção de biodiesel microalgal. A microalga *Scenedesmus obliquus* foi capaz de armazenar energia suficiente para sustentar o crescimento celular por períodos de até 2h no escuro, sem afetar as taxas de crescimento. Ao fracionar o fotoperíodo de 22:2 h (claro: escuro) em vários ciclos por dia, verificou-se um aumento progressivo na produtividade celular à medida que aumentava o número de ciclos. Nos fotoperíodos de curta duração foi verificada uma elevada produtividade celular, porém um baixo teor de lipídeos e, consequentemente de produtividade em lipídeos e valor calorífico. Em termos qualitativos, observou-se que os fotoperíodos influenciaram significativamente no perfil de ácidos graxos e, consequentemente na qualidade do biodiesel produzido.

Quanto a caracterização do perfil de carotenoides em cianobactérias cultivadas em condições livre estresse fisiológico, três carotenoides esterificados foram identificados. Especificamente, observamos os ésteres de miristoil-zeinoxantina e miristoil-β-criptoxantina em *Aphanothece microscopica* Nägeli e mixoxantofila em *Phormidum autumnale.* Essa identificação gera novas possibilidades para a indústria de alimentos, uma vez que quando esterificados, os carotenoides são mais estáveis, possuem maior capacidade antioxidante e, sua biodisponibilidade é maior.

Vinte e nove pigmentos, entre carotenoides e clorofilas foram identificados em amostras de biomassa microalgal de *Chlorella vulgaris*, Scenedesmus *obliquus*, *Aphanothece microscopica* Nägeli e *Phormidum autumnale*, através da metodologia pepiline. Dois carotenoides ainda não encontrados em cianobactérias foram encontrados em *Aphanothece microscopica* Nägeli: 5,6-epoxy-β-criptoxantina, cis-5,8-furanoide-β-criptoxantina e 2’-

dehidrodeoximixol. Um carotenoide nunca antes identificado foi encontrado na biomassa de *Phormidum autumnale* (*Desertifilum*), a desertixantina.

REFERÊNCIAS BIBLIOGRÁFICAS

ABOMOHRA, A. E. F.; JIN, W.; EL-SHEEKH, M. Enhancement of lipid extraction for improved biodiesel recovery from the biodiesel promising microalga *Scenedesmus obliquus.* **Energy Conversion and Management**, v.108, p.23-29, 2016.

BLANKEN, W.; CUARESMA, M.; WIJFFELS, R. H.; JANSSEN, M. Cultivation of microalgae on artificial light comes at a cost. **Algal Research**, v. 2, p.333-340, 2013.

BOROWITZKA, M. A. Biology of Microalgae. In: Levine, I.; Fleurence, J. **Microalgae in Health and Disease Prevention.** Elsevier, 2018, p.23–72.

BOROWITZKA, M. A. Commercial production of microalgae: ponds, tanks, tubes and fermenters. **Journal of Biotechnology**. v.70, p.313-321, 1999.

CHANG, J. S.; SHOW, P. L.; LING, T. C.; CHEN, C. Y.; HO, S. H.; TAN, C. H., NAGARAJAN, D.; PHONG, W. N. Photobioreactors, in: Larroche, C.; Sanroman, M.; Du, G.; Pandey, A. (Eds). **Current Developments in Biotechnology and Bioengineering: Bioprocesses, Bioreactors and Controls.** Atlanta: Elsevier inc., 2017, p. 313-352.

CHEN, Y.; WANG, J.; ZHANG, W.; CHEN, L.; GAO, L.; LIU, T. Forced light/dark circulation operation of open pond for microalgae cultivation. **Biomass and bioenergy**, v.56, p.464-470, 2013.

DESHMUKH, S.; KUMAR, R.; BALA, K. Microalgae biodiesel: A review on oil extraction, fatty acid composition, properties and effect on engine performance and emissions. **Fuel Processing Technology**, v.191, p.232–247, 2019.

EL-SHEEKH, M.; ABOMOHRA, A. E.-F.; ELADEL, H.; BATTAH, M.; MOHAMMED, S. Screening of different species of Scenedesmus isolated from Egyptian freshwater habitats for biodiesel production. **Renewable Energy**, v.129, p.114–120, 2018.

FALKOWSKI, P.G.; RAVEN, J.A. **Aquatic Photosynthesis**. Princeton: Princeton University Press; 2007.

FAY, P. **The blue-greens(Cyanophytacyanobacteria).** 5ª ed. London: ed. Edward Arnold, (Publishers), 88p. (Studies in Biology nº 160). 1983.

FERNANDES, A. S.; NOGARA, G. P.; MENEZES, C. R.; CICHOSKI, A. J.; MERCADANTE, A. Z.; JACOB-LOPES, E.; ZEPKA, L. Q. Identification of chlorophyll molecules with peroxyl radical scavenger capacity in microalgae *Phormidium autumnale* using ultrasound-assisted extraction. **Food Research International**, v.99, p.1036-1041, 2017.

FERNÁNDEZ, F, G, A.; SEVILLA, J. M. F.; GRIMA, E, M. Photobioreactors for the production of microalgae. **Environ Sci Biotechnol,** v.12, p.131-151, 2013.

FERREIRA, V. S.; SANT'ANNA, C. Impact of culture conditions on the chlorophyll content of microalgae for biotechnological applications. **World Journal of Microbiology and Biotechnology**, v.33, p.20, 2017.

FERRUZZI, M. G.; BLAKESLEE, J. Digestion, absorption, and cancer preventative activity of dietary chlorophyll derivatives. **Nutrition Research**, v.27, p.1-12, 2007.

GARCÍA-CAÑEDO, J. C.; Cristiani-Urbina, E.; Flores-Ortiz, C. M.; Ponce-Noyola, T.; ESPARZA-GARCÍA, F.; CAÑIZARES-VILLANUEVA, R. O. Batch and fed-batch culture of *Scenedesmus incrassatulus*: Effect over biomass, carotenoid profile and concentration, photosynthetic efficiency and non-photochemical quenching. **Algal Research**, v.13, p.41-52, 2016.

GEORGE, B.; PANCHA, I.; DESAI, C.; CHOKSHI, K.; PALIWAL, C.; GHOSH.; MISHRA, S. Effects of different media composition, light intensity and photoperiod on morphology and physiology of freshwater microalgae *Ankistrodesmus falcatus* – A potential strain for bio-fuel production. **Bioresource Technology**, v.171, p.367-374, 2014.

GIFUNI, I.; POLLIO, A.; SAFI, C.; MARZOCCHELLA, A.; OLIVIERI, G. Current Bottlenecks and Challenges of the Microalgal Biorefinery. **Trends in Biotechnology**. v.37, p. 242-252 2018.

GROBBELAAR, J. U. Upper limits of photosynthetic productivity and problems of scaling. **Journal of Applied Phycology**, v.21, p.519-522, 2009.

HOLDMANN, C.; SCHMID-STAIGER, U.; HIRTH, T. Outdoor microalgae cultivation at different biomass concentrations — Assessment of different daily and seasonal light scenarios by modeling. **Algal Research**. v.38, p.101405-101412, 2019.

HU, H.; LI, J. Y.; PAN, X. R.; ZHANG, F.; MA, L.L.; WANG, H.J.; ZENG, R.J. Different DHA or EPA production responses to nutrient stress in the marine microalga Tisochrysis lutea and the freshwater microalga Monodus subterraneus. **Science Total Environmental**, v. 656, p.140-149, 2019.

HU, J.; NAGARAJAN, D.; ZHANG, Q.; CHANG, J. S.; LEE, D. J. Heterotrophic cultivation of microalgae for pigment production: A review. **Biotechnology Advances**, v. 36, p. 54-67, 2017.

JACOB-LOPES, E., MARONEZE, M. M.; DEPRÁ, M. C.; SARTORI, R. B.; DIAS, R. R.; ZEPKA, L. Q. Bioactive food compounds from microalgae: An innovative framework on industrial biorefineries. **Current Opinion in Food Science**. v.25, p. 1-7, 2019.

JACOB-LOPES, E.; LACERDA, L. M. C. F.; FRANCO, T. T. Biomass production and carbon dioxide fixation by *Aphanothece microscopica Nägeli* in a bubble column photobioreactor. **Biochemical Engineering Journal**, v. 40, p.27-34, 2008.

JACOB-LOPES, E.; SCOPARO, C. H, G.; LACERDA, L. M. C. F.; FRANCO, T. T. Effect of light cycles (night/day) on CO_2 fixation and biomass production by microalgae in photobioreactors. **Chemical Engineering and Processing**, v. 48, p.306-310, 2009.

JANSSEN, M.; KUIJPERS, T. C.; VELDHOEN, B.; TERNBACH, M. B.; TRAMPER, J.; MUR, L. R.; WIJFFELS, R. H. Specific growth rate of *Chlamydomonas reinhardtii* and *Chlorella sorokiniana* under medium duration light:dark cycles: 13–87 s. **Journal of Biotechnology**, v.70, p.323-333, 1999.

JANSSEN, M.; SLENDERSA, P.; TRAMPER, J.; MUR, L. R.; WIJFFELS, R. H. Photosynthetic efficiency of *Dunaliella tertiolecta* under short light/dark cycles. **Enzyme and Microbial Technology**, v.29, p.298-305, 2001.

JANSSEN, M.; TRAMPER, J.; MUR, L. R.; WIJFFELS, R. H. Enclosed outdoor photobioreactors: Light regime, photosynthetic efficiency, scale up and future prospects. **Biotechnology and Bioengineering**, v.81, p.193-210, 2003.

KRZEMINSKA, I.; PAWLIK-SKOWRONSKA, B.; TRZCINSKA, M.; TYS, J. Influence of photoperiods on the growth rate and biomass productivity of green microalgae. **Bioprocess Biosystem Engineering**, v.37, p.735-741, 2014.

LAURITANO, C.; FERRANTE, M. I.; ROGATO, A. Marine Natural Products from Microalgae: An -Omics Overview. **Marine Drugs**, v.17, p.269, 2019.

MAEDA, Y.; YOSHINO, T.; MATSUNAGA, T.; MATSUMOTO, M.; TANAKA, T. Marine microalgae for production of biofuels and chemicals. **Current Opinion in Biotechnology**, v.50, p.111–120, 2018.

MARONEZE, M. M.; QUEIROZ, M. I. Microalgal Production Systems with Highlights of Bioenergy Production. In Jacob-Lopes, E.; Zepka, L. Q.; Queiroz, M. I. **Energy from Microalgae.** Springer, 2018, p.5-34.

MATA, T. M.; MARTINS, A. A.; CAETANO, N. S. Microalgae for biodiesel production and other application: A review. **Reviews of Sustainable Energy**, v. 14, p. 217-232, 2010.

MENEGAZZO, M. L.; FONSECA, G. G. Biomass recovery and lipid extraction processes for microalgae biofuels production: A review. **Renewable and Sustainable Energy Reviews**, v.107, p.87–107, 2019.

NEGISHI, T.; RAI, H.; HAYATSU, H. Antigenotoxic activity of natural chlorophylls. **Mutation Research/fundamental & Molecular Mechanisms of Mutagenesis**, v.376, p.97–100, 1997.

NWOBA, E. G.; PARLEVLIET, D. A.; LAIRD, D. W.; ALAMEH, K.; MOHEIMANI, N. R. Light management technologies for increasing algal photobioreactor efficiency. **Algal Research**. v.39, p.101433, 2019.

OGBONNA, J. C.; SOEJIMA, T.; TANAKA, H. An integrated solar and artificial light system for internal illumination of photobioreactors. **Journal of biotechnology**, v.70, p.289-297, 1999.

PALIWAL, C.; GHOSH, T.; GEORGE, B.; PANCHA, Y.; MAURYA, R.; CHOKSHI, K.; GHOSH, A.; MISHRA, S. Microalgal carotenoids: Potential nutraceutical compounds with chemotaxonomic importance. **Algal Research**, v.15, p.24-31, 2016.

PATIAS, L. D.; FERNANDES, A. S.; PETRY, F. C.; MERCADANTE, A. Z.; JACOB-LOPES, E.; ZEPKA, L. Q. Carotenoid profile of three microalgae/cyanobacteria species with peroxyl radical scavenger capacity. Food Research International, v.100, p.260–266, 2017.

PEREIRA, H.; PÁRAMO, J.; SILVA, J.; MARQUES, A.; BARROS, A.;, MAURÍCIO, D.; SANTOS, T.; SCHULZE, P.; BARROS, R.; GOUVEIA, L.; BARREIRA, L.; VARELA, J.

Scale-up and large-scale production of *Tetraselmis* sp. CTP4 (*Chlorophyta*) for CO_2 mitigation: from an agar to 100-m3 industrial photobioreactors. **Nature Science Reports**. v.8, p.1-13, 2018.

POSTEN, C. Design principles of photobioreactors for cultivation of microalgae. **Engineering in Life Sciences**, v.9, p.165-177, 2009.

QUEIROZ, M. I.; MARONEZE, N. M.; MANETTI, A. G. S.; VIEIRA, J. G.; ZEPKA, L. Q.; JACOB-LOPES, E. Enhanced single-cell oil production by cold shock in cyanobacterial cultures. Ciência Rural, v.48, p.11-19, 2018.

QUEIROZ, M.I. HORNES, M., MANETTI, A.G.S., ZEPKA, L.Q., JACOB-LOPES, E. Fish processing wastewater as a platform of the microalgal biorefineries. **Biosystems Engineering**, v.115, p.195-202, 2013.

RASHID, N. Current status, issues and developments in microalgae derived biodiesel production. **Renewable and Sustainable Energy Reviews**, v.40, p.760–778, 2014.

RAZZAK, S. A. Integrated CO2 capture, wastewater treatment and biofuel production by microalgae culturing - A review. **Renewable and Sustainable Energy Reviews**, v.27, p.622–653, 2013.

RIVIERS, B. **Biologia e Filogenia das Algas**. Traducao: FRANCESCHINI, I. M. Porto Alegre, MG, Ed. Artmed, p.21-27; 66-94; 153-183, 2006.

RIZWAN, M.; MUJTABA, G.; MEMON, S. A.; LEE, K.; RASHID, N. Exploring the potential of microalgae for new biotechnology applications and beyond: A review. **Renewable and Sustainable Energy Reviews**, v.92, p.394–404, 2018.

RODRIGUES, D. D.; FLORES, E. M. M.; BARIN, J. S. MERCADANTE, A. Z.; JACOB-LOPES, E.; ZEPKA, L. Q. Production of carotenoids from microalgae cultivated using agroindustrial wastes. **Food Research International**, v. 65, p.144-148, 2014.

SAFI, C.; ZEBIB, B.; MERAH, O.; PONTALIER, P.-Y.; VACA-GARCIA, C. Morphology, composition, production, processing and applications of *Chlorella vulgaris*: A review. **Renewable and Sustainable Energy Reviews**, v.35, p.265–278, 2014.

SAINI, R. K.; KEUM, Y. S. Omega-3 and omega-6 polyunsaturated fatty acids: dietary sources, metabolism, and significance - a review. **Life Sciences**, v. 203 p.255-267, 2018.

SATHASIVAM, R.; RADHAKRISHNAN, R.; HASHEM, A.; ABD-ALLAH, E. F. Microalgae metabolites: A rich source for food and medicine. **Saudi Journal of Biological Sciences**, v.26, p.709-722, 2017.

SCHADE, S.; MEIER, T. A comparative analysis of the environmental impacts of cultivating microalgae in different production systems and climatic zones: A systematic review and meta-analysis. **Algal Research**, v.40, p.101485, 2019.

SHISHIDO, T. K.; JOKELA, J.; HUMISTO, A.; SUURNÄKKI, S.; WAHLSTEN, M.; ALVARENGA, D. O.; SIVONEN, K.; FEWER, D.P. The Biosynthesis of Rare Homo-Amino Acid Containing Variants of Microcystin by a Benthic Cyanobacterium. **Marine Drugs**, v.17, p.271, 2019.

SU, F.; LI, G.; FAN, Y.; YAN, Y. Enhanced performance of lipase via microcapsulation and its application in biodiesel preparation. **Nature Science Reports**, v.6, p.29670-29682, 2016.

SUN, X.-M.; REN, L.-J.; ZHAO, Q.-Y.; JI, X.-J.; HUANG, H. Enhancement of lipid accumulation in microalgae by metabolic engineering. **Biochimica et Biophysica Acta (BBA) - Molecular and Cell Biology of Lipids**, v.1864, p.552-566, 2019.

VASUMATHI, K. K.; PREMALATHA, M.; SUBRAMANIAN, P. Parameters influencing the design of photobioreactor for the growth of microalgae. Renewable and **Sustainable Energy Reviews**, v.16, p.5443–5450, 2012.

VENDRUSCOLO, R. G.; FAGUNDES, M. B.; MARONEZE, M. M.; DO NASCIMENTO, T. C.; DE MENEZES, C. R.; BARIN, J. S.; ZEPKA, L. Q.; JACOB-LOPES, E.; WAGNER, R. Scenedesmus obliquus metabolomics: effect of photoperiods and cell growth phases. **Bioprocess and Biosystems Engineering**, v.42, p.727-739, 2019.

Vesenick, D. C.; Paula, N. A.; Niwa, A. M.; Mantovani, M. S. Evaluation of the effects of chlorophyllin on apoptosis induction, inhibition of cellular proliferation and mRNA expression of CASP8, CASP9, APC and b-catenin. **Current Research Journal of Biological Sciences**, v.4, p.315-322, 2012.

WIJFFELS, R, H.; KRUSE, O; HELLINGWERF, K, J. Potential of industrial biotechnology with cyanobacteria and eukaryotic microalgae. **Current Opinion in Biotechnology**, v.24, p.405–413, 2013.

WILLIAMS, P. B. LAURENS, M. L. Microalgae as biodiesel and biomass feedstocks & analysis of the biochemistry, energetic and economics. **Energy & Environmental Science**, v.3, p.554-590, 2010.

Xavier, A. A. O.; Pérez-Gálvez, A. (2016). Carotenoids as a Source of Antioxidants in the Diet. In Stange, C (Ed.). **Carotenoids in Nature**. Springer International Publishing, 2016, p. 359-375.

XU, X.; GU, X.; WANG, Z.; SHATNER, W.; WANG, Z. Progress, challenges and solutions of research on photosynthetic carbon sequestration efficiency of microalgae. **Renewable and Sustainable Energy Reviews**, v.110, p.65–82, 2019.

ZEPKA, L. Q. et al. Production and biochemical profile of the microalgae *Aphanothece microscopica Nägeli* submitted to different drying conditions. **Chemical Engineering and Processing**, v.47, p.1311-1316, 2008.

ZHAO, B.; SU, Y. Process effect of microalgal-carbon dioxide fixation and biomass production: A review. **Renewable and Sustainable Energy Reviews**, v.31, p.121–132, 2014.

ZHOU, Q.; ZHANG, P.; ZHAN, G.; PENG, M. Biomass and pigments production in photosynthetic bacteria wastewater treatment: Effects of photoperiod. **Bioresource Technology**, v.190, p.196-200, 2015.